

RP66G Synthesis Report

Gully mapping and drivers in the grazing lands of the Burdekin catchment

Remote Sensing Centre

November 2014

Prepared by

Dan Tindall, Bleuenn Marchand, Uri Gilad, Nicholas Goodwin, Robert Denham, Skye Byer
Remote Sensing Centre, Land Surface Sciences
Science Division
Department of Science, Information Technology, Innovation and the Arts
PO Box 5078
Brisbane QLD 4001

On behalf of
Reef Water Quality
Environmental Policy and Planning
Department of Environment and Heritage Protection

© The State of Queensland (Department of Science, Information Technology, Innovation and the Arts) 2014

The Queensland Government supports and encourages the dissemination and exchange of its information. The copyright in this publication is licensed under a Creative Commons Attribution 3.0 Australia (CC BY) licence



Under this licence you are free, without having to seek permission from DSITIA, to use this publication in accordance with the licence terms.

You must keep intact the copyright notice and attribute the State of Queensland, Department of Science, Information Technology, Innovation and the Arts as the source of the publication.

For more information on this licence visit <http://creativecommons.org/licenses/by/3.0/au/deed.en>

Disclaimer

This document has been prepared with all due diligence and care, based on the best available information at the time of publication. The department holds no responsibility for any errors or omissions within this document. Any decisions made by other parties based on this document are solely the responsibility of those parties. Information contained in this document is from a number of sources and, as such, does not necessarily represent government or departmental policy.

If you need to access this document in a language other than English, please call the Translating and Interpreting Service (TIS National) on 131 450 and ask them to telephone Library Services on +61 7 3170 5725

Acknowledgements

This report has been prepared by the Department of Science, Information Technology, Innovation and the Arts. Acknowledgement is made of Reef Water Quality, Department of Environment and Heritage for funding and support for this project and for reviewing this document. Acknowledgement is also made to Shawn Darr, Dave Waters and the team in DNRM who are contributing to the catchment-scale mapping guidelines and mapping effort. The support and advice of Scott Wilkinson, Anne Henderson, and Rebecca Bartley in CSIRO, Jacky Croke, Dan Brough (and team) and Jo Burton in DSITIA, Bob Shepherd and the Charters Towers team in DAFF and staff at NQDT Regional NRM Group is also gratefully acknowledged. Finally, we wish to thank the producers in the Burdekin who gave us their valuable time and advice.

Executive summary

Recent studies of sediment sources in the Great Barrier Reef (GBR) lagoon have shown that gully erosion is a dominant contributor of sediment, particularly in the Burdekin and Fitzroy catchments. Gully erosion also presents a significant challenge to the grazing industry, impacting land condition and reducing productivity. There has been limited work undertaken to comprehensively map gully locations, and to quantify and monitor gully erosion processes in GBR catchments at scales or resolutions appropriate for land management decision-making. Where mapping studies have been conducted, the information has been of limited use due to low accuracy, scale limitations or the maps being of limited geographic extent. This project aimed to provide spatially-comprehensive mapping and monitoring of gully erosion in the Burdekin catchment to improve knowledge of where gullies occur and to attempt to better understand the processes and drivers of gully erosion, particularly in the grazing lands of the catchment. The outcomes are intended to serve multiple needs including: providing improved information for targeting erosion prevention and remediation efforts; to support grazing extension programs aimed at improving grazing land management to improve sustainability of the grazing industry in GBR catchments; and, to help improve water quality models.

Improved mapping of gully locations in the Burdekin was achieved by visual observation of satellite and aerial imagery and predictive modelling. Mapping was produced at two resolutions, 5km and 1km. The 5km resolution mapping combined high resolution mapping, a predictive model of gully presence and visual observations of gully prevalence across the entire catchment. Gully presence was mapped in 7 classes relating to the amount of gulying present, where gulying was observed. The 1km resolution mapping was achieved entirely through visual interpretation of a 1km grid, each grid divided into one hundred, 100m x 100m cells to provide a count or percentage of gulying evident in each 1km grid cell. Mapping was targeted at key areas identified in the 5km map as having high gully presence. A mapping guideline has also been developed to support ongoing application of this mapping approach in other parts of the GBR grazing lands.

Changes in gully extent and volume were mapped and quantified over multiple time scales and at different resolutions in an effort to improve knowledge on rates of change and volumes of sediment loss when changes occur. Very high resolution LiDAR data was captured for a number of transects over at least two dates and digital elevation models developed. Differences in elevation between the dates were compared by first classifying where gullies occur, and then determining the depth and volume of gullies to provide quantitative estimates of change. Elevation thresholds were required to account for potential errors in the LiDAR data due to different sensor configuration and acquisition specifications for different capture dates, the processing applied to the data by the supplier, and issues of classifying complex terrain, where vegetation and other land cover features are present. Long-term gully change was mapped at ten sites for dominant land types using historical imagery. The mapping was limited by available historical imagery, difficulty in image rectification and identifying features in imagery of varying resolution and quality. Gully extents were mapped over time (up to nearly 60 years at some sites) using a grid cell-based approach, at 30m resolution. Extents were compared over the time-series to quantify the two-dimensional expansion of gullies and proportional rates of change.

The 5km and 1km resolution gully maps showed that nearly 60% of the Burdekin catchment has very low to low gulying present. This means there are very few or no gullies apparent in the imagery used for the mapping. Sub-catchments with the highest prevalence of gulying were the Upper Burdekin, Bowen-Broken and the northern part of the Suttor where sedimentary and granitic

geologies dominate. The predictive modelling showed a strong relationship between gully presence and elevation above drainage lines with most gullies occurring within the first 1.5m. This is consistent with observations from aerial and satellite imagery, where alluvial gullies occur close to major drainage lines and the higher order drainage in the topographic data has mapped gullies as drainage features in the colluvial slope environments. The predictive model also found that where there was a high probability of gullies occurring, there was still only around 5% chance of an actual gully being present, suggesting that gullies are rare features in a whole-of-landscape context.

The gully change monitoring approaches showed that where sampling was undertaken, some active gullying was detected. There is some uncertainty in the change estimates from the LiDAR data due to thresholds used and differences between sites and issues with the data. The LiDAR analysis showed that gullying could be up to about 10% of a site and the change analysis indicated that large changes of over 10,000m³ have taken place in some areas in a three year period. The LiDAR data also showed a high correlation between gully area and gully volume, suggesting that mapping of gully area may provide a proxy for volume, where volume data is not available. The results of the LiDAR change analysis and the long-term change analysis also suggested that larger gully changes may be episodic or event-based, driven by intense, localised rainfall events and possibly exacerbated by low ground cover. This could highlight the need for land management approaches that protect at-risk areas when they are most vulnerable, such as at the end of a drought or the break of dry season.

Future mapping and monitoring efforts should focus on continuing catchment-scale mapping of gully locations using simple and consistent mapping approaches. Developing appropriate management strategies for gullies relies on first knowing where gullies are in the landscape, and then understanding the erosion processes which have led to their formation and ongoing activity. This project has developed multiple lines of evidence to help improve understanding of where gullies are and how they are changing. However, large knowledge gaps remain including understanding the fate and timing of sediment delivered from gullies, and developing the most appropriate technologies and approaches for managing and monitoring gullied areas. Research issues still remain about how to best use airborne LiDAR for determining gully volumes and changes over time. Emerging technologies such as terrestrial laser scanning, sediment tracing and digital soils mapping all present opportunities to help improve our understanding of gully processes to enable effective management strategies for improving land condition and water quality in the grazing lands of the GBR.

Contents

Overview	xi
1 Introduction	1
1.1 Gully erosion in the Burdekin catchment	1
1.2 Gully modelling and mapping	1
1.3 Recent mapping and modelling in the Burdekin	2
1.4 Objectives	3
2 Methods	3
2.1 Mapping gully locations	3
2.1.1 Imagery and data	3
2.1.2 5km resolution gully presence map	6
2.1.3 1km Gully Presence Map	17
2.2 Mapping gully extent, volume and change using airborne LiDAR	20
2.2.1 LiDAR data and pre-processing	20
2.2.2 Classifying gully extents	24
2.2.3 Quantifying gully depth, volume and change	27
2.2.4 Multi-temporal Terrestrial Laser Scanning of gullies	28
2.3 Gully chronosequence mapping	29
2.3.1 Selection of gully locations for chronosequence mapping	29
2.3.2 Aerial photography and satellite imagery	34
2.3.3 Identifying gully change	35
3 Results	38
3.1 Gully locations in the Burdekin	38
3.1.1 'No Gully' location map	38
3.1.2 Manual gully extent mapping	39
3.1.3 Predictive model of gullies	40
3.1.4 5km Gully Presence Map	44
3.1.5 Converting the 5km Gully Presence Map to gully density	49
3.1.6 1km Gully Presence Map	50
3.2 Gully extent, volume and change using airborne LiDAR	53
3.2.1 Gully extents	53
3.2.2 Gully depth, volume and change	55
3.2.3 Gully change between 2010 and 2013	58

3.3 Gully chronosequence mapping	62
4 Discussion	69
4.1 Mapping of gully locations	69
4.1.1 Broad-scale (5km resolution) mapping	69
4.1.2 Medium scale (1km resolution) mapping	71
4.2 Mapping gully extent, volume and change using airborne LiDAR	72
4.3 Gully chronosequence mapping	74
5 Conclusions.....	77
5.1 Key outputs	77
5.2 Key findings	78
5.3 Recommendations for future work	81
6 Data publication	82
7 References	83

List of tables

Table 1 Data layers used for predictive mapping.....	4
Table 2 Relative gully probability classes based on explanatory variables. Class 8 was assigned 'very low' because gullies that occur within this layer are not well explained by the explanatory variables.	8
Table 3 Explanatory variables used for development of the predictive model. Variables were generated in SAGA software and were based on the SRTM 1" DEM.	9
Table 4 Gully presence values.....	11
Table 5 Information sources and methods used to interpret them, ranked in order of confidence for mapping gully presence.	12
Table 6 Values assigned to 5km grid cells based on observed gullying.	15
Table 7 Simplifying gully density classes based on mean density from visual observations and high resolution mapping.....	15
Table 8 Proportion of 5km Gully Presence Map that has been mapped at 1km resolution	19
Table 9 LiDAR capture specifications.....	22
Table 10 Quality assurance checks for LiDAR captures.....	23
Table 11 Erodible soils characteristics of gully chronosequence mapping locations.....	32
Table 12 Imagery years and image type (BW: black and white, C: colour, S: satellite), soil types and gully shapes.....	34
Table 13 Classes used for the predictive model of gullies.	40
Table 14 Gully presence for each sub-bioregion. Cells in sub-bioregions where >95% of the already assigned cells had 'low' or 'very low' gully presence were assigned 'low' gully presence in the final map. These are shown in red text.....	46
Table 15 Total count, percentage and sum of cells, categorised by 'gully count' values.....	50
Table 16 Summary of the 'gully count' values found in the major sub-catchments.	51
Table 17 A comparison of general statistics for the 5km Gully Presence Map and 1km Gully Presence Map.....	52
Table 18 Classified gully statistics for the 13 processed Burdekin LiDAR sites for 2010 and 2013. Note: percentage cover refers to the percentage of pixels containing a return > 2m (vegetation overstorey) and > 0.5 and <2.0m (vegetation understorey).	56
Table 19 Summary of gully chronosequence mapping results, sorted by original size (largest to smallest)	65
Table 20 The soil erosion characteristics and ranking of the gullies (based on products developed by RWQ Science Project RP63G), sorted by the proportional growth of gullies.	66
Table 21 List of data sources to be released as Open Data from this project.....	82

List of figures

Figure 1 Quickbird and SPOT imagery coverage on Google Earth and randomly selected sampling sites.....	5
Figure 2 Schematic of 5km resolution gully presence mapping methodology.....	6
Figure 3 Area Under Curve (AUC) represents the relationship between gully occurrence and elevation above drainage line in areas defined as gully sensitive. The triangles indicate elevation above drainage line. A random prediction (shown on the graph as dashed line) is expected to be linear throughout the examined area and therefore would have an AUC of 50%. The model (solid line) shows an AUC of 80%. This means that elevation above drainage line can explain the distribution of most mapped gullies and can improve prediction ability compared with the other variables examined. For example, the model locates 60% of the (mapped) gullies within the first 15% of the gully sensitive area closest to drainage line (<75cm).....	10
Figure 4 Sources of information used to develop the gully map. Darker greens indicate information sources with the highest confidence. The predictive model had the lowest confidence and was therefore used only where other sources were not able to provide sufficient information. Note: QB imagery refers to Quickbird satellite imagery (resolution <1m).....	13
Figure 5 Deriving gully density classes based on proportion gullied as determined by high resolution mapping and visual observation of gully prevalence. The graph at top shows the overlap between some classes and provided the basis for simplification of the classification from seven to four classes.....	16
Figure 6 Gully mapping at different resolutions. The 5km cell (red lines) extracted from the 5km Gully Presence Map is shown in the image on the left. The 1km cells (white lines) from the 1km Gully Presence Map are also shown. The '1' indicates the presence of gullying within the 1km grid cell. The image on the right is a zoom of the grid cell labelled '1' and shows the 100m grid cells which are used to help interpret gully presence as a percentage within the 1km grid cell.....	17
Figure 7 This diagram illustrates how the 1km Gully Presence Map provides improved resolution for the gully presence mapping than the 5km Gully Presence Map. The red square outline is the 5km Gully Presence Map and the smaller coloured squares are the 1km Gully Presence Map symbolised according to 'gully count' values. The image on the right shows the presence of gullies within the 1km grid cell. This example was interpreted as having >65% of gullying present within the 1km x 1km area.	18
Figure 8 Location of LiDAR transects in the Burdekin and Fitzroy catchments. Site numbers correspond with site names in Table 10. Sites 1 (Blue Range) and 8 (Mount Ravenswood) were excluded from reporting due to processing errors.	21
Figure 9 Example of 50% LiDAR scan overlap. The two opposing scan orientations limit occlusion by vegetation and overhangs and increase the detection of gully walls.....	24
Figure 10 Sections of gullies were chosen for each transect for gully classification and subsequent change analysis. The subsets used for the Lyall Creek transect are shown with ortho-photography. The image below is a zoom of the north-east corner of the transect.....	26
Figure 11 Schematic diagram showing how gully depth was calculated. The gully extent (red line) was removed from LiDAR data and the DEM was re-interpolated across the gullied area to create a continuous surface (black line). Gully depth is the difference between red and black lines across the defined gully extents.	27
Figure 12 Example of a Terrestrial Laser Scanning instrument. The instrument shown is a Riegl VZ-400 full waveform instrument (source: www.riegl.com).....	28

Figure 13 Reconstruction of a DEM for a gully system in the Burdekin (Spyglass Research Station) based on scans obtained using a TLS. 29

Figure 14 Gully chronosequence mapping locations in the Burdekin catchment 31

Figure 15 Gully location 4 mapped in 1945. Grid cells are 30m x 30m. 36

Figure 16 Example of gullied cells selected over three different dates with the earliest available date shown (Gully 4 and Gully 1).. 37

Figure 17 ‘No-gully’ areas and ‘gully sensitive areas’ 38

Figure 18 Map of the Burdekin showing where gully mapping has been completed (within available Quickbird imagery)..... 39

Figure 19 Example of gully mapping based on Quickbird imagery 40

Figure 20 Sub-section of the predictive model with mapped gullies overlaid. There is generally good agreement between mapped gullies and areas of high gully probability in the predictive model..... 43

Figure 21 Observed gully presence at 5x5km grid cells vs. extent of no-gully area. Observed 5x5km cells were divided according to gully presence classes (x-axis; number in box indicates cell count). The y-axis indicates the mean extent of no-gully area throughout observed cells as a percentage. Horizontal lines in the boxes indicate mean percentage of no-gully area for the gully presence class. Boxes show the interquartile range while the vertical line indicates where 95% of the data lies for each class. Outliers are marked as points. For example, in the ‘very low’ gully class: 331 cells were observed as having very low gully presence. These cells had an average of about 80% no-gully area. 75% of these cells had 60%-95% of their area classified as a no-gully area. Only five of these cells had no-gully area between 0% and 5%..... 45

Figure 22 Final 5km gully presence map. This map shows gully presence is greatest in the Upper and Lower Burdekin and Bowen-Broken sub-catchments. 48

Figure 23 5km resolution gully density map. The relationship between density derived from manual mapping and observed gully presence was used to extrapolate density across the 5km gully presence map. 49

Figure 24 Distribution of ‘gully count’ values for all cells mapped. 53

Figure 25 Distribution of ‘Gully count’ values for cells that intersect ‘High’ and ‘Very High’ within the 5km Gully Presence Map. 53

Figure 26 Example of a LiDAR derived DEM (a), the difference from mean elevation (b) and the classified gully extent (c) for a subset at one of the LiDAR sites (Blue Range). In the difference from mean elevation image (b), lighter shades indicate greater difference from mean elevation. This information is used to automatically classify the gully extent. Subset extent 200 x 200 m; DEM elevation range 360 to 375m; Difference layer elevation range = -59cm to 76cm..... 54

Figure 27 Example of gully extent classification based on LiDAR. Left image shows the orthophoto for the area and right image shows the classified gully extent in red. 54

Figure 28 Relationship between gully area and volume. As gully area increases, the gully volume increases. 57

Figure 29 Example of gully change mapping using LiDAR at one of the Fitzroy sites: (a) DEM in 2007. Deeper gullied areas are darker shades. (b) DEM in 2010. Note the clear expansion of the gully. (c) Change in gully extent and volume between 2007 and 2010 (white areas)..... 57

Figure 30 Example of a cross-sectional profile of a gully in the Fitzroy showing the difference between 2007 and 2010. The profile represents the horizontal red line dissecting the expanded gully head in Figure 29..... 58

Figure 31 Fraction of gully area mapped in 2010 only (blue), 2013 only (green), and mapped in both years (red). 59

Figure 32 Total difference between 2010 and 2013 digital elevation models..... 60

Figure 33 Impact of change threshold on the fraction of gully change (2010 DEM minus 2013 DEM). The value is calculated as the total difference between dates (i.e. 2013 minus 2010) divided by the difference greater than the threshold value. To facilitate visual comparison between sites the values were rescaled as the fraction of the total change rather than the magnitude..... 61

Figure 34 Total difference between 2010 and 2013 digital elevation models with a 0.45m noise threshold applied (i.e. only change >0.45m is included in this figure). 62

Figure 35 Proportional gully growth, in relation to gully sizes measured in the first available images.63

Figure 36 Top: high resolution aerial photography, Bottom: DEM derived from LiDAR data of the same area..... 76

Overview

This report describes project RP66G Gully mapping and drivers in the grazing lands, undertaken on behalf of the Reef Water Quality (RWQ) Science Program. The project aimed to map and quantify gully extent and rates of change at a range of scales in the Burdekin catchment, Queensland. The work is part of a larger program which aimed to improve understanding of sediment sources and erosion processes within grazing lands of the Burdekin catchment.

This report focuses on the method development and delivery of a range of gully mapping products to:

- improve understanding of gully locations, activity, and longer-term processes that influence gully formation and evolution
- highlight areas that are more likely to have gullies or be at risk of gully formation
- help government, industry and natural resource management groups to focus grazing extension and land management investment efforts to vulnerable areas
- assist the Paddock to Reef monitoring, modelling and reporting program (under Reef Water Quality Protection Plan) to improve model parameterisation for gullies in select areas.

1 Introduction

1.1 Gully erosion in the Burdekin catchment

Present knowledge of gully locations, processes and contribution to the sediment budget in the Burdekin catchment is limited. In a review of sediment sources in the Burdekin catchment, Bartley (2011) highlighted that there is a large disparity between studies (e.g. Prosser et al. 2001; Kinsey-Henderson et al. 2005) about the scale of gully erosion in the catchment. This is mainly attributed to the poor quality gully data used in models and uncertainty in predictive methods. Further, a range of findings have been reported in the literature regarding where sediment is originating within the catchment, which sediment fractions pose the greatest risk to the Great Barrier Reef (GBR), and which erosion processes and land management types can be attributed to the source of the sediment (e.g. Lewis et al., 2006; Bartley et al., 2007; Bainbridge et al., 2008).

In a summary of the scientific evidence, the 2013 Scientific Consensus Statement (Brodie et al., 2013) has identified gullies as a dominant contributor to the sediment load in the GBR receiving waters. This is particularly relevant in the Burdekin and Fitzroy catchments, the largest contributor of sediment to the GBR of all reef catchments. There is a clear need for consistent mapping of landscapes susceptible to gully erosion and mapping of past and present gully extent and volume. These data should be at a range of scales and in formats that are suitable for prioritisation of prevention, rehabilitation, and investment and extension activities and for use in catchment-scale water quality models.

1.2 Gully modelling and mapping

A number of studies in the literature have undertaken spatial mapping and quantification of gullies (e.g. Meyer and Martínez-Casasnovas, 1999; Zinck et al., 2001; Martínez-Casasnovas et al., 2004; Bou Kheir et al., 2007; Vrieling et al., 2007; Vanwallegem et al., 2008; Gómez Gutiérrez et al., 2009; Perroy et al., 2010; Baruch and Filin, 2011; Shruthi et al., 2011). Most of the studies have used very high resolution imagery and focused on relatively small areas (1-100km²) where gullies are prominent. These methods are not readily transferable to regional scales and large areas.

Regional and local scale modelling and mapping of gullies has been attempted in Australia for a range of locations and environments. These have been based on various biophysical and remotely-sensed data, and have used a range of methods. As part of the National Land and Water Resources Audit, Hughes et al. (2001) interpreted aerial photography to derive gully locations for selected areas in the Burdekin and other Australian catchments. They then modelled gully density based on a geostatistical approach applied to biophysical variables (e.g. geology, land use, climate and terrain). Their work was aimed at national and regional scale measures of gully density and validation of the outputs was minimal. Prosser et al. (2002) and Lorimer et al. (2011) produced gully and erosion hazard maps for the Burdekin. Hazard maps do not directly indicate where gullies are present, but are useful to

highlight areas that may be at risk of gully formation. However, the accuracy of these maps is limited by available data, including aerial imagery and information about soils and terrain. Kuhnert et al. (2010) applied a random forest modelling approach to the mapping data from Hughes et al. (2001) to predict gully density and associated error of the prediction. They found that the error associated with prediction was considerable and concluded that the poor mapping of gullies led to the poor predictions. They noted that only a very small proportion (~0.88%) of the Burdekin had been mapped with a focus on gully presence.

Eustace et al. (2011) also used a random forest modelling approach to predict the risk of gully presence in the Fitzroy catchment. They used gully mapping derived from LiDAR data at eight sites in the Fitzroy as the training data. They also had modest results and, like Kuhnert et al. (2010), attributed this mainly to the lack of gully mapping information and limitations of the resolution and accuracy of biophysical data, especially soils information.

Other studies from Queensland have applied object-oriented and decision-tree based approaches to medium- and high-resolution imagery to map gullies. For example, Johansen et al. (2011) used SPOT imagery and other derived surfaces (e.g. ground cover, slope) to map gullies in the Burdekin catchment while Knight et al. (2009) used ASTER imagery, airborne LiDAR and aerial photography to map alluvial gully systems in the Mitchell river catchment. Both of these studies had limited quantitative validation but results indicated moderate levels of accuracy in the output maps.

1.3 Recent mapping and modelling in the Burdekin

In response to the lack of information about gully locations in the Burdekin catchment, the Remote Sensing Centre (RSC) undertook a mapping project to identify areas where gullies were present. This work was primarily funded internally by DSITIA (as part of the former QScape program) and the outputs have provided a foundation for this current project (RP66G). For example, we have used this information to target areas for multi-temporal mapping of gully activity and erosion rates in the current project, historical air photos, airborne and terrestrial LiDAR, and satellite imagery. As part of the synthesis of information for this report, some methods and outputs of lead-in work completed under the former QScape program is included in sections 2.1, 3.1 and 5.1 below.

RSC has also previously investigated the use of high resolution LiDAR data for multi-temporal, quantitative measurement of volumetric change to gullies in the Burdekin and Fitzroy catchments. Four dates of LiDAR data (2007; 2008; 2010; 2013) now exist for four sites in the Fitzroy. Preliminary analysis shows that LiDAR data has sufficient accuracy and resolution to quantify changes in extent and volume of gullies. Further research is needed to quantify uncertainties in the estimates due to sensor configurations, capture specifications and variations in landscapes. In the Burdekin catchment, 15 transects of LiDAR data were acquired in 2010 and again in 2013 through Reef Water Quality Protection Plan (Reef Plan) funding. When analysing this data, this project has extended the techniques developed for the Fitzroy analysis.

The transects include investment areas of the North Queensland Dry Tropics (NQDT) regional group and repeat monitoring will enable evaluation of practice effectiveness for minimising erosion and improving land condition in these areas.

1.4 Objectives

This project aims to produce information at a range of scales to improve knowledge of sediment sources and erosion processes in the Burdekin catchment by using remote sensing, statistical modelling, manual digitising and field survey methods. The specific objectives are to:

1. Map gully locations in the Burdekin catchment at a range of scales to provide multiple sources of information about gully presence, gully absence, and risk of gully formation.
2. Identify and map active and dormant gully systems using historical aerial photography and satellite imagery to improve understanding of gully processes and help identify areas where the greatest current activity is occurring in the catchment.
3. Quantify changes in gully extent and volume using multi-date airborne LiDAR. This provides measures of volumetric changes to actively eroding gullies in a range of landscapes.
4. Develop a suite of simple, repeatable methods that can be used to map and quantify gully erosion activity in other GBR catchments, and more generally, in Queensland and elsewhere.
5. Where possible, link these data and information to other lines of evidence obtained from sediment tracing (RP65G) and soil attribute mapping (RP63G) Reef Water Quality R&D projects to enhance landscape understanding in the Burdekin for improved decision-making and policy implementation.

2 Methods

2.1 Mapping gully locations

This section describes the methods used to develop broad-scale and large-area coverage gully maps for the Burdekin catchment.

2.1.1 Imagery and data

2.1.1.1 Imagery

DSITIA has a complete coverage of SPOT imagery at 2.5m spatial resolution for the entire Burdekin catchment. Google Earth™ imagery for the Burdekin includes a variety of image sources including Quickbird and GeoEye imagery at ~0.6m spatial resolution and SPOT imagery at 2.5m spatial resolution. Extensive preliminary observations showed that gullies in the Burdekin can be visually identified with high certainty on Quickbird and GeoEye imagery (~0.6 m/pixel), but not on SPOT imagery (~2.5 m/pixel). All gully sampling was therefore limited to Quickbird and GeoEye imagery available on Google Earth™. This limited our sampling to about 30% of the total area of the Burdekin (Figure 1).

2.1.1.2 Data

Table 1 lists and describes the data compiled as potential explanatory variables for gully location in the predictive map. These data were tested for use as explanatory variables, as described in Section 2.1.2.3 below.

Table 1 Data layers used for predictive mapping

Data layer name	Spatial resolution/scale	Description
Geology	Vector, various scales	Mapping of dominant geological unit
Soils	Vector, various scales	Mapping of dominant soil unit
Regional Ecosystems	1:100,000	Data produced by Queensland Herbarium (v6.0b)
Ground Cover Index (GCI)	30m	Vegetation cover in areas of <15% FPC (Scarth et al., 2006)
Foliage Projective Cover (FPC)	30m	Wooded vegetation cover derived from Landsat TM/ETM+ imagery (Armston et al., 2009)
Digital Elevation Model (DEM)	30m	Derived from SRTM 1" DEM
Slope	30m	Derived from SRTM 1" DEM
Distance from nearest drainage line	30m	Derived from 1:100,000 topographic drainage line mapping
Elevation above drainage line	30m	Derived from SRTM 1" DEM



Figure 1 Quickbird and SPOT imagery coverage on Google Earth and randomly selected sampling sites.

2.1.2 5km resolution gully presence map

The methodology to map gullies included four main steps. Each step resulted in a standalone product that contributed to the creation of the next product. The overall process is shown schematically in Figure 2.

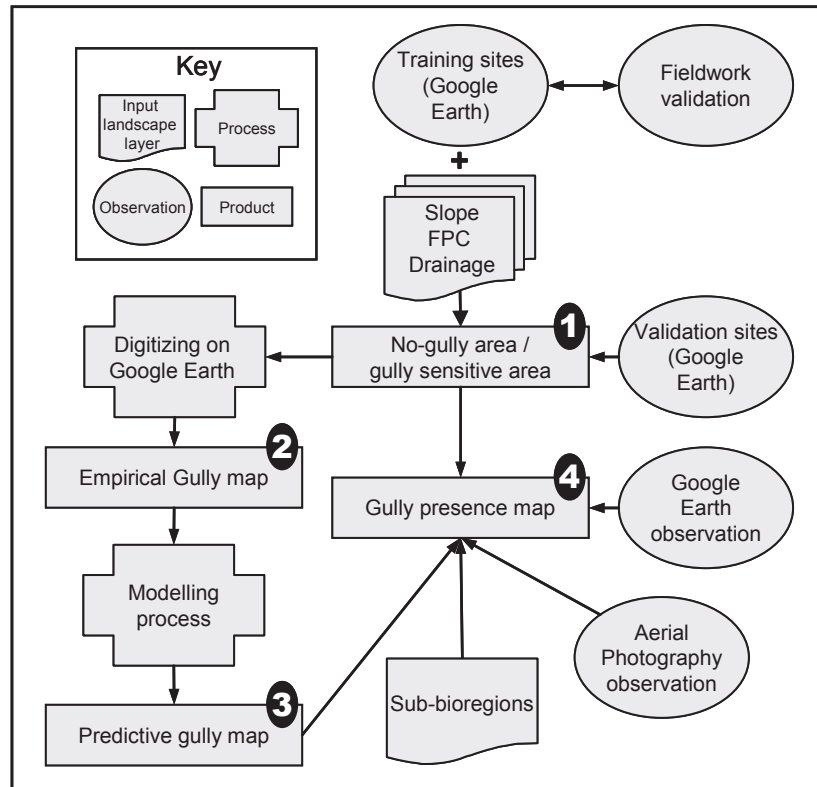


Figure 2 Schematic of 5km resolution gully presence mapping methodology.

2.1.2.1 Identifying 'No-gully' areas

This step aimed to identify areas of the Burdekin catchment where gullies are less likely to occur or are not present, and do not pose significant risk to the formation of gullies in future. The identification of these areas helped to target mapping efforts in subsequent stages and provided information about areas at low risk of gully erosion.

Five hundred and eighty two training sites were randomly generated for areas in the Burdekin where Quickbird or GeoEye image scenes were available on Google Earth™. Sites were buffered by a 300m radius, resulting in a training site area of approximately 28.3ha. Sites were visually inspected on the imagery for the presence or absence of gullies. Of the 582 training sites:

- 104 sites had gullies present
- 433 sites were absent of gullies or gullies were not visible
- 45 sites were removed from the data set as determination of gully presence/absence was uncertain due to vegetation or similarity to other erosion features.

Validation of gully presence or absence was undertaken by field observation. Expert local knowledge was also obtained. Sites that were assigned as having gullies present usually had gullies only over a small part of the site. Assigning the entire

area as a gullied site led to an overestimation of gully presence. To increase the spatial accuracy of observations, a further 456 validation sites at a size of 50m x 50m (0.25ha) were assessed for gully presence or absence. Of these, 12 sites had gullies present and 444 sites had gullies absent or not visible.

Using the training data, the presence of gullies was examined against the explanatory variables. Gully presence had greatest association with areas of low FPC (<20%), slopes generally less than 5°, and distance from drainage line less than 400m. Further assumptions were made about presence or absence of gullies based on information provided by local experts and further visual inspection of imagery and field observations. These included:

- basaltic soils of the Burdekin are unlikely to have gullies or where they do occur, they do not pose significant risk to sediment generation from gully
- gullies that occur at areas where human activity is prevalent (mine sites, towns, industrial areas, cropping) are often not related to natural processes and are also less likely to drain into the GBR
- gullies cannot form in water bodies (lakes, reservoirs).

Using the associations with the explanatory variables and applying the abovementioned assumptions, a set of 8 classes were established. These classes capture the range of conditions (i.e. combination of variables) and indicate the relative probability of a gully occurring in a given class (Table 2).¹

The conditions in Table 2 were spatially applied in ArcGIS to create an 8-class map indicating the likely occurrence of a gully. The classes can be interpreted in terms of probability, presented as the range of results obtained from the training and validation sites. For example:

$$P(\text{class } 1,2,3|\text{gully}) = 0.95 \text{ with a } 95\% \text{ CI of } (0.93, 1) \text{ or similar.}$$

OR the probability that a gullied location falls in class 1, 2 or 3 is 93%-100%.

In other words, 93%-100% of all gullies are found in classes 1, 2 or 3. Considering the low probabilities associated with finding gullies in classes 4-8, all areas with these landscape characteristics were classified as very low probability and excluded from further examination. All areas in classes 1, 2, 3 were classified as *gully-sensitive* areas.

Table 2 Relative gully probability classes based on explanatory variables. Class 8 was assigned 'very low' because gullies that occur within this layer are not well explained by the explanatory variables.

Class	Relative gully probability	Explanatory variables				% of total gullies (training)	% of total gullies (validation)	% of total area
		Distance from drainage line (m)	FPC (%)	Slope (°)	Basalt			
1	Very high	0-300	<20	<10	No	69%	75%	40.2%
2	High	300-400	<20	<5	No	18%	17%	5.2%
3	Medium	400-600	<20	<5	No	6%	8%	7.6%
4	Low	600+	<20	<5	No	7%	0%	22.0%
5	Very low	600+	>20	>5	Yes	~0%	0%	22.7%
6	Very low	Water bodies				~0%	0%	0.8%
7	Very low	Cropping				~0%	0%	1.2%
8	Very low	Towns, mines, industry				~0%	0%	0.2%

2.1.2.2 Manual gully extent mapping

To develop gully maps, 50 randomly selected 5x5km squares were selected, along with several other areas where high-resolution imagery was available. Mapping targeted only those areas with low or higher gully probability (i.e. classes 1-3 in

Table 2). Within the 50 sites, gullied and non-gullied areas were manually digitized on Google Earth using the polygon tool and then imported into ArcGIS, smoothed and cleaned.

2.1.2.3 Developing a predictive model of gullies

The gully mapping from Step 2 was used to develop a predictive model of gully presence within the *gully sensitive* areas identified from Step 1.

A set of biophysical explanatory variable products were generated using SAGA software (Table 3). All products were based on the Shuttle Radar Topography Mission one second Digital Elevation Model (SRTM 1" DEM), which is available at ~30m spatial resolution. The variables were chosen based on expert knowledge of a likely relationship to gully presence. The resolution of the SRTM 1" DEM was considered the lowest resolution that could be used given the size of gullies and very low resolution of previous models for the Burdekin.

The usefulness of these products as explanatory variables for gully occurrence was assessed by comparing them with the gully maps produced in Step 2. The Area Under the Curve (AUC) for a plot of cumulative mapped gullies against cumulative area from predicted high to low probability was used to quantify the predictive ability of explanatory variables. The AUC provides an effective measure of how much of the response variable's distribution (in this case gully presence) is explained by a particular explanatory variable. Most products offered a higher than random, yet still modest gully prediction ability (AUC 60-70%, compared with AUC of 50% for a random prediction) (Table 3). A further test using a multivariate logistic regression model combining several layers did not show significantly improved results. The one variable which showed high correlation with gully occurrence was the *elevation above drainage line*, which had an AUC of 80% (Figure 3). The final predictive model was therefore based on probability values from elevation above drainage line in areas that were initially classified as *gully-sensitive* areas.

Table 3 Explanatory variables used for development of the predictive model. Variables were generated in SAGA software and were based on the SRTM 1" DEM.

Variable	Spatial resolution
Aspect	30m
Flow accumulation	30m
Slope length	30m
Curvature	30m
Catchment area	30m

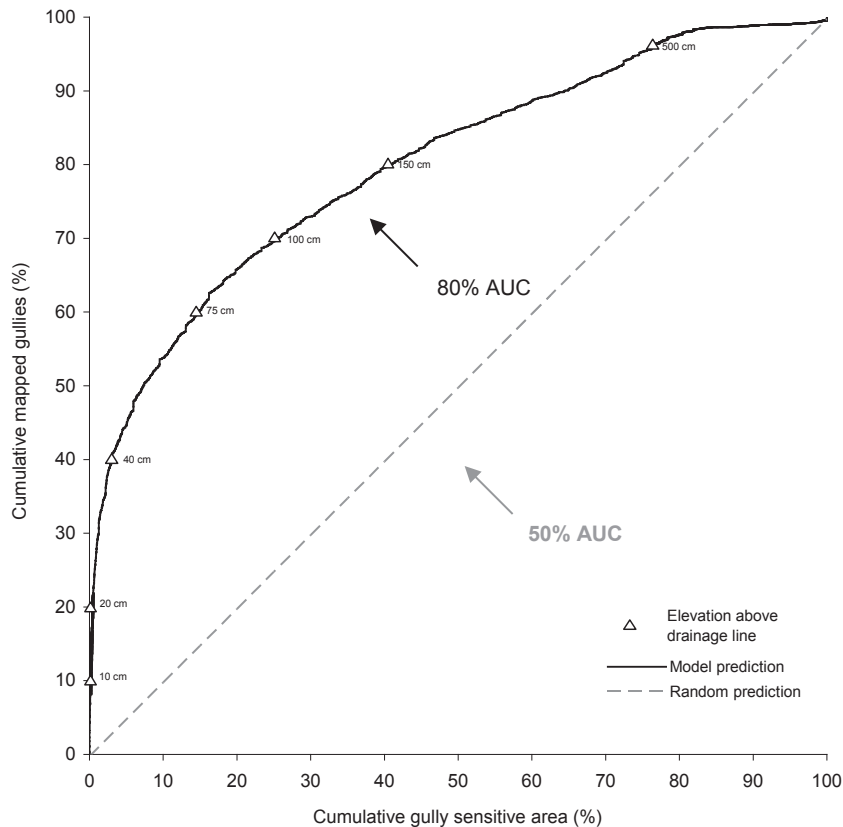


Figure 3 Area Under Curve (AUC) represents the relationship between gully occurrence and elevation above drainage line in areas defined as gully sensitive. The triangles indicate elevation above drainage line. A random prediction (shown on the graph as dashed line) is expected to be linear throughout the examined area and therefore would have an AUC of 50%. The model (solid line) shows an AUC of 80%. This means that elevation above drainage line can explain the distribution of most mapped gullies and can improve prediction ability compared with the other variables examined. For example, the model locates 60% of the (mapped) gullies within the first 15% of the gully sensitive area closest to drainage line (<75cm).

2.1.2.4 Production of the 5km Gully Presence Map

A broad-scale gully presence map was developed using a range of mapping techniques and extrapolation rules. This was intended to be a comprehensive map of the Burdekin, incorporating information from Steps 1-3. It was also intended to address some of the uncertainty in the predictive map derived at Step 3.

To develop the 5km Gully Presence Map, the Burdekin catchment was divided into 5521 cells of 5x5km. Each cell was assigned with one of seven gully presence values (Table 4). The gully presence values were determined by a number of methods, based on a range of information sources. Each method was ranked by its level of confidence, according to the source of information available to map gully presence (Table 5; Figure 4).

Table 4 Gully presence values.

Gully presence value	Description
Very high	Severe gullying. Extensive systems and individual gullies within most of 5x5km cell
High	Numerous gullies at various sizes. Easily observed over large areas of the 5x5km cell
Med-high	Frequent individual gullies. A few systems
Medium	Frequent gullies. Mostly individual (i.e. no systems)
Low-medium	Several (3-10) small to medium sized gullies
Low	A few (1-3) small, scattered gullies
Very low	No apparent gullies

Table 5 Information sources and methods used to interpret them, ranked in order of confidence for mapping gully presence.

Information source	Confidence level	Gully mapping method	Number of cells mapped	% of total area
High resolution (<1m) imagery (Quickbird, GeoEye, LiDAR, aerial photography)	Very high	Visual inspection of imagery for extent of gully presence per cell.	1595	28.9
Medium resolution (<10m) imagery (SPOT pan-sharpened)	High	Visual inspection of imagery for extent of gully presence per cell. Adjacent high-resolution imagery assisted interpretation.	579	10.5
Extent of no-gully area in a cell	Medium	The extent of no-gully area (derived from Step 1) in a 5x5km cell was plotted against the observed value. Observed cells with >70% of no-gully area had low or very low observed gully presence.	1120	20.3
Association with IBRA sub-region (Interim Biogeographic Regionalisation for Australia)	Medium	Gully presence per cell was compared with 13 sub-regions in the Burdekin (Figure 4). Sub-regions which had over 95% of observed cells within very low to low-medium gully presence were assigned a low gully presence value.	922	16.7
Predictive map (Step 3)	Medium confidence if prediction is low. Low confidence if prediction is high.	Gully presence value assigned to cell based on mean value of predictive model (derived from Step 3).	1399	25.3

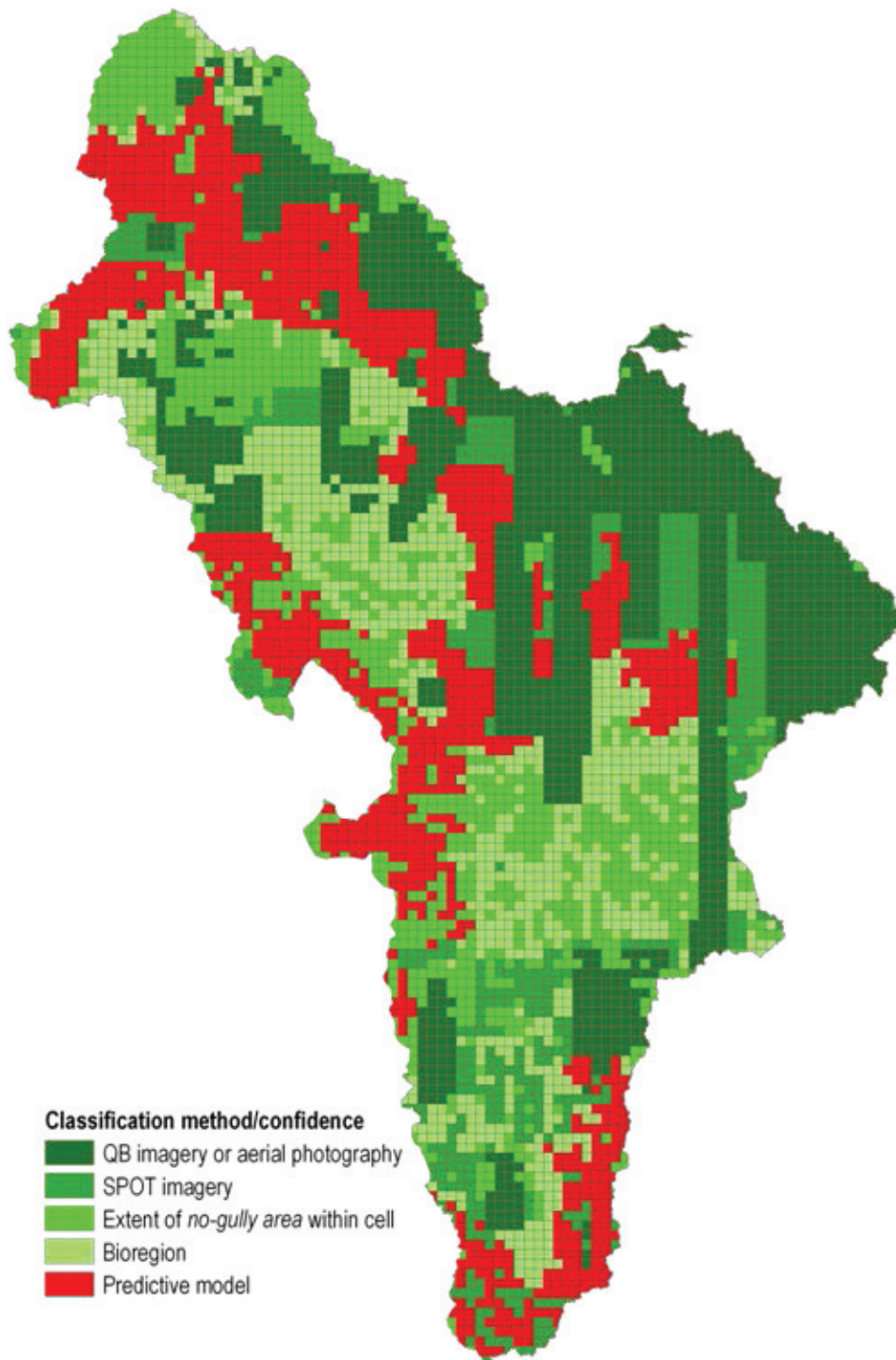


Figure 4 Sources of information used to develop the gully map. Darker greens indicate information sources with the highest confidence. The predictive model had the lowest confidence and was therefore used only where other sources were not able to provide sufficient information. Note: QB imagery refers to Quickbird satellite imagery (resolution <1m).

2.1.2.5 Converting gully presence to density

Parameterisation for gully erosion in the Paddock to Reef catchment water quality model, Source, requires that gully information be represented as either a linear density or area-based density per square kilometre. To meet this requirement the 5km gully presence map was converted to a density map expressed as a percentage of a 5km grid cell that was gullied.

Gully density was calculated by examining the extent of the mapped gullied areas (see section 2.1.2.2) against the semi quantitative gully presence value which was assigned based on visual observation described in section 2.1.2.4 above. While the first was performed only on selected areas in the Burdekin, the second was derived for the entire catchment. Since these two methods are independent of each other, a proved relationship between them in parts of the area would allow us to interpolate the results into unmapped areas. The following is a short description of the two methods, and the approach taken to combine them to produce a gully density value for each 5km x 5km square in the Burdekin.

- i. *Gully mapping*: Presence and absence of gullies was mapped in 330 squares (5km x 5km) where high-resolution imagery was available. Gullied and non-gullied areas were manually digitized on Google Earth using the polygon tool and then imported into ArcGIS, smoothed and cleaned. The final product included three classes: Gully, No gully, or area classified as not likely to have gullies by a previous model. The latter two were combined into one class. For each square, the percentage of gullied area was then calculated by dividing the gullied area (in km²) by the total area of the square (25km²).
- ii. *Gully observations*: One of seven semi-quantitative values was assigned to each 5km x 5km square for the whole of the Burdekin after visual observation on high resolution imagery (Table 6).
- iii. *Examining the relationship between the outputs of the methods*: The observation values were independent of the mapping, and therefore the two features could be used to validate each other – assuming that the higher the % of mapped gullies in a square the higher would be its observed value and vice versa. If this relationship could be established, it would be possible to determine the gully density for all other unmapped squares. The following graph and table show that there is clear relationship between the mapping and the observations. However, the variation in mapping was minimal between some adjacent observed values (e.g. Very high and High Very low and Low). To simplify the classification and provide better differentiation between the classes several values were grouped (Table 7, Figure 5).

Table 6 Values assigned to 5km grid cells based on observed gulying.

Gully presence	Description
Very high	Severe gulying. Extensive systems and individual gullies within most of 25km ² square.
High	Numerous gullies at various sizes. Easily observed over large areas of the 25km ² square.
Medium-high	Frequent individual gullies. A few systems.
Medium	Frequent gullies. Mostly individual (i.e. no systems).
Low-medium	Several (3-10) small to medium sized gullies.
Low	A few (1-3) small, scattered gullies.
Very low	No apparent gullies.

Table 7 Simplifying gully density classes based on mean density from visual observations and high resolution mapping.

Old Classes	Mean*	SD [^]	New classes	Mean*	SD [^]
Very high	10.70%	5.80%	High	11.20%	4.50%
High	11.50%	4.70%			
Medium-high	7.10%	3.70%	Medium	5.80%	3.30%
Medium	5.10%	3.00%			
Low-medium	1.20%	1.10%	Low	1.30%	1.10%
Low	0.20%	0.50%	Very low	0.00%	0.00%
Very low	0.00%	0.00%			

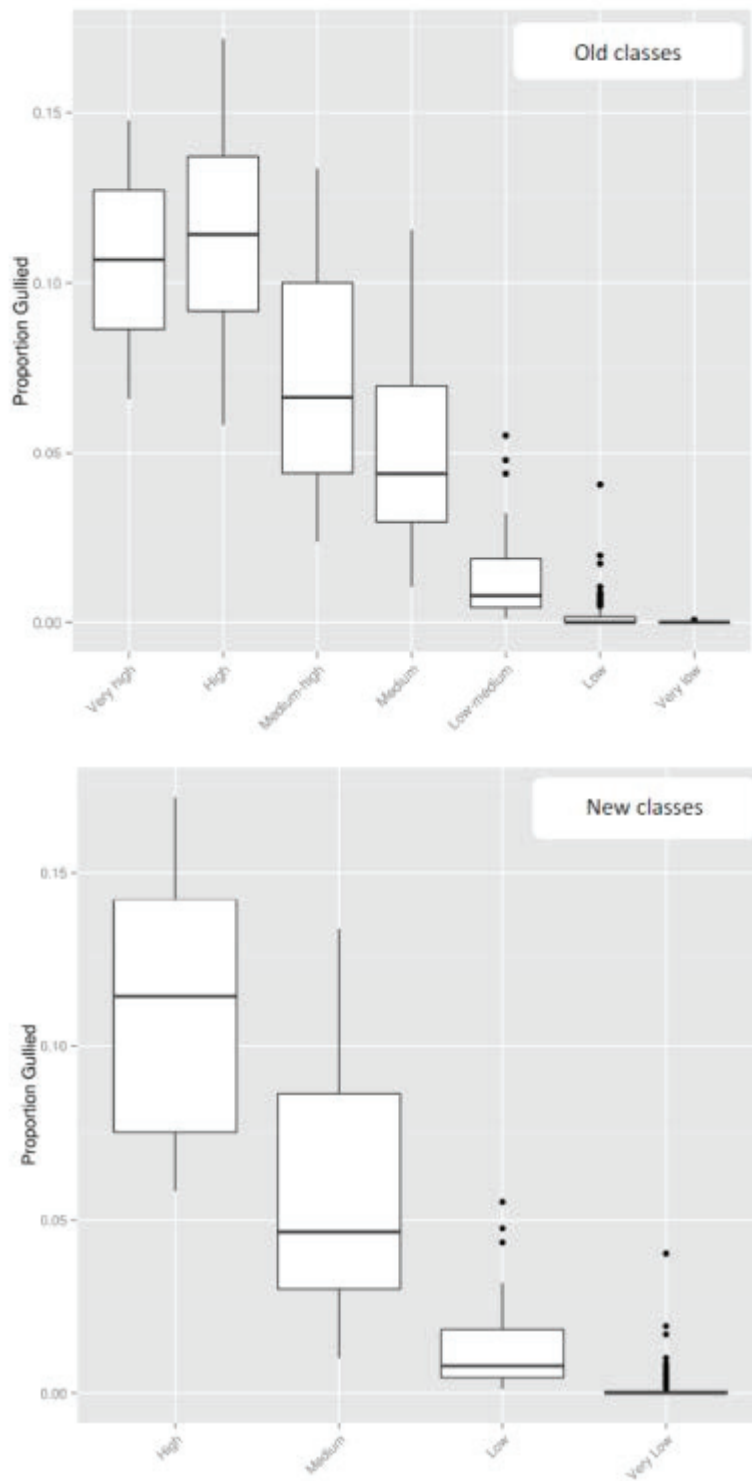


Figure 5 Deriving gully density classes based on proportion gullied as determined by high resolution mapping and visual observation of gully prevalence. The graph at top shows the overlap between some classes and provided the basis for simplification of the classification from seven to four classes.

2.1.3 1km Gully Presence Map

Cells classified as 'High' and 'Very high' in the 5km Gully Presence Map were refined to a 1x1km scale in the 1km Gully Presence Map. The 129 cells classified 'Very High' and 'High' were divided into 3,224 1km cells and visually assessed for gully presence, using high resolution Google Earth and Spot imagery.

To determine the extent of gullying, each 1km cell was overlaid by a grid of 100 cells, each measuring 100m x 100m. The number of 100m cells that contained any form of gullying was manually counted, and that count was applied to the corresponding 1km cell (Figure 6). A set of guiding rules and principles were followed when counting grid cells to maintain consistency across areas (DSITIA and DNRM, 2014). The 'gully count' values provide a relative percentage of gullying in comparison to other mapped cells. Figure 7 is an example of the improvement in mapping resolution between the 5km product and the 1km product.

The 1km Gully Presence Map has been mapped solely through visual interpretation, using a combination of Spot 2009 and 2012 imagery and high resolution Google Earth imagery (Quickbird and GeoEye) available over multiple recent dates. Topographic drainage line and elevation contour data sets were also used to guide decisions, as described in DSITIA and DNRM (2014).

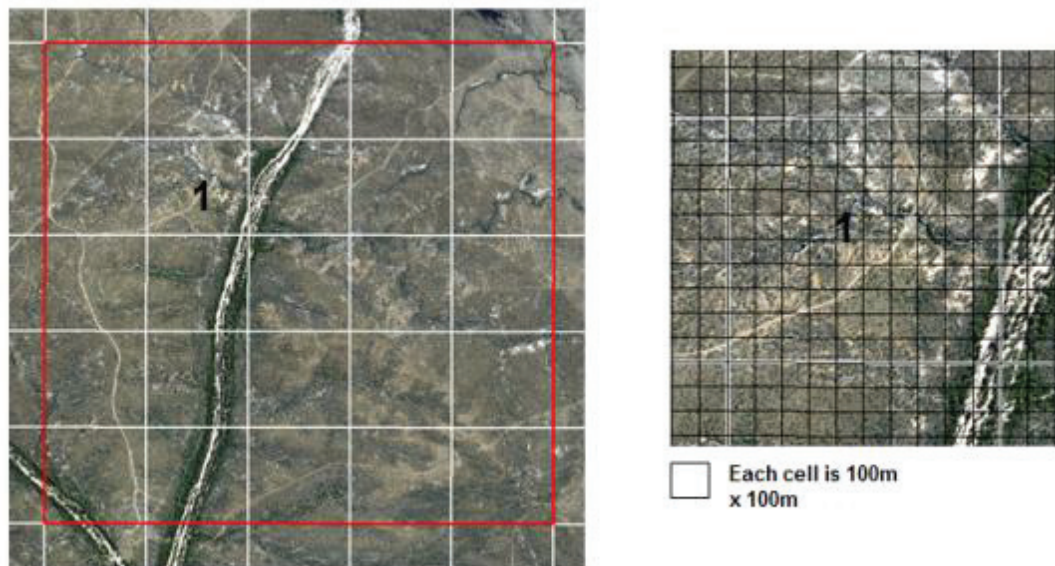


Figure 6 Gully mapping at different resolutions. The 5km cell (red lines) extracted from the 5km Gully Presence Map is shown in the image on the left. The 1km cells (white lines) from the 1km Gully Presence Map are also shown. The '1' indicates the presence of gullying within the 1km grid cell. The image on the right is a zoom of the grid cell labelled '1' and shows the 100m grid cells which are used to help interpret gully presence as a percentage within the 1km grid cell.

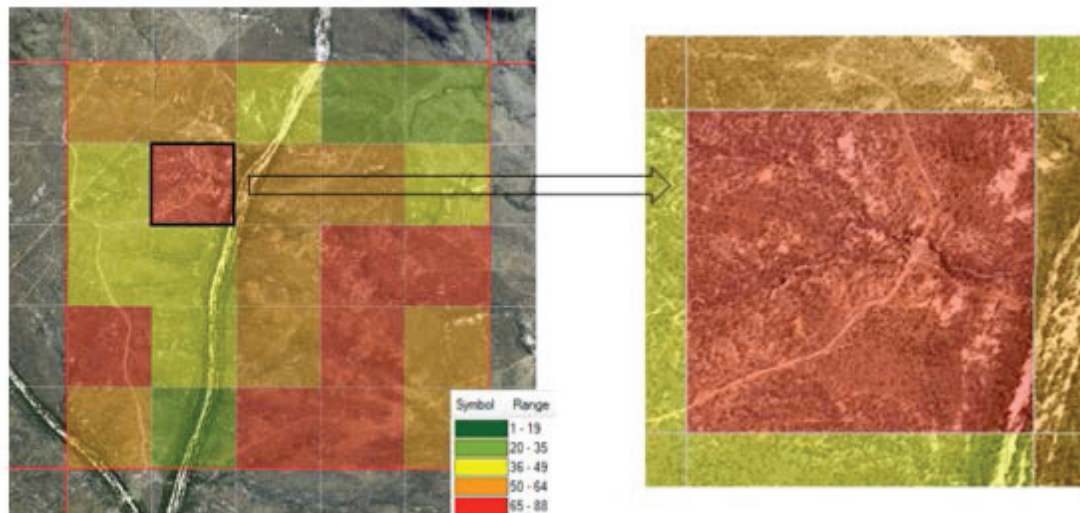


Figure 7 This diagram illustrates how the 1km Gully Presence Map provides improved resolution for the gully presence mapping than the 5km Gully Presence Map. The red square outline is the 5km Gully Presence Map and the smaller coloured squares are the 1km Gully Presence Map symbolised according to 'gully count' values. The image on the right shows the presence of gullies within the 1km grid cell. This example was interpreted as having >65% of gullying present within the 1km x 1km area.

Where time and resources permitted, some cells classified as 'Medium High', 'Medium', 'Low Medium', 'Low' and 'Very Low' in the 5km Gully Presence Map were interpreted and mapped in the 1km Gully Presence Map. Table 8 provides an overview of the 1km Gully Presence Map relative to the 5km Gully Presence Map. At the time of writing, 7,603 1km cells have been analysed as part of this project. Further mapping is ongoing through arrangements with Department of Natural Resources and Mines (DNRM). The mapping guidelines (DSITIA and DNRM, 2014) continue to be refined as part of this process.

Table 8 Proportion of 5km Gully Presence Map that has been mapped at 1km resolution

5km Gully Presence Map Classification	Total number 1km cells within 5km cells	Number of mapped 1km cells	Percentage of 5km cells mapped at 1km resolution
Very high	600	600	100%
High	2,700	2,649	98.1%
Medium high	6,677	774	11.6%
Medium	15,591	88	0.6%
Low medium	20,463	86	0.4%
Low	52,111	3,285	6.3%
Very low	676	121	17.9%

2.2 Mapping gully extent, volume and change using airborne LiDAR

2.2.1 LiDAR data and pre-processing

A multi-date LiDAR dataset was captured for 15 gullied sites in the Burdekin and 4 sites in the Fitzroy catchment (Figure 8). The Burdekin sites were captured on two dates in 2010 and 2013 using a similar capture configuration between dates. The Fitzroy sites were captured on 3 dates in 2007, 2010 and 2013 with the 2007 capture using a different sensor and capture configuration. A fourth date was captured for the Fitzroy sites in 2008 however this data set was not used in the analysis due to poor data calibration. A detailed list of the airborne survey parameters are provided in Table 9.

To ensure the supplied data matched required specifications and to provide confidence that detected change corresponded to real events, a series of data pre-processing checks were undertaken to assess the data quality. This included checking the spatial extents, pulse densities, horizontal and vertical accuracies, and overlap of flight-runs. Of the 19 sites captured in 2013, five did not meet the RSC's initial quality assessment (QA). These sites were recaptured in April 2014, however, they once again did not pass the RSC's QA and two have been excluded from reporting here due to relative horizontal error exceeding 0.5m. These sites are highlighted on Figure 8 and will be processed when the data is resupplied.

For the 2010 and 2013 captures, the sensors were configured to sample the gully environment with an average pulse density of 4.2 m² (each pulse was able to record up to 5 returns) and an overlap of 50% between flight runs to minimise the impact of occlusion from variable terrain and vegetation (Figure 9); an average of 8 pulses/m². Digital orthophotos (15cm resolution) were acquired coincident with the LiDAR data in 2010 and 2013.

DEM surfaces were interpolated for each of the sites using the natural neighbour algorithm (Sibson, 1981) at a spatial resolution of 50cm using the LiDAR returns classified as ground. No hydrological conditioning of the DEM was performed. Water bodies (e.g. dams, rivers) which recorded no LiDAR returns were set to a null value and excluded from the analysis. A maximum height layer (i.e. maximum return height relative to the ground surface) was produced using all the LiDAR returns.

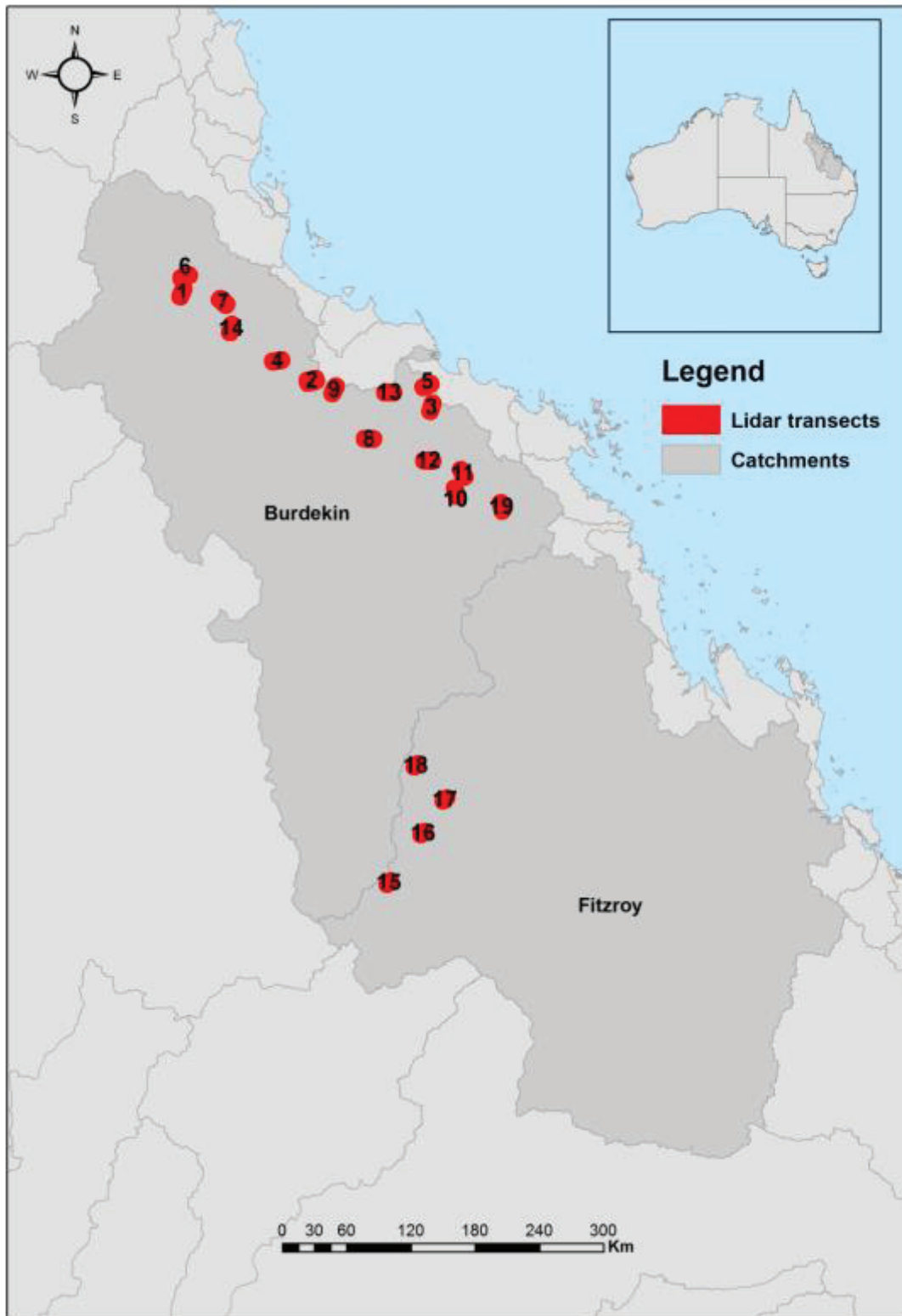


Figure 8 Location of LiDAR transects in the Burdekin and Fitzroy catchments. Site numbers correspond with site names in Table 10. Sites 1 (Blue Range) and 8 (Mount Ravenswood) were excluded from reporting due to processing errors

Table 9 LiDAR capture specifications.

Metadata Element	2007	2010	2013
Company Name	AAMHatch	Terranean	RPS Mapping
Acquisition Start Date	3rd February 2007	May 2010	03-08-2013
Acquisition End Date	6th February 2007	June 2010	08-08-2013
LiDAR Sensor	Optech 3100	TopoSys Harrier 56 (Riegl 560)	TopoSys Harrier 68i (Riegl 680)
Senor Wavelength (nm)	1064	1550	1550
Platform	Fixed wing	Fixed wing	Fixed wing
Flying Height(AGL)	~550	550m (+/-50m)	480m(+/-50m)
INS/IMU Used	N/A	Applanix POS/AV 410	Applanix POS/AV 410
Swath Width	~250 m	456m	550 m - 580 m
Swath Overlap	N/A	50%	50%
Horizontal Datum	GDA 94	GDA 94	GDA 94
Vertical Datum	AusGeoid98	AusGeoid98	AHD (Ausgeoid09)
Map Projection	MGA zone 55	MGA Zone 55	MGA Zone 55
Spatial Accuracy- Horizontal	N/A	+/- 0.45m RMSE	+/- 0.5m RMSE
Spatial Accuracy- Vertical	N/A	+/- 0.15m RMSE (1s)	+/- 0.1m RMSE (1s)
Average Point Spacing	N/A	8.4 points / m ²	8 points / m ²
Laser Return Types	Multiple echo	Multiple echo	Multiple echo
Data Thinning	N/A	No thinning applied	No thinning applied
Laser Footprint Size	0.16 m	0.28 m	0.24m
Orthophotography	No	Yes	Yes*

Table 10 Quality assurance checks for LiDAR captures.

Site No.	Site	Region	Year	QA issue
1	Blue Range	Burdekin	2010, 2013	Horizontal errors
2	Fanning	Burdekin	2010, 2013	Pass
3	Fish Creek	Burdekin	2010, 2013	Pass
4	Keelbottom Creek	Burdekin	2010, 2013	Pass
5	Kirknie Creek	Burdekin	2010, 2013	Pass
6	Lyll Creek	Burdekin	2010, 2013	Pass
7	Marshes Creek	Burdekin	2010, 2013	Pass
8	Mount Ravenswood	Burdekin	2010, 2013	Horizontal errors
9	Oaky Creek	Burdekin	2010, 2013	Pass
10	Parrot Creek	Burdekin	2010, 2013	Pass
11	Pelican Creek	Burdekin	2010, 2013	Pass
12	Red Hill Creek	Burdekin	2010, 2013	Pass
13	Spring Creek	Burdekin	2010, 2013	Pass
14	Starbright	Burdekin	2010, 2013	Pass
15	T1-T2	Fitzroy	2007, 2010	Pass
16	T3-T4	Fitzroy	2007, 2010, 2013	Pass
17	T5-T6	Fitzroy	2007, 2010, 2013	Pass
18	T7-T8	Fitzroy	2007, 2010, 2013	Pass
19	Turrawulla	Burdekin	2010, 2013	Pass

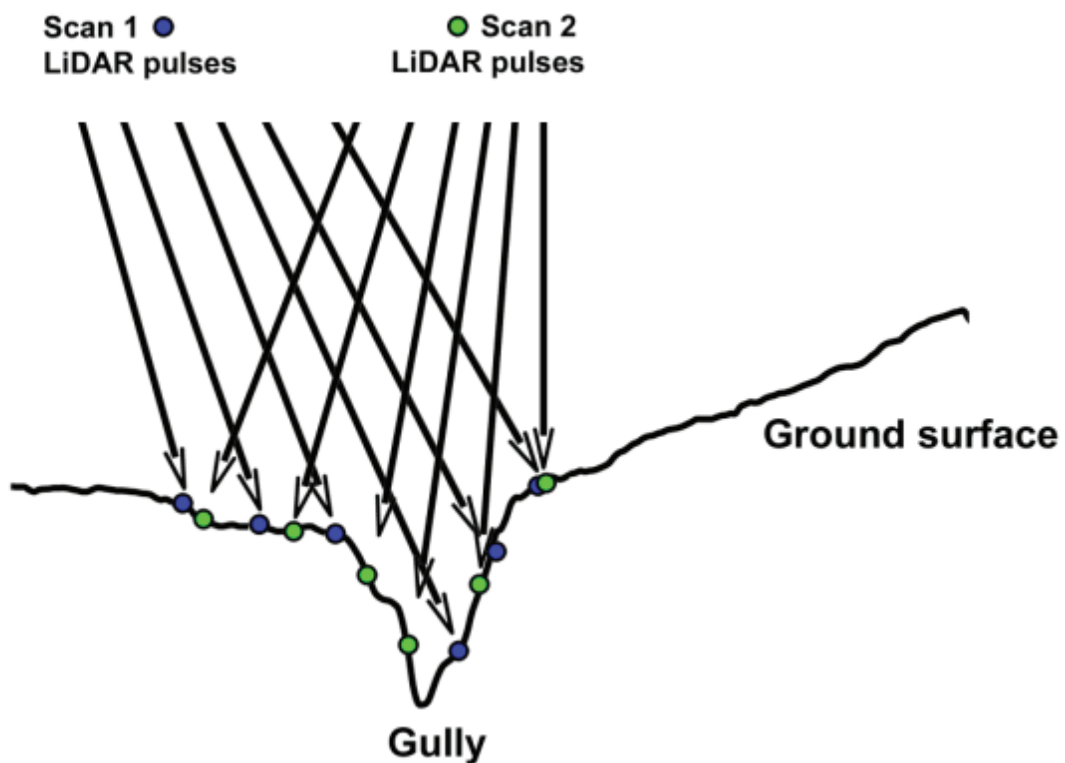


Figure 9 Example of 50% LiDAR scan overlap. The two opposing scan orientations limit occlusion by vegetation and overhangs and increase the detection of gully walls.

2.2.2 Classifying gully extents

LiDAR data provides very accurate data for studying elevation differences in the landscape. However, the morphology of gullied environments remains complex and highly variable making the classification of LiDAR ground returns and gully extents difficult. A depression in the landscape, vegetation returns which have been misclassified as ground, or a natural component of a stream network, for example, may be difficult to separate from a gully based on DEM morphology alone. These features can lead to commission errors ('false gullies') in any classification. To reduce the impact of these errors, gully areas from each transect were manually identified, subset and analysed.

Mapping the location of gullies in the DEM first involved a moving circular window to be passed over the DEM to calculate the 'average elevation'. The circle size (diameter) should approximate the gully width and may involve some optimisation for different landscapes. Circle sizes of 3m, 5m and 8m diameter were tested and outputs inspected with the DEM and very high resolution orthophotos. The 5m circle was deemed most appropriate representation of the gullies observed. This average DEM value was then differenced to the centre pixel elevation value to produce a layer showing the 'difference from mean elevation' (DFME). This follows a method described by Evans and Lindsay (2010). A seeded 'region grow' operation was also applied to the DFME layer with spatially contiguous clumps of five or more pixels exceeding a threshold of 20cm used to seed a region grow filter with a fixed lower limit of 2cm. Incorporating a region grow filter was considered necessary to maximise the area of gully mapped whilst limiting commission errors. This approach, which is

based on detecting differences in landscape elevation and morphology, in effect maps depressions in the landscape. The approach may therefore include non-gully depressions. In some areas it may not be a reliable classification of gully extent. To account for this, the maps of gully extent for each transect were manually edited to remove any obvious errors.

Figure 10 shows an example of the areas that have been selected within the Lyall Creek transect, overlaid with the DFME outputs and the 2013 orthophoto.



Figure 10 Sections of gullies were chosen for each transect for gully classification and subsequent change analysis. The subsets used for the Lyall Creek transect are shown with ortho-photography. The image below is a zoom of the north-east corner of the transect.

2.2.3 Quantifying gully depth, volume and change

2.2.3.1 Gully depth

Quantifying gully depths at the pixel scale followed Evans and Lindsay (2010). This included:

- I. removing the LiDAR ground returns that intersect the gully classification;
- II. re-interpolating the non-gully ground return using a natural neighbour interpolator with a pixel resolution of 50cm - basically putting a 'lid' across the top of the gully; and,
- III. differencing this layer with the original DEM

This is schematically represented in Figure 11.

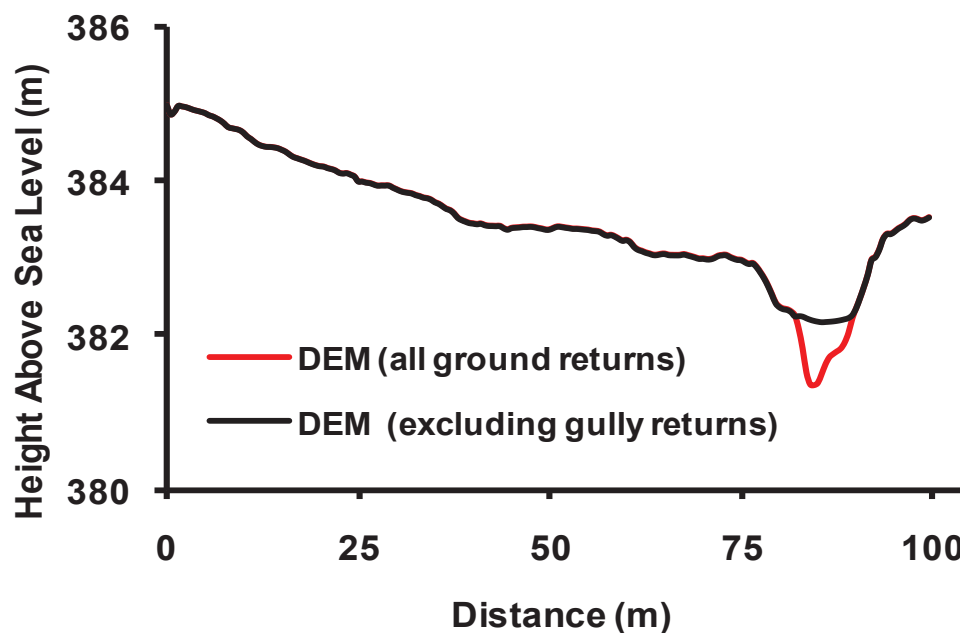


Figure 11 Schematic diagram showing how gully depth was calculated. The gully extent (red line) was removed from LiDAR data and the DEM was re-interpolated across the gullied area to create a continuous surface (black line). Gully depth is the difference between red and black lines across the defined gully extents.

2.2.3.2 Gully volume

Gully volume was calculated by summing the gully depth pixel values (as described above) and converting these values into volumetric units (i.e. cubic metres).

2.2.3.3 Gully change

Gully change can be defined in terms of both lateral expansion/contraction (widening or narrowing) and volumetric erosion/deposition (deepening or shallowing/infilling). This requires at least two dates of gully attribute mapping. To quantify gully change, we compared mapped extents and gully volume estimates between LiDAR dates.

2.2.4 Multi-temporal Terrestrial Laser Scanning of gullies

RSC and University of Queensland, through the JRSRP, have purchased a Terrestrial Laser Scanner (TLS). A TLS is a ground-based LiDAR device that enables relatively rapid, 3-dimensional scanning of surrounding features at high spatial resolutions. An example of an instrument is shown in Figure 12. The data produced can be used to quantify size, extent and volumes of biophysical features such as gullies. When scans are obtained on multiple dates, volumetric changes through time may be quantified and compared in a similar way that airborne LiDAR has been used. Figure 13 shows an example reconstruction of a gully head from Virginia Park in the Burdekin, derived from a number of scans collected from different viewing angles.

Four gully locations in the Burdekin catchment have been scanned twice during this project, in October 2012, and in October/November 2013. These data are yet to be analysed as significant research and development will be required to determine appropriate scanning specifications and to develop algorithms for the quantification of gullies using TLS data.



Figure 12 Example of a Terrestrial Laser Scanning instrument. The instrument shown is a Riegl VZ-400 full waveform instrument (source: www.riegl.com).

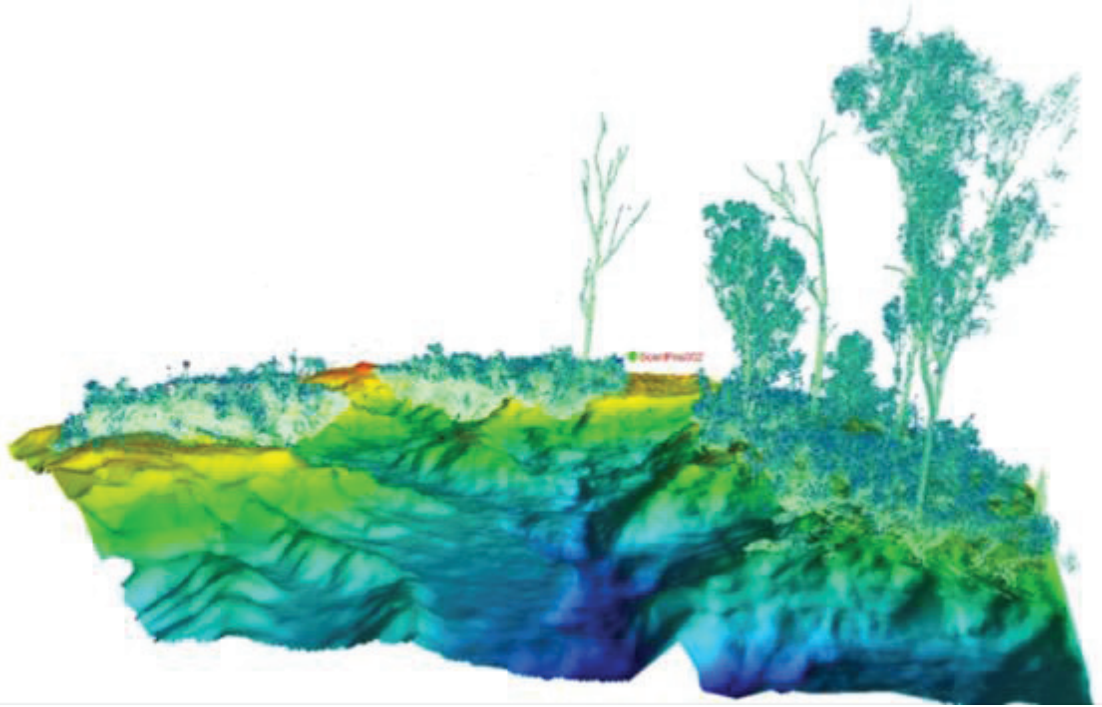


Figure 13 Reconstruction of a DEM for a gully system in the Burdekin (Spyglass Research Station) based on scans obtained using a TLS.

2.3 Gully chronosequence mapping

Gully chronosequence mapping refers to the mapping of long term change in extent of gullies using historical imagery. Over 40 sites were assessed for application of the approach. In total, the change in extent at ten gully locations has been documented through a chronosequence mapping process (Figure 14). The exclusion of the other sites assessed was due to lack of suitability of these sites resulting from issues with imagery or being located in non-dominant land types.

2.3.1 Selection of gully locations for chronosequence mapping

Gully locations were selected to best represent the most prevalent land types as mapped in the *Burdekin Regional Grazing Land Management Land Types* dataset. These land types include Box and napunyah; Goldfields country (red soils); Box country; Narrow leaved ironbark on shallow soils; and Red basalt. This approach ensures that a range of land types were sampled in order to develop an improved understanding of rates of change across different landscapes in the Burdekin. Specifically, the following lithological characteristics were represented:

- Clay, silt, sand, gravel, flood-plain alluvium (Gully 1)
- Lithofeldspathic arenite, mudstone and minor polymictic conglomerate; local melange (Gully 2)
- Grey, medium-grained, hornblende-biotite tonalite, minor diorite (Gully 3)
- Sand and subordinate silt and clay; residual soil and colluvium (Gully 4)

- Locally red-brown mottled, poorly consolidated sand, silt, clay, minor gravel; high-level alluvial deposits, generally dissected, and related to present stream valleys (Gully 5)
- Clay, silt, sand, gravel and soil; colluvial and residual deposits (generally on older land surfaces) (60%) and Biotite gneiss, mica schist, quartzite, leucogneiss, laminated amphibolite and minor marble (40%) (Gully 7)
- Altered aphyric tholeiitic basalt, locally pillowed; minor chert and jasper (Gully 8), and
- Olivine basalt (Gullies 9 and 10).



Figure 14 Gully chronosequence mapping locations in the Burdekin catchment

The soil erodibility profile (as mapped under RWQ Science Project RP63G) of each gully is listed in Table 11. RP63G's Inherent Vulnerability to Erosion ranking system was used to assess any links between the gully erosion rates and the soil erodibility profiles.

Table 11 Erodible soils characteristics of gully chronosequence mapping locations.

Gully	Erosion Vulnerability - Surface Soil	Erosion Vulnerability - Subsoil Dispersibility	Erosion Vulnerability - Combined
1	80% Non-cohesive surface soils, 20% Dispersive surface soils	80 % Non-dispersive subsoils, 20% a Weakly dispersive subsoils	80% Non-cohesive surface soils over non-dispersive subsoils, 20% Weakly dispersive clayey soils
2	40% Non-dispersive surface soils, 60% Dispersive surface soils	100% Non-dispersive subsoils	40% Non-cohesive surface soils over non-dispersive subsoils, 60% Weakly dispersive clayey soils
3	85% Non-cohesive surface soils, 15% Dispersive surface soils	65% Non-dispersive subsoils, 45% Highly dispersive subsoils	50% Non-cohesive surface soils over non-dispersive subsoils, 10% Weakly dispersive clayey soils, 20% Non-cohesive surface soils over highly dispersive subsoils, 20% Dispersive clayey surface soils over highly dispersive subsoils

Gully	Erosion Vulnerability - Surface Soil	Erosion Vulnerability - Subsoil Dispersibility	Erosion Vulnerability - Combined
4	85% Non-cohesive surface soils, 5% Moderately stable surface soils, 10% Dispersive surface soils	100% Non-dispersive subsoils	85 % Non-cohesive surface soils over non-dispersive subsoils, 5% Moderately stable surface soils over non-dispersive subsoils, 10 % Weakly dispersive clayey soils
5	100% Dispersive surface soils	90% Non-dispersive subsoils, 10% Moderately dispersive subsoil	90% Weakly dispersive clayey soils, 10% Dispersive clayey soils
6	40% Dispersive surface soils, 30% Non-cohesive surface soils, 30% Moderately stable surface soils	100% Non-dispersive subsoils	40% Water Supply Division, 30% Non-cohesive surface soils over non-dispersive subsoils, 30 % Moderately stable surface soils over non-dispersive subsoils
7	90% Non-cohesive surface soils, 10 % Moderately stable surface soils	100% Non-dispersive subsoils	90% Non-cohesive surface soils over non-dispersive subsoils, 10% Moderately stable surface soils over non-dispersive subsoils
8	60% Dispersive surface soils, 40% Non-cohesive surface soils	100% Non-dispersive subsoils	60% Weakly dispersive clayey soils, 40% Non-cohesive surface soils over non-dispersive subsoils
9	100% Non-cohesive surface soils	100% Non-dispersive subsoils	100% Non-cohesive surface soils over non-dispersive subsoils
10	75% Moderately stable surface soils, 25% Non-cohesive surface soils	100% Moderately stable surface soils	75% Moderately stable surface soils over non-dispersive subsoils, 25% Non-cohesive surface soils over non-dispersive subsoils

2.3.2 Aerial photography and satellite imagery

Aerial photography and satellite imagery were obtained at approximately 10 year intervals from around the 1940s onwards, with each gully averaging 6 observations (Table 12). These images span from the 1940s (2 sites), 1950s (3 sites) and 1960s (5 sites) through to 2012. Older aerial photography was captured in black and white and identification of gullies was often difficult. All 2009 and 2012 images are high resolution Spot satellite images (~2.5 m/pixel), and all other images are a combination of colour and black and white aerial photography with varying resolutions. When choosing imagery, all of the photos available were obtained and checked and the best quality images were selected and used in the analysis.

Digital copies of the aerial imagery were provided by SmartMap Information Services provided by the Department of Natural Resources and Mines. Each aerial photograph was ortho-rectified using high resolution 2009 Spot imagery. This involved selecting control points using standard photogrammetric methods.

Approximately 25 to 35 control points (predominantly located around the gully site) were manually selected to geo-reference each image. Due to the issues of accurate geo-referencing and the difficulty of interpreting the some of the aerial photography, the study was limited to the ten sites reported on here.

Table 12 Imagery years and image type (BW: black and white, C: colour, S: satellite), soil types and gully shapes.

Gully	Aerial and satellite image capture date								Land type	Gully morphology
	1 st	2 nd	3 rd	4 th	5 th	6 th	7 th	8 th		
1	1961 BW	1979 BW	1991 BW	2002 C	2009 S	2012 S	NA	NA	Box and napunyah	Linear
2	1945 BW	1964 BW	1970 BW	1979 BW	1991 BW	2000 C	2009 S	2012 S	Box and napunyah	Dendritic
3	1962 BW	1980 BW	1999 C	2009 S	2012 S	NA	NA	NA	Goldfields country (red soils)	Dendritic
4	1945 BW	1962 BW	1976 BW	1999 C	2009 S	2012 S	NA	NA	Goldfields country	Linear
5	1961 BW	1980 BW	1991 BW	1998 C	2009 S	2012 S	NA	NA	Box country	Linear

Gully	Aerial and satellite image capture data								Land type	Gully morphology
	1st	2nd	3rd	4th	5th	6th	7th	8th		
6	1959 BW	1972 BW	1985 BW	2009 S	2012 S	NA	NA	NA	Box country	Linear
7	1952 BW	1973 BW	1991 BW	2009 S	2012 S	NA	NA	NA	Narrow Leaved Ironbark on Shallower Soils	Dendritic
8	1951 BW	1980 BW	1991 BW	2002 C	2009 S	NA	NA	NA	Narrow Leaved Ironbark on Shallower Soils	Linear
9	1964 BW	1978 BW	1991 BW	2002 C	2009 S	2012 S	NA	NA	Red basalt	Linear
10	1964 BW	1978 BW	1991 BW	2002 C	2009 S	2012 S	NA	NA	Red basalt	Linear

2.3.3 Identifying gully change

A digital grid of 30m x 30m grid cells was created and overlaid onto each of the ten gully sites (Figure 15). Beginning with the earliest available image date, the number of cells that showed gulying was counted and the area (in m²) calculated. This follows the same approach for the gully presence mapping. For example, if a gully covered 10 cells, the size of that gully would be calculated as 9,000 m². Gulying needed to extend to at least 50% of a grid cell before the cell was included in the count. This rule made counts more conservative and, to some extent, compensated for any image warping or minor misregistrations.

The next image, in chronological order, was then analysed and the gully extent again counted, independent of the count in the earlier image. It is important to note that images were not compared to each other when cells were being counted. However, where small sections of a gully were difficult to interpret due to poor image quality, other images were observed for guidance only. Figure 16 shows the change in the number of cells selected over three separate dates. All results were then tabulated for analysis.

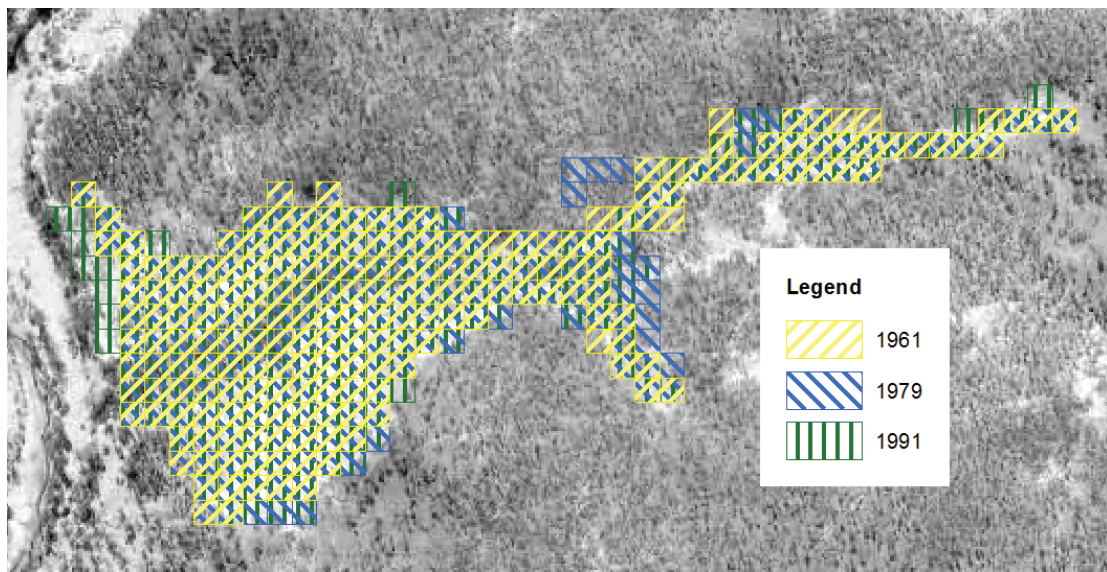
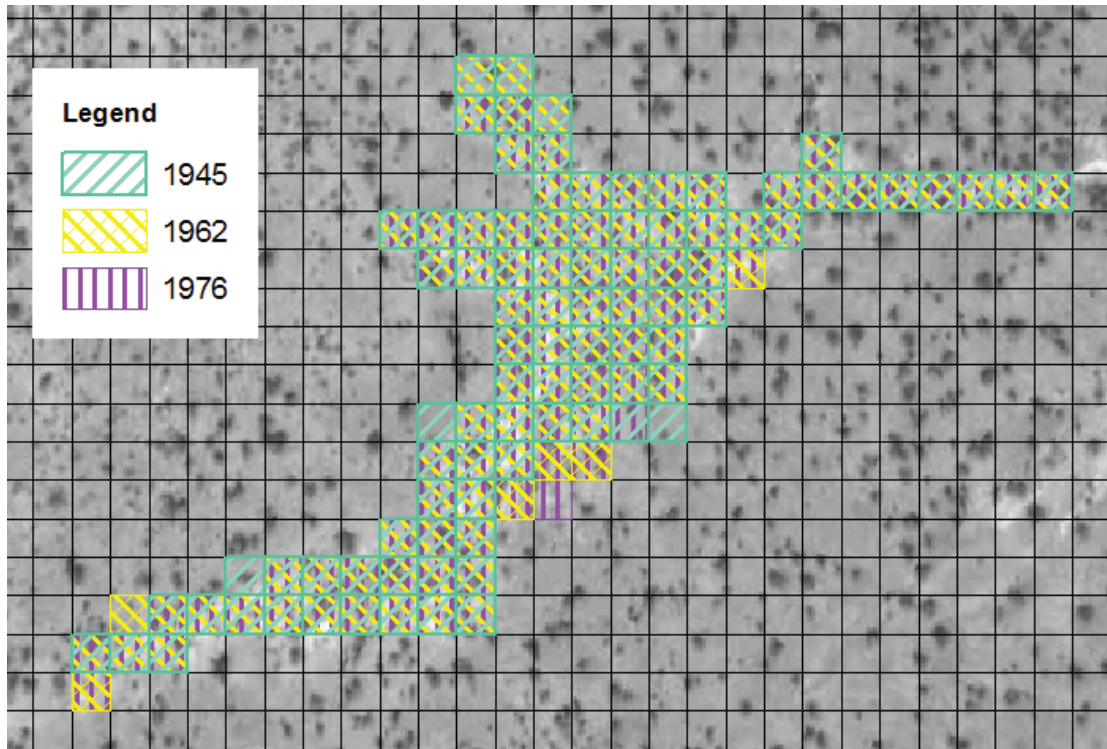


Figure 16 Example of gullied cells selected over three different dates with the earliest available date shown (Gully 4 and Gully 1)..

3 Results

3.1 Gully locations in the Burdekin

3.1.1 'No Gully' location map

Approximately 47% of the total area of the Burdekin was mapped as highly unlikely to have gullies or as having no significant risk of gully formation (Figure 17). These areas were mainly in basalt, with steep slopes and relatively high FPC, and generally large distance from drainage lines.

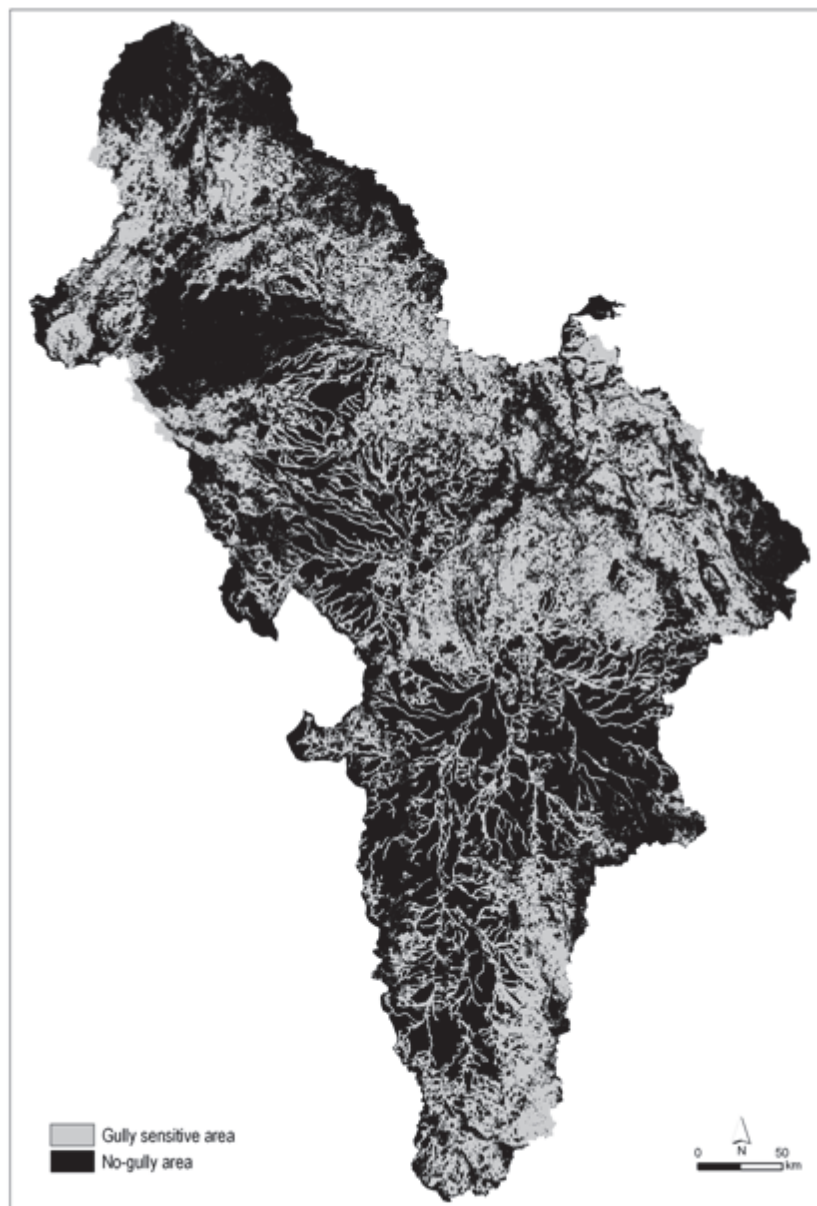


Figure 17 'No-gully' areas and 'gully sensitive areas'

3.1.2 Manual gully extent mapping

The gully mapping described in section 2.1.2.2 resulted in a total area of approximately 3500km² or 2.7% of the Burdekin catchment being mapped (Figure 18). 5,100 gullied areas were identified and delineated (total area of ~230km²). An example of the mapping is shown in Figure 19. Due to time limitations and difficulties in gully identification and delineation on the imagery, some non-gullied areas may be included in polygons classified as gullies. Those areas usually were around gully edges or areas between adjacent gullies.

Assuming the “no-gully” areas from Step 1 are accurate, results indicate that almost 50% of the Burdekin catchment was mapped or classed as having no gullies. Figure 19 shows a mapped area with high gully occurrence.

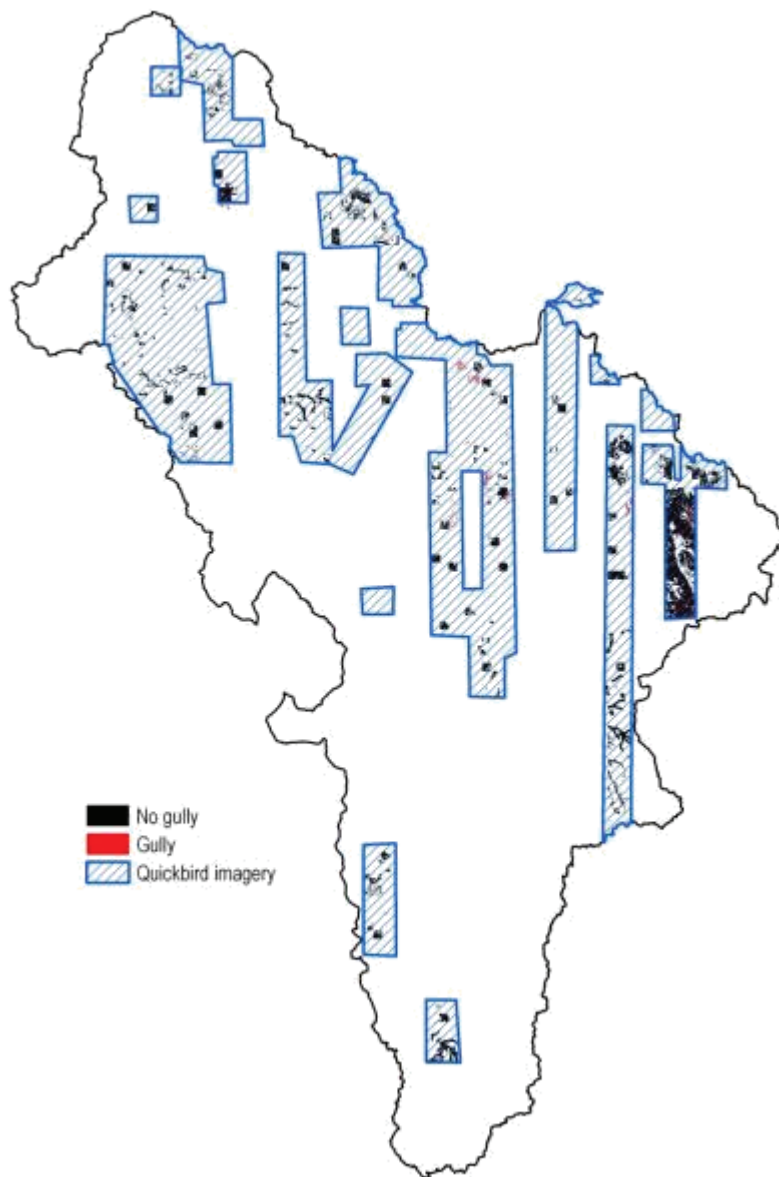


Figure 18 Map of the Burdekin showing where gully mapping has been completed (within available Quickbird imagery)



Figure 19 Example of gully mapping based on Quickbird imagery

3.1.3 Predictive model of gullies

The gully predictive model used 37 classes to quantify the probability of gully occurrence, based on gully mapping, elevation above drainage line, and ‘No Gully’ mapping (Table 13). This model found that 96% of mapped gullies were within 1m of elevation above the drainage line. However, the probability of finding a gully in these areas is only around 4-5%. This suggests that although the model can identify areas where gully probability is higher, the prevalence of gullies in the landscape is still low.

Figure 20 shows a sub-section of the predictive model with the mapped gullies (from Step 2) overlaid. There is generally very good agreement between the gully mapping (which is assumed to be an accurate representation) and the areas of higher probability (4-5%) in the predictive model.

Table 13 Classes used for the predictive model of gullies.

Class	Description	% of total gullies	% of total area	Probability
1	0m above drainage line	61%	7.8%	5%
2	0.1m above drainage line	5%	0.7%	4%

Class	Description	% of total gullies	% of total area	Probability
3	0.2m above drainage line	12%	1.8%	5%
4	0.3m above drainage line	8%	2.3%	5%
5	0.4m above drainage line	3%	2.3%	4%
6	0.5m above drainage line	2%	2.2%	4%
7	0.6m above drainage line	1%	2.0%	4%
8	0.7m above drainage line	1%	1.8%	3%
9	0.8m above drainage line	1%	1.6%	3%
10	0.9m above drainage line	1%	1.5%	3%
11	1m above drainage line	0%	1.3%	3%
12	1.1m above drainage line	0%	1.2%	3%
13	1.2m above drainage line	0%	1.1%	3%
14	1.3m above drainage line	0%	1.0%	2%
15	1.4m above drainage line	0%	1.0%	2%
16	1.5m above drainage line	0%	0.9%	2%
17	1.6m above drainage line	0%	0.9%	2%
18	1.7m above drainage line	0%	0.8%	2%
19	1.8m above drainage line	0%	0.8%	2%

Class	Description	% of total gullies	% of total area	Probability
20	1.9m above drainage line	0%	0.7%	2%
21	2m above drainage line	0%	0.7%	2%
22	2.1m above drainage line	0%	0.7%	2%
23	2.2m above drainage line	0%	0.6%	2%
24	2.3m above drainage line	0%	0.6%	2%
25	2.4m above drainage line	0%	0.6%	2%
26	2.5m above drainage line	1%	0.5%	2%
27	3m above drainage line	1%	2.4%	2%
28	4m above drainage line	1%	3.7%	1%
29	5m above drainage line	1%	2.6%	1%
30	6m above drainage line	0%	1.8%	1%
31	7m above drainage line	0%	1.2%	1%
32	8m above drainage line	0%	0.8%	0%
33	9m above drainage line	0%	0.6%	0%
34	10m above drainage line	0%	0.4%	0%
35	100m above drainage line	0%	1.6%	1%
36	More than 600 m from watercourse, slope<5° and FPC<20%. No basalt.	0%	22.1%	0%

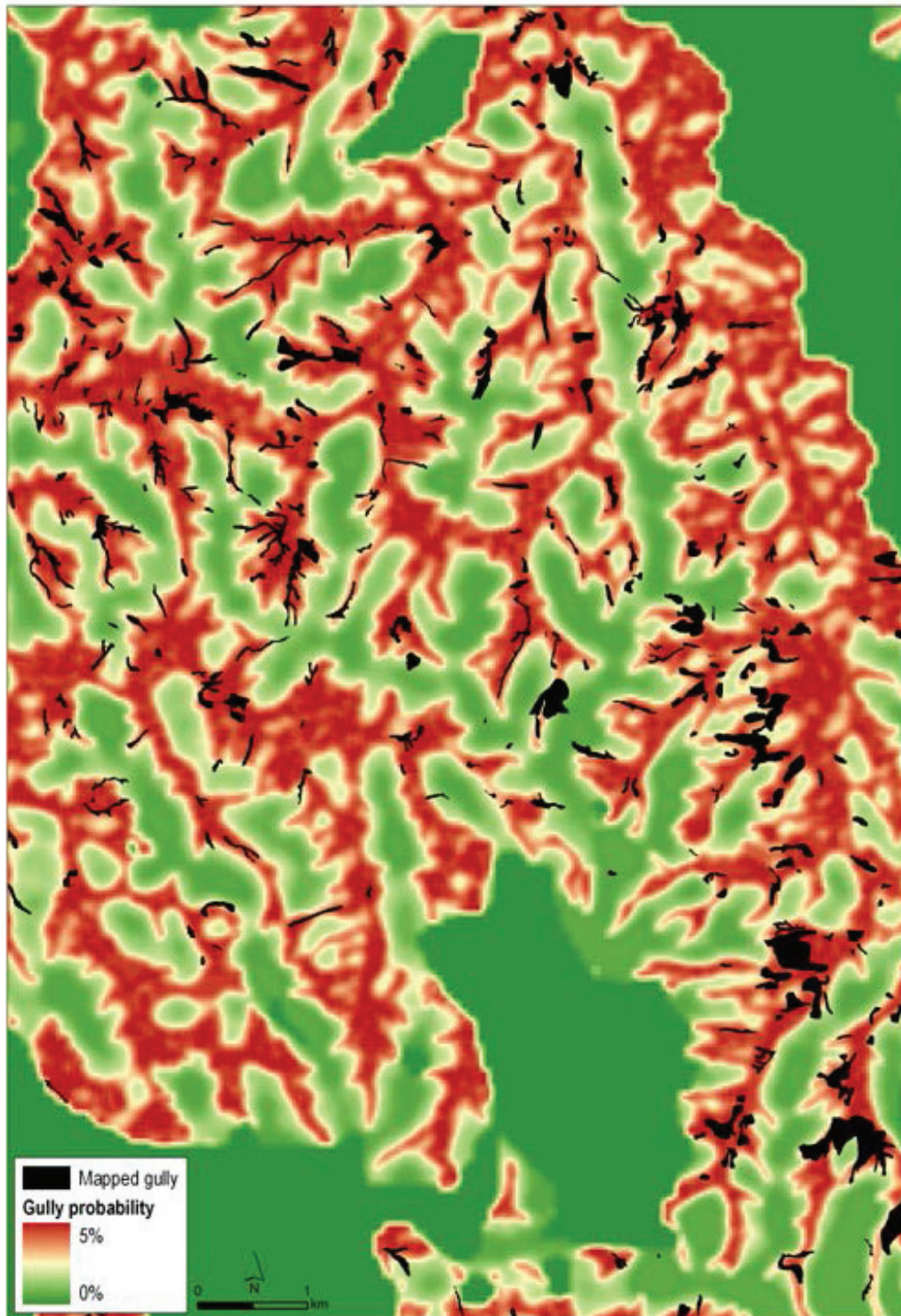


Figure 20 Sub-section of the predictive model with mapped gullies overlaid. There is generally good agreement between mapped gullies and areas of high gully probability in the predictive model.

3.1.4 5km Gully Presence Map

Results from the gully presence map show that of the 5,521 5km x 5km cells in the Burdekin:

- 2,080 or 37.7% of total cells were assigned a gully value according to the visual interpretation of gully presence on the imagery.
- 1,120 or 20.3% of total cells were found to have >70% of 'no-gully' area and were therefore classified as having 'low' gully presence. This assumption was tested by plotting the 2,080 visually interpreted cells against the extent of cell area classified as 'no-gully' area (Figure 21). This showed that cells with more than 70% of 'no-gully' area (403 in total) were almost all classified as 'low' or 'very low' gully presence.
- 922 or 16.7% of total cells were found to be in sub-bioregions where >95% of the cells were interpreted as having 'low' to 'low-medium' gully presence (Table 14). These were assigned a 'low' gully presence in the final map.
- the remaining 1,399 or 25.3% of total cells were mapped based on the value assigned by the predictive model.

The 5,521 5x5km cells were classified into 7 gully presence classes ranging from 'very high' presence to 'very low' presence using high and medium-resolution imagery. The final map is shown in Figure 22.

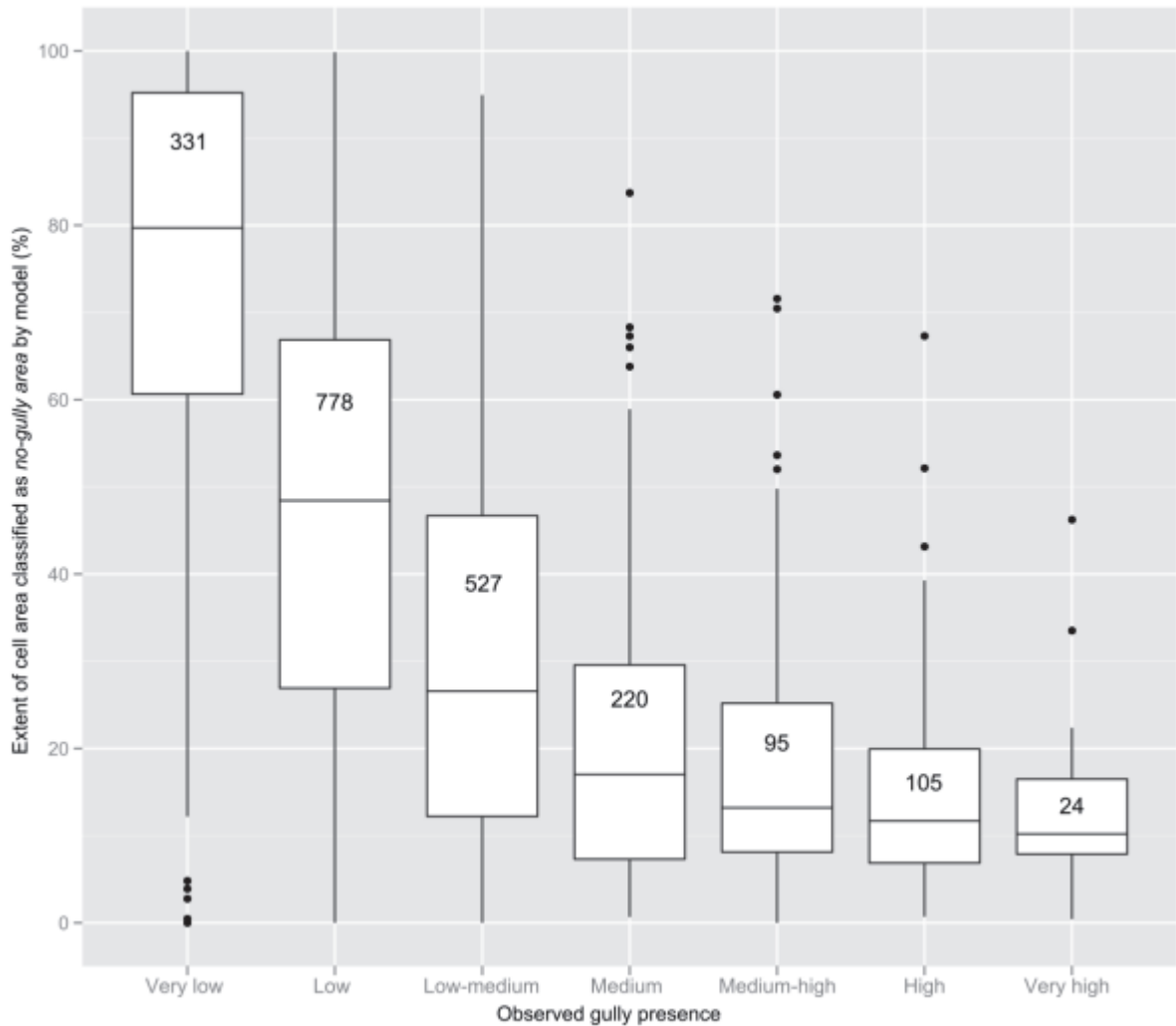


Figure 21 Observed gully presence at 5x5km grid cells vs. extent of no-gully area. Observed 5x5km cells were divided according to gully presence classes (x-axis; number in box indicates cell count). The y-axis indicates the mean extent of no-gully area throughout observed cells as a percentage. Horizontal lines in the boxes indicate mean percentage of no-gully area for the gully presence class. Boxes show the interquartile range while the vertical line indicates where 95% of the data lies for each class. Outliers are marked as points. For example, in the 'very low' gully class: 331 cells were observed as having very low gully presence. These cells had an average of about 80% no-gully area. 75% of these cells had 60%-95% of their area classified as a no-gully area. Only five of these cells had no-gully area between 0% and 5%.

Table 14 Gully presence for each sub-bioregion. Cells in sub-bioregions where >95% of the already assigned cells had 'low' or 'very low' gully presence were assigned 'low' gully presence in the final map. These are shown in red text.

Bioregion	Very low to Low-Medium gully presence	Medium to Very High gully presence	Undetermined cells	Total cells	% of cells with Very Low to Low – Medium gully presence
Paluma-Seaview	54	0	0	54	100
Clarke – Connors Rangers	48	0	0	48	100
Anakie Inlier	40	0	4	44	100
Bogie River Hills	270	30	0	300	90
Carnarvon Ranges	7	0	1	8	100
Undara – Toomba Basalts	363	0	73	436	100
Basalt Downs	71	0	21	92	100
Jericho	140	0	45	185	100
Northern Bowen Basin	157	60	1	218	72

Bioregion	Very low to Low-medium gully presence	Medium to Very High gully presence	Undetermined cells	Total cells	% of cells with Very Low to Low – Medium gully presence
Townsville Plains	62	29	1	92	68
Herberton – Wairuna	45	0	30	75	100
Belyando Downs	411	1	301	713	100
Alice Tableland	257	0	291	548	100
Upper Belyando Floodout	85	1	98	184	99
Cape – Campaspe Plains	159	6	234	399	96
Cape River Hills	112	53	135	300	68
Claude River Downs	47	12	70	129	80
South Drummond Basin	79	11	129	219	88
Broken River – West	55	3	100	158	95
Wyarra Hills	54	30	72	156	66
Broken River – East	307	208	602	1117	60
Beucazon Hills	5	22	10	37	19

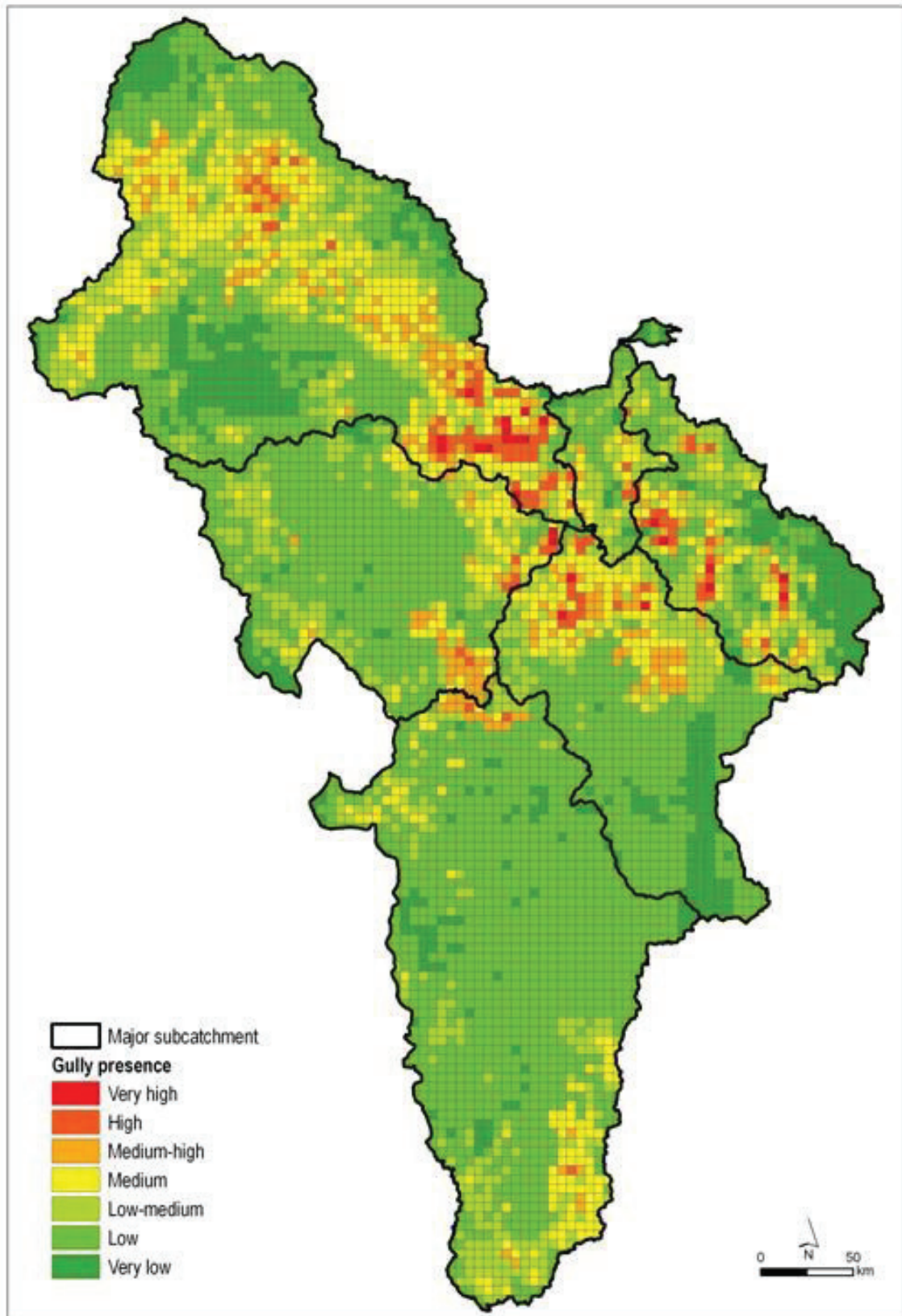


Figure 22 Final 5km gully presence map. This map shows gully presence is greatest in the Upper and Lower Burdekin and Bowen-Broken sub-catchments.

3.1.5 Converting the 5km Gully Presence Map to gully density

Manual mapping and observations were used to simplify the seven classes of gully presence into four classes of gully density. These classes were then applied to the 5km gully presence map based on the mean density of gullies observed for each class. The resulting 5km resolution gully density map is shown in Figure 23. As would be expected, the gully density reflects the gully presence map with the Upper and Lower Burdekin and Bowen-Broken sub-catchments having those areas of high gully density relative to other areas.

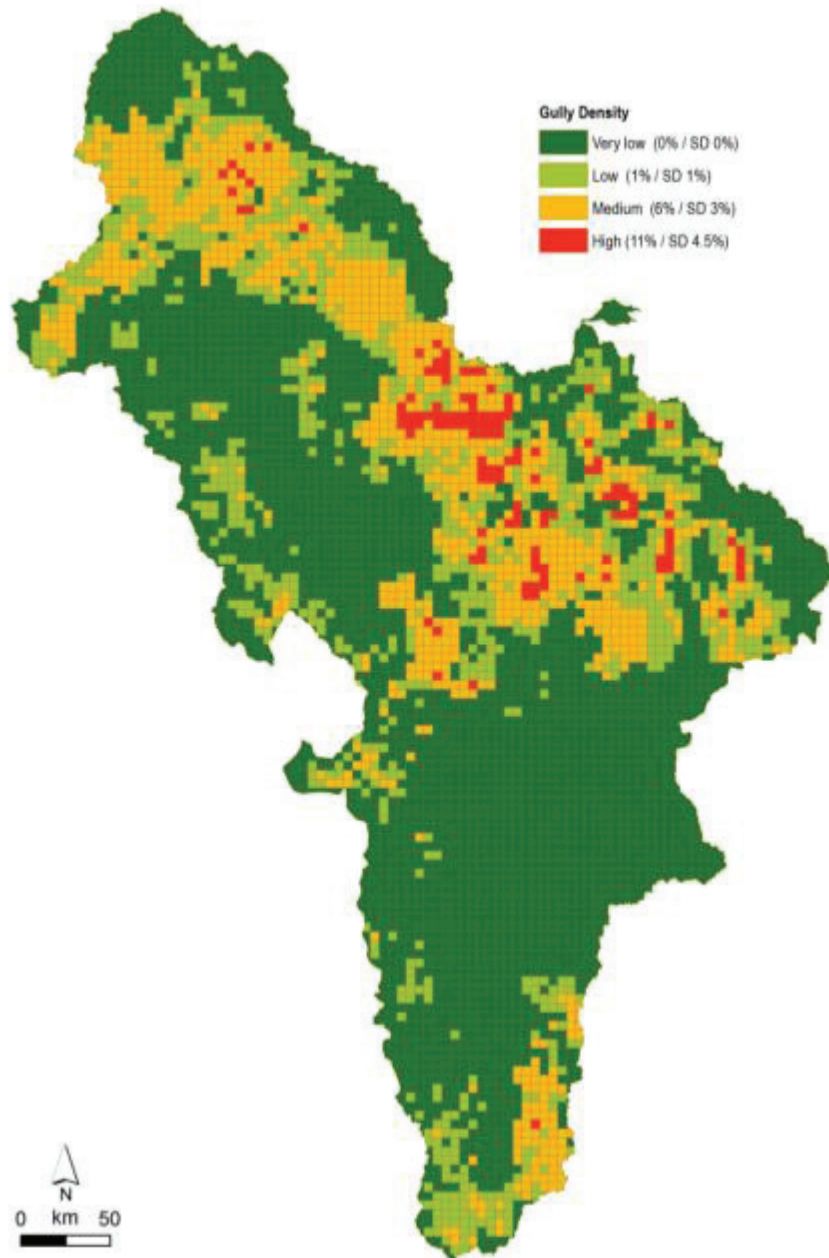


Figure 23 5km resolution gully density map. The relationship between density derived from manual mapping and observed gully presence was used to extrapolate density across the 5km gully presence map.

3.1.6 1km Gully Presence Map

The 1km Gully Presence Map is shown in Appendix A, in map-book format. At 1km resolution, the map highlights sections of the Burdekin where high rates of gullying were observed (within those areas which were mapped as per Table 8 above).

Of the 7,603 cells assessed, the highest 'gully count' (number of 100m² cells gullied) was 98 and the lowest count was 0. The 'gully counts' have been divided into 6 categories (Table 15). Approximately half of all 'gully counts' had a value of 4 or lower indicating very little gully presence. Only 0.24 per cent of the 1km Gully Presence Map featured 'gully count' values greater than 79 and less than two per cent of the Map featured 'gully count' values higher than 59. In terms of area represented, (i.e. the total sum of 100m² cells counted within each 1km cell²) the 20-39 'gully count' category is the largest with a total of 40,593 cells, representing 409.53km². 'Gully counts' are also summarised in Table 16 for major sub-catchments.

Table 17 (below) outlines some standard statistics associated with the 5km Gully Presence Map and the 1km Gully Presence Map. There is a strong correlation between both datasets for areas mapped 'Very Low' and a general correlation for other areas. The Average count and Maximum count trends aligns with the 5km Gully Presence Map categories. Figure 24 below shows the distribution of the 1km Gully Presence Cells and Figure 25 show the distribution of these cells that intersect the 'High' and 'Very High' 5km Gully Presence Map cells. These results support the previous finding in the gully predictive model that even where gully presence is high, the actual prevalence of gullies at these locations is still relatively low.

Table 15 Total count, percentage and sum of cells, categorised by 'gully count' values.

'Gully count' value	No of cells counted	% of total count	Total sum of counts (i.e. 100m ² cells within the 1km ² cells)
0-4	3,816	50.19%	4,752
5 – 19	1,757	23.11%	20,077
20-39	1,437	18.9%	40,593
40-59	489	6.43%	23,114
60-79	86	1.13%	5,835
80-100	18	0.24%	1,569
Total	7,603	100%	95,940

Table 16 Summary of the ‘gully count’ values found in the major sub-catchments.

‘Gully count’ value per 1km x 1km cell	Upper Burdekin count	% of Upper Burdekin count total	Lower Burdekin count	Percentage of Lower Burdekin count total	Bowen River count	Percentage of Bowen River count total	Suttor River count	Percentage of Suttor River count total
0-4	857	47.37%	462	21.82%	335	40.12%	2,162	76.07%
5-19	365	20.18%	671	31.70%	297	35.57%	424	14.92%
20-39	420	23.22%	679	32.07%	155	18.56%	183	6.44%
40-59	144	7.96%	250	11.81%	38	4.55%	57	2.01%
60-79	19	1.05%	50	2.36%	10	1.20%	7	0.25%
80-100	4	0.22%	5	0.24%		0.00%	9	0.32%
Total	1,809	100	2,117	100	835	100	2,842	100

Table 17 A comparison of general statistics for the 5km Gully Presence Map and 1km Gully Presence Map.

5km Gully Presence Map value	No. of 1km grid cells counted and % of 5km Gully Presence Map overlap	Average count	Maximum count	Minimum count	Standard deviation
Very high	600 (100%)	34	98	1	21
High	2649 (98.1%)	19	95	1	14
Medium-high	774 (11.6%)	19	76	0	14
Medium	88 (0.6%)	25	76	1	16
Low-medium	86 (0.4%)	14	61	1	12
Low	3285 (6.3%)	2	88	1	7
Very low	121 (17.9%)	1	6	1	21

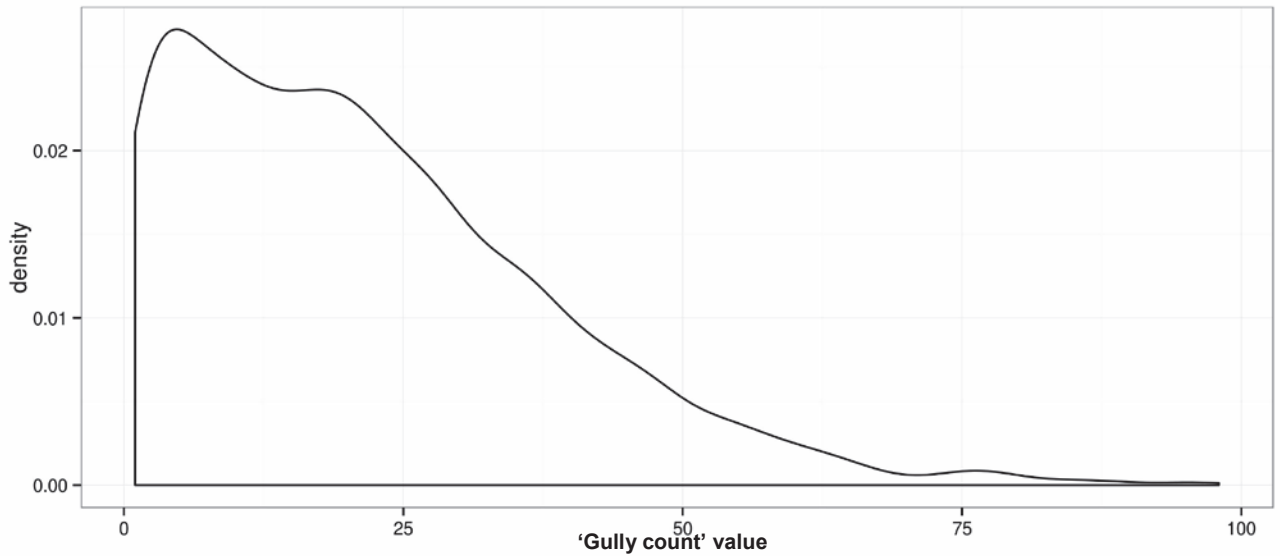


Figure 24 Distribution of 'gully count' values for all cells mapped.

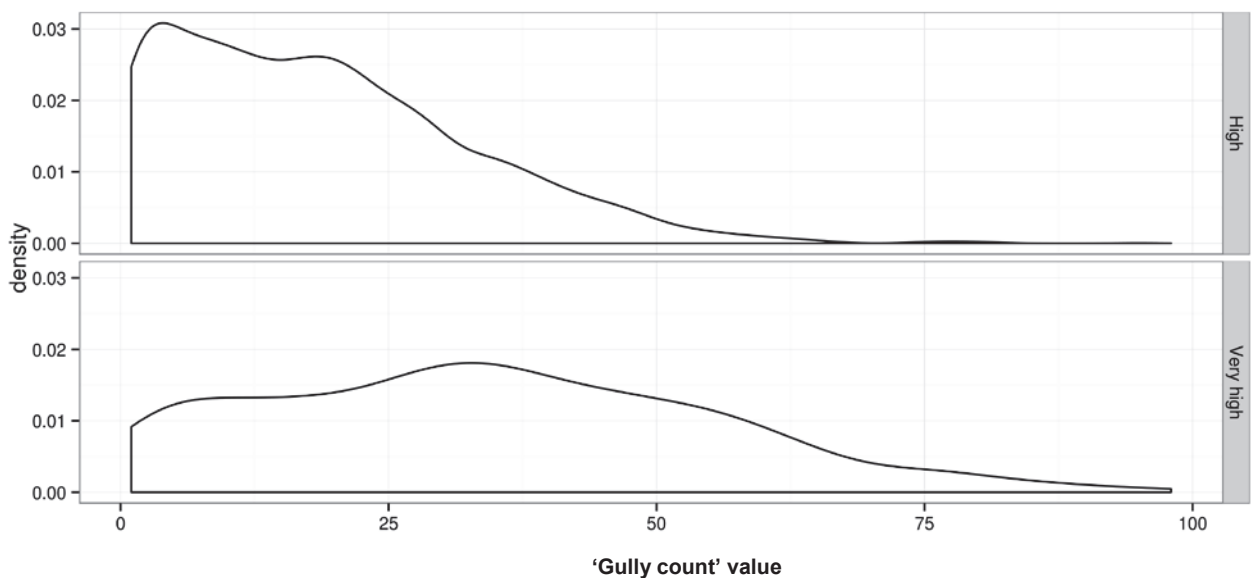


Figure 25 Distribution of 'Gully count' values for cells that intersect 'High' and 'Very High' within the 5km Gully Presence Map.

3.2 Gully extent, volume and change using airborne LiDAR

3.2.1 Gully extents

Gully extent was calculated using the 'difference from mean elevation', which highlights the change in elevation within gullied environments, while suppressing background noise and undulations in the DEM (Figure 26 a and b). An example is shown in Figure 26 (b) where brighter shades of green to white indicate larger differences from the surrounding mean elevation. Using this layer and region growing, gully extent is classified (Figure 26, c).

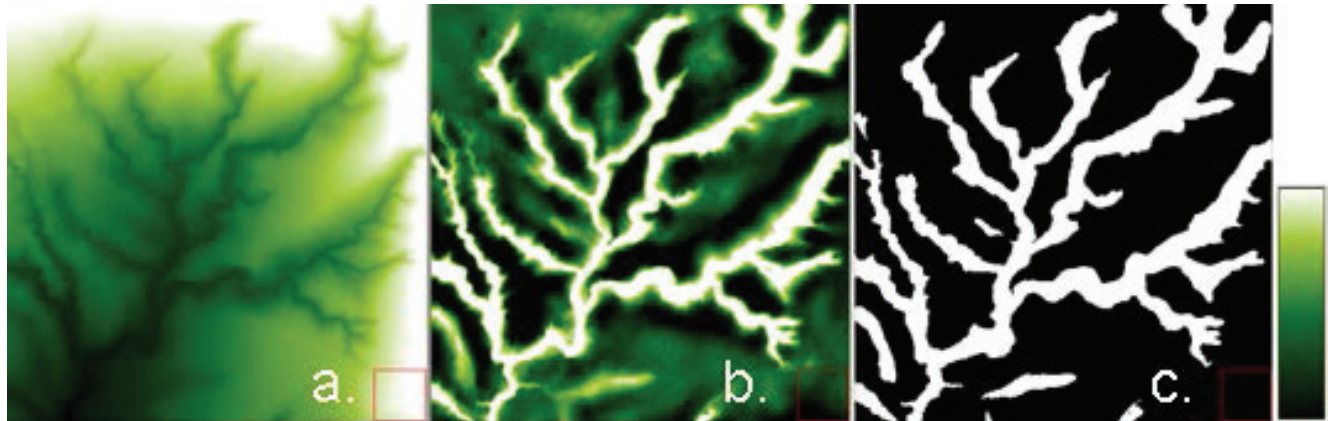


Figure 26 Example of a LiDAR derived DEM (a), the difference from mean elevation (b) and the classified gully extent (c) for a subset at one of the LiDAR sites (Blue Range). In the difference from mean elevation image (b), lighter shades indicate greater difference from mean elevation. This information is used to automatically classify the gully extent. Subset extent 200 x 200 m; DEM elevation range 360 to 375m; Difference layer elevation range = -59cm to 76cm.

An example of classified gully extent overlaid on corresponding orthophotos is shown in Figure 27. The results generally show good visual agreement between the LiDAR classification and orthophotography. It was evident however, that vegetated drainage lines appear morphologically similar to gullies and as a result were sometimes misclassified as gullies. Additionally, wide, shallow gullies (i.e. greater than 15m wide) were not always mapped to their full extent. This is probably due to a low difference from mean elevation as a result of the size and depth of the gully system. Further work that is beyond the scope of this report is required to validate the results and determine the best possible automated approach for mapping different gully morphologies.



Figure 27 Example of gully extent classification based on LiDAR. Left image shows the orthophoto for the area and right image shows the classified gully extent in red.

3.2.2 Gully depth, volume and change

Gully extent and volume results for 2010 and 2013 for each of the (thirteen) Burdekin LiDAR transects that have been processed are shown in Table 18. All sites surveyed had gullies present. The extent of gullying across each of the transects varied with Marshes Creek having the highest area of gullying and Spring Creek having the lowest area gullied. It is interesting to note about 20 per cent of pixels classified as gullies also contained LiDAR returns from overstorey vegetation. This indicates that technologies such as LiDAR, which can pass through small canopy gaps, are suitable for gully classification even in woodland and forest environments provided appropriate ground filters are applied to the data.

Figure 29 shows the relationship between gully area and volume. There is a strong relationship ($R^2 = 0.91$) between gully area and volume. This suggests that two-dimensional mapping of gully area may provide a reasonable surrogate for three-dimensional information about gully volume. However, it is important to note that gully volume does not provide direct information about rates of change or sediment delivery and other data such as tracing and additional LiDAR analysis is required to better understand these processes.

An example of gully change from one of the Fitzroy transects is shown in Figure 29 and Figure 30 for demonstration purposes. When the elevation differences are averaged across the LiDAR capture area, it equates to an elevation change ranging between 0.9 and 8.4 cm.

Table 18 Classified gully statistics for the 13 processed Burdekin LiDAR sites for 2010 and 2013. Note: percentage cover refers to the percentage of pixels containing a return > 2m (vegetation overstorey) and > 0.5 and <2.0m (vegetation understorey).

Site Name	Area Captured (km ²)	Gully Area (km ²) (2010 ; 2013)	Gully Volume (m ³) (2010; 2013)	Overstorey; Understorey Cover (%)*
Fanning	31.8	1.05 ; 1.05	250170 ; 240507	18; 2
Fish Creek	14.4	0.37 ; 0.34	77828 ; 74013	24; 2
Keelbottom Creek	14.2	0.20 ; 0.19	42739 ; 43203	15; 2
Kirknie Creek	14.5	0.29 ; 0.26	39872 ; 36024	19; 1
Lyll Creek	12.2	0.20 ; 0.19	46698 ; 46150	24; 2
Marshes Creek	20.1	1.47 ; 1.39	521816 ; 521416	27; 3
Oaky Creek	13.3	0.55 ; 0.53	125781 ; 109352	24; 2
Parrot Creek	14.5	1.40 ; 1.32	423307 ; 418570	22; 4
Pelican Creek	14.2	0.16 ; 0.15	38964 ; 39639	12; 2
Red Hill Creek	13.0	0.57 ; 0.56	176243 ; 149360	18; 1
Spring Creek	13.3	0.14 ; 0.13	20889 ; 19150	21; 3
Starbright	12.9	0.96 ; 0.89	245325 ; 244563	23; 3
Turrawulla	14.1	1.32 ; 1.24	349051 ; 364878	15; 3

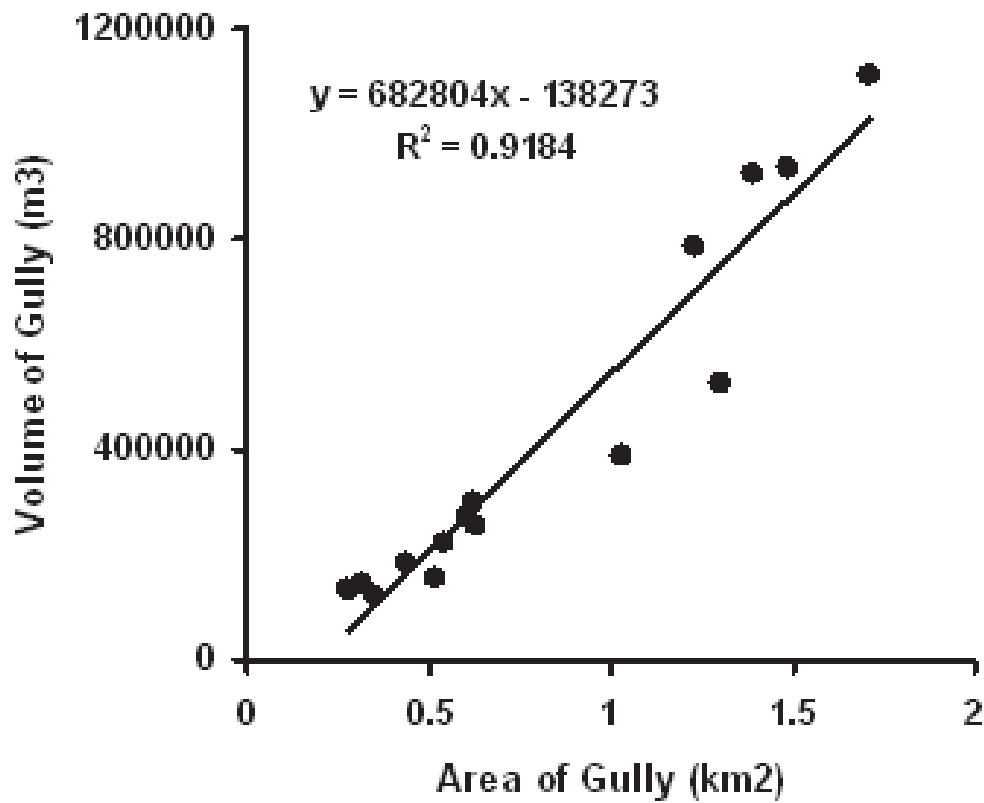


Figure 28 Relationship between gully area and volume. As gully area increases, the gully volume increases.

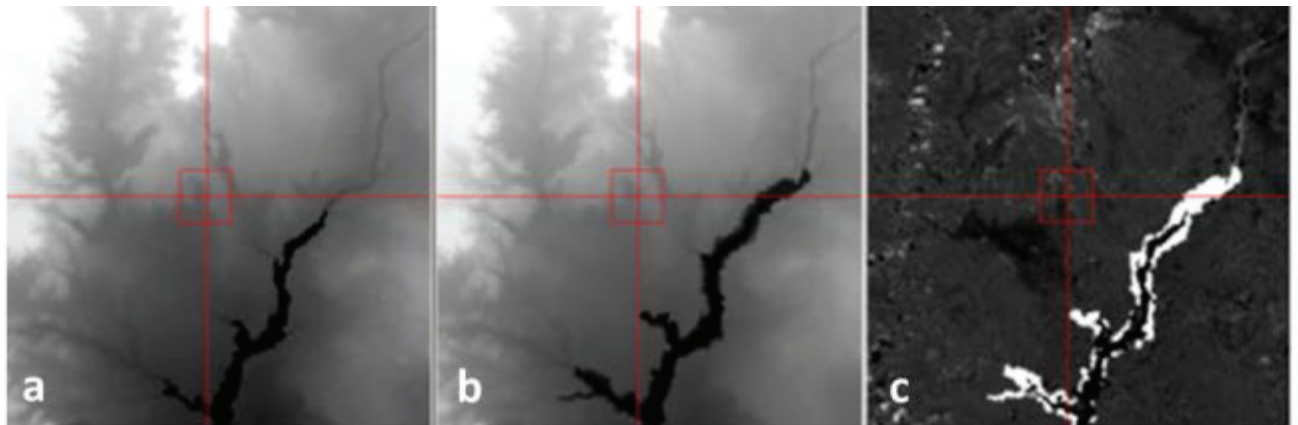


Figure 29 Example of gully change mapping using LiDAR at one of the Fitzroy sites: (a) DEM in 2007. Deeper gullied areas are darker shades. (b) DEM in 2010. Note the clear expansion of the gully. (c) Change in gully extent and volume between 2007 and 2010 (white areas).

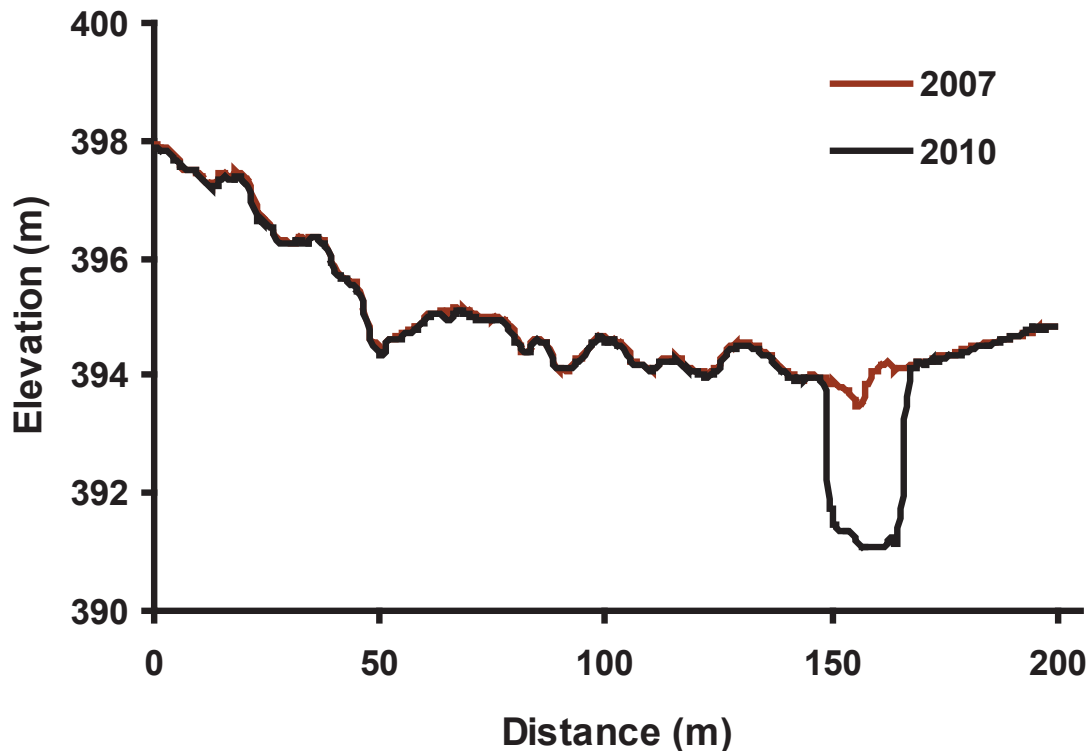


Figure 30 Example of a cross-sectional profile of a gully in the Fitzroy showing the difference between 2007 and 2010. The profile represents the horizontal red line dissecting the expanded gully head in Figure 29.

3.2.3 Gully change between 2010 and 2013

An identical approach and set of thresholds were used to map gully extents in the 2010 and 2013 LiDAR datasets. The comparison assumed that gullies would show a net increase in extent over time due to erosion. Results showed nearly 90% of the area mapped as gullies in 2010 were also mapped as gullies in 2013 (Figure 31). Interestingly, however, our results found that the area of gully extent actually declined over time with a larger gully area being mapped in 2010; a result consistent across all sites. This trend is not real and most likely due to differences in LiDAR's sampling of these complex environments and complexities in processing the LiDAR data and classifying the ground surface within the data sets. These findings suggest the gully extent method, as parameterised, is not suitable for monitoring change when it represents only a small portion of the total gullied area (*i.e.* the error in the classification exceeds the true change).

Once the gully extent was mapped, two approaches were applied for assessing gully volume change and to report an averaged result for each of the sites. In the first approach, a 'lid' was interpolated over gullied areas and this surface was subtracted from the DEM. The 2010 dataset volume was then subtracted from 2013. Results indicate variability in the direction of change between sites. Most sites show a positive change over time as we would have expected (*i.e.* increase in gully volume) while some show a negative change (*i.e.* reduction in gully volume), with Turrawulla in

particular recording a large reduction in gully volume. In the second approach, the 2010 DEM is subtracted from the 2013 DEM within mapped gully areas (Figure 32). The results show the two approaches often provide different and sometimes contrasting results. For example, Parrot Creek and Turrawulla invert from positive to negative change. This might be caused by sub-optimal mapping of gully extents, inability to separate noise from true change, mis-registration between datasets or limitations in the ability of LiDAR to characterise gully volume.

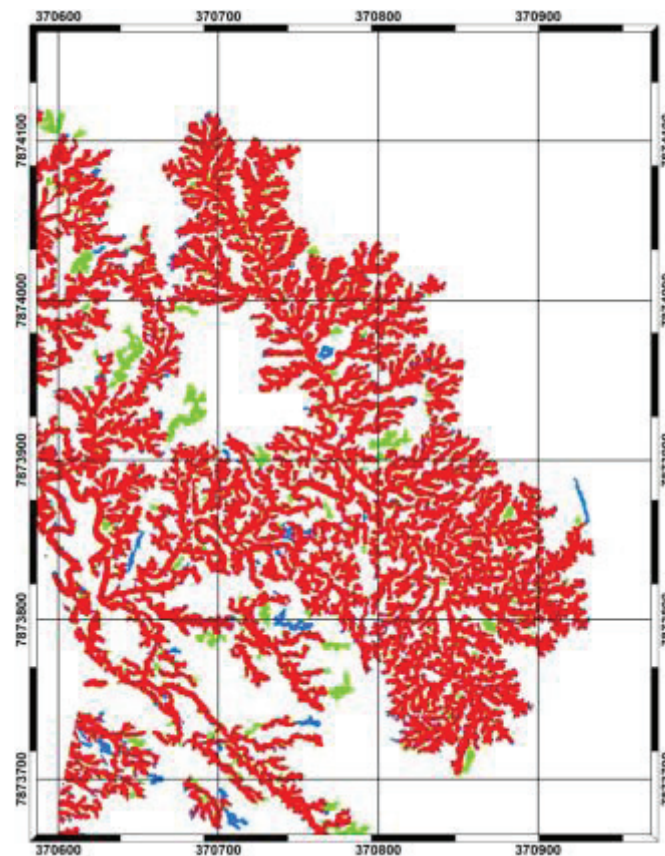
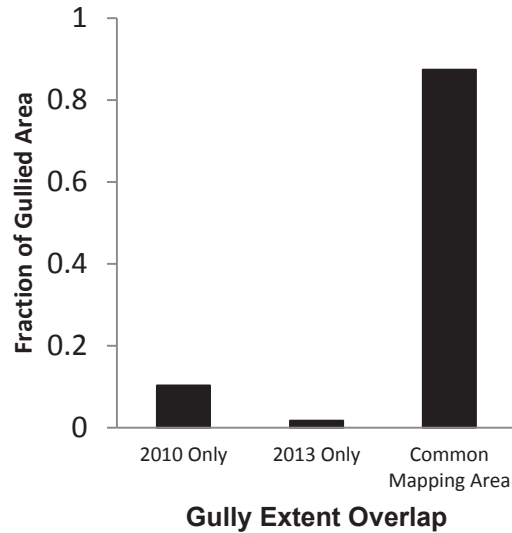


Figure 31 Fraction of gully area mapped in 2010 only (blue), 2013 only (green), and mapped in both years (red).

To assess the impact of a 'noise' threshold on gully change estimates, gully change greater than a series of thresholds was compared. Thresholds were between 0 and 1.0m (). Ideally, a threshold of change can be applied which separates the effects of noise/change unrelated to gully morphology (e.g. grass misclassified as the ground surface) from real change. The results shown in Figure 33 demonstrate that a large proportion of detected gully change occurs at lower magnitudes of change and no obvious single noise threshold would be applicable between sites. This might explain why the gully change results above are highly variable as the noise in the LiDAR data is dominating the amount of change detected. At +/-40cm for example, only one site (Parrot Creek) had greater than 50% of gully change remaining. Overall this suggests the selection of the 'noise' threshold has a large impact on the estimate of gully change. Previous studies which have used LiDAR for erosion estimates also support this finding (Croke et al., 2013, Brasington et al., 2003) with Croke et al. (2013), for example, applying a noise threshold of 0.45m for stream bank change mapping in South-East Queensland. To illustrate the importance of a noise threshold in change calculations, we applied threshold similar to Croke et al. (2013) of 0.45m; although we acknowledge this may not be the optimal value. Notably the results indicate a more stable result between DEM and volume differencing methods (Figure 34). Assuming these results are more representative of the true change in gully volume, this indicates that Marshes Creek, Parrot Creek, Starbright and Turrawulla experienced the largest change in gully volume of all of the LiDAR sample sites (Figure 34).

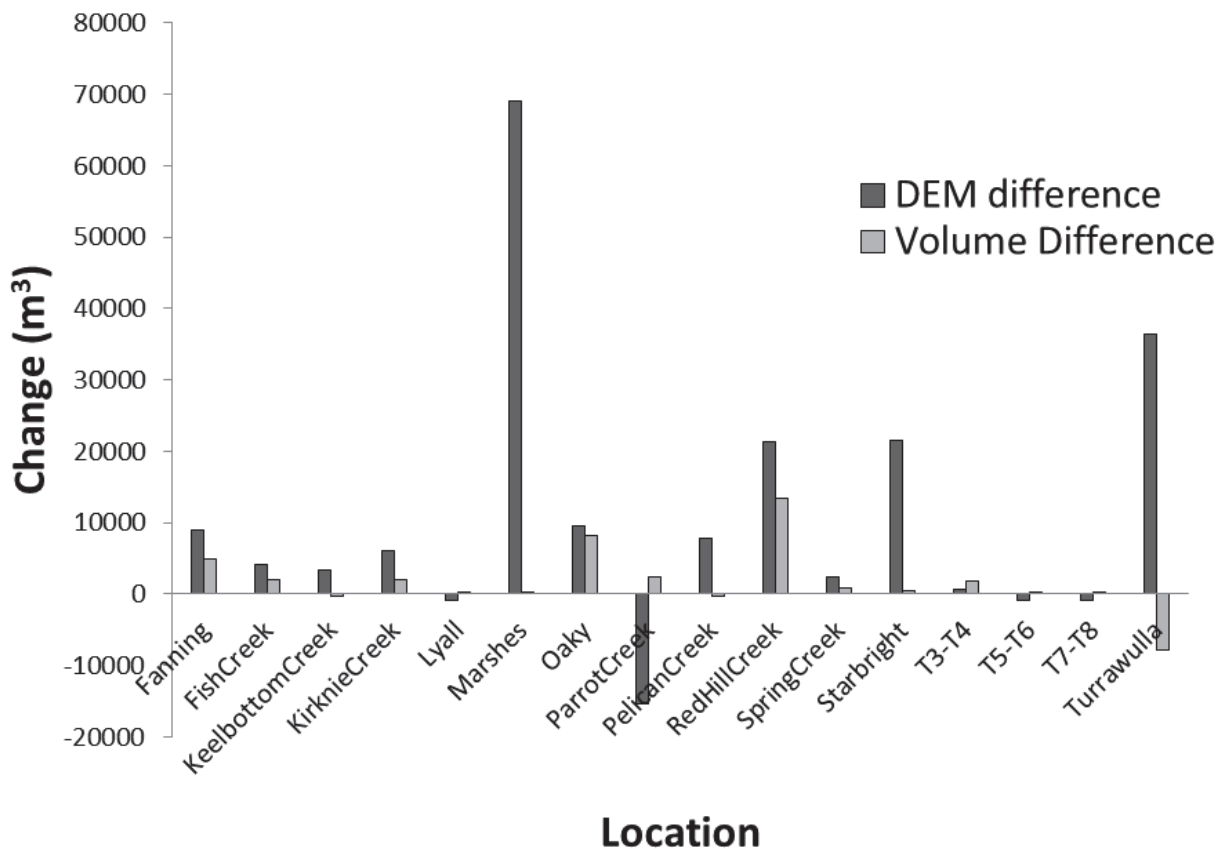


Figure 32 Total difference between 2010 and 2013 digital elevation models.

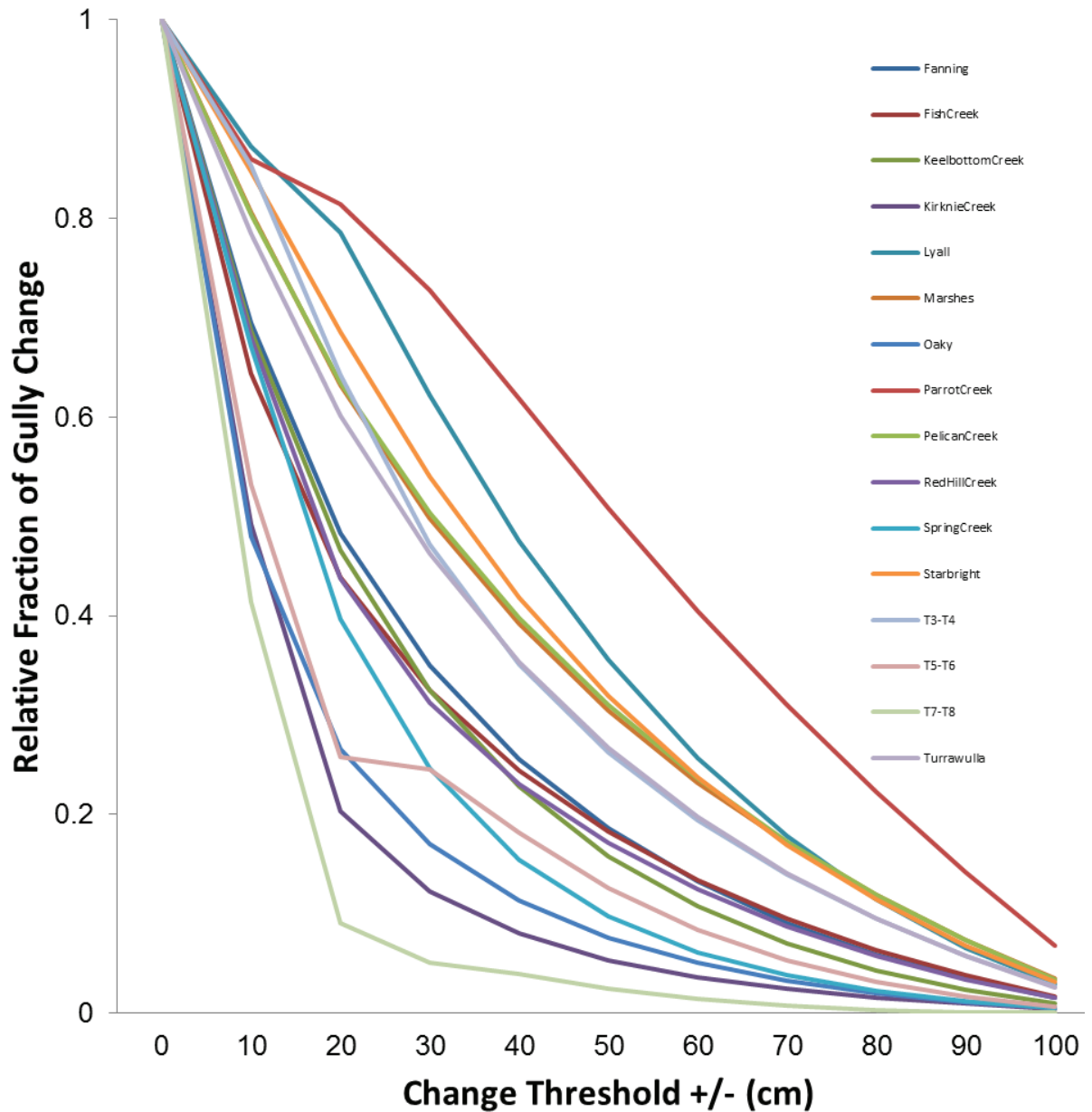


Figure 33 Impact of change threshold on the fraction of gully change (2010 DEM minus 2013 DEM). The value is calculated as the total difference between dates (i.e. 2013 minus 2010) divided by the difference greater than the threshold value. To facilitate visual comparison between sites the values were rescaled as the fraction of the total change rather than the magnitude.

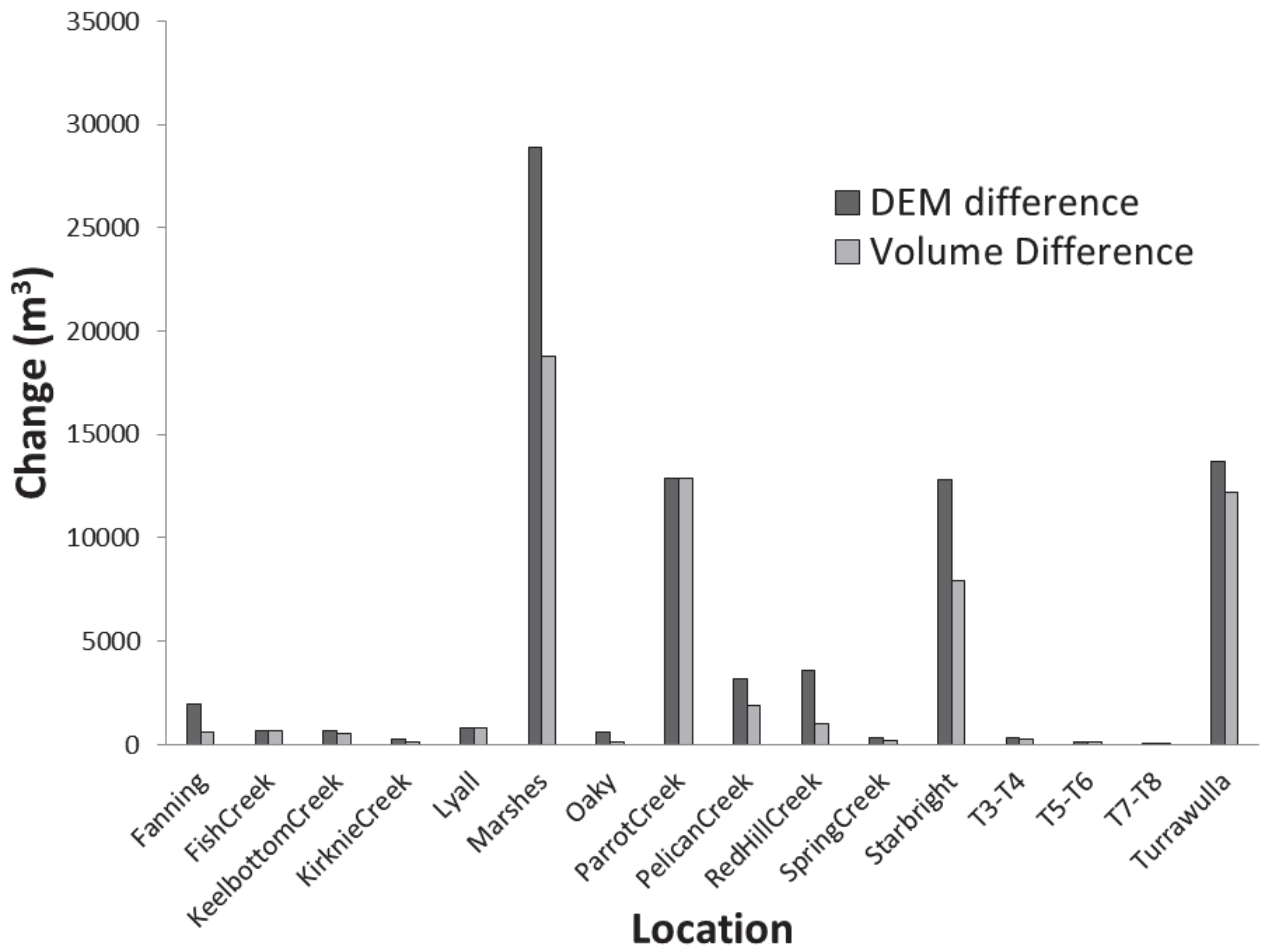


Figure 34 Total difference between 2010 and 2013 digital elevation models with a 0.45m noise threshold applied (i.e. only change >0.45m is included in this figure).

Classifying ground returns in gully environments is a difficult task and the performance of standard algorithms is largely unknown. Tests were conducted to determine whether the classified returns used to develop the DEMs had actually used the lowest elevation points within a gully environment; returns should not occur below the ground surface (interactions with water being a possible exception). This found that on average, the DEM should be 3-7cm lower than mapped when averaged across the different sites. It is unclear whether this is cancelled out by positive errors (non-ground features being selected) but highlights more work is needed to classify ground returns within gully environments. This may require LiDAR providers to use different filtering approaches to achieve improved ground return classifications, and the consistent application of these filters between capture dates.

3.3 Gully chronosequence mapping

The gully chronosequence mapping was limited to only ten sites due to issues of comparing older imagery with more recent imagery and the difficulty of accurately mapping gullies in different imagery sources. However, despite this relatively small sample, a range of different landscapes were observed and some trends were evident. The most notable trend relates to gully activity; nine gullies were found to be active. The activity of the other remaining gully was not able to be determined due to ambiguity in defining gully boundaries between within and between dates because of

unclear features in the aerial photography and satellite imagery. The rates of change between dates are summarised in Figure 35 and given for each site in Appendix B. Most of the gullies observed showed expansion over the observation period of up to about 60 years. These figures are based on the results outlined in the Appendix C. A summary of Appendix C is provided in Table 19 below.

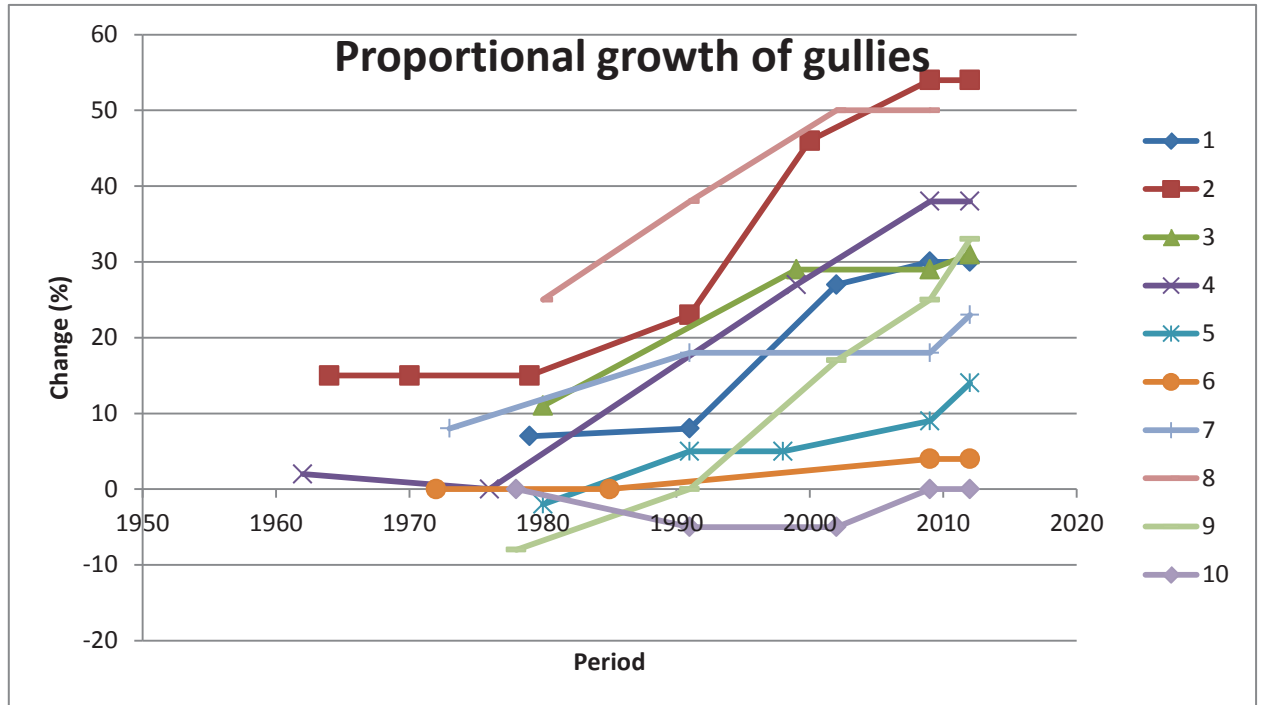


Figure 35 Proportional gully growth, in relation to gully sizes measured in the first available images.

As is shown in Table 19, the yearly rates of gully expansion vary widely; some gullies eroded at a yearly rate of over 100m², while others eroded at a rate of less than 20m². The average yearly rate (excluding two outliers) was 50.4m²/year. These rates were not linear over the observation period and large expansions appear to have occurred during short periods, possibly driven by particular rainfall events. There was no particular period during which all, or even most, gullies expanded at a similar elevated rate. This also supports the suggestion that gully evolution is driven by rainfall events, with rainfall intensity due to localised storms possibly resulting in changes at particular times.

Of the active gullies studied, the larger gullies showed greater expansion than the smaller gullies (Table 19). They also expanded at a higher yearly rate, on a m² expansion/year basis when comparing changes in size between the first and last available image dates. These larger gullies did not, however, grow at a higher proportional rate. No obvious trends were observed between gully size and proportional growth rates. The average proportional growth of the gullies, between the first and last available image dates, was 28 per cent.

There was no obvious relationship between land type and yearly rate of growth, or actual growth. Lower than average proportional growth occurred on land categorised as Box country and above average proportional growth occurred on land classified as Box and napunyah, and Goldfield country. However, these results are probably more reflective of the original gully size than impacts from actual land type characteristics.

Much of the erosion for these gullies may already have occurred, prior to the first image date available for this study. A larger sample is required to determine such relationships. Also, no discernible relationship was found between the morphology or shape of gullies and yearly rates of growth, actual growth, or total proportional growth. This is probably also due to the small sample size. However, it was observed that most of the linear gullies expanded more in width than length. This suggests that linear density of gullies, as it often used in water quality models, may not be an accurate representation of the true contribution of gullies to the sediment budget.

Table 19 Summary of gully chronosequence mapping results, sorted by original size (largest to smallest)

Gully Id No.	Original Size (m ²)	Change between 1 st and last year (m ²)	Proportional change from first image date (%)	Rate of change between 1 st and last year (m ² /year)	Gully Shape	Land type
3	339,300	103,500	31	2070	Dendritic	Goldfields country - red soils
1	177,300	54,000	30	1059	Linear	Box and napunyah
5	38,700	5,400	14	106	Linear	Box country (BD & DU)
10	38,700	0	0	0	Linear	Red basalt
7	36,000	8,100	23	135	Dendritic	Narrow Leaved Ironbark on Shallower Soils
6	21,600	900	4	17	Linear	Box country (BD & DU)
2	11,700	6,300	54	94	Dendritic	Box and napunyah
9	10,800	3,600	33	75	Linear	Red basalt
8	7,200	3,600	50	62	Linear	Narrow Leaved Ironbark on Shallower Soils
4	2,700	1,020	38	15	Linear	Goldfields country - red soils

The ten gully locations were compared with the mapping of Soil Erosion Vulnerability, as mapped under RWQ Science Project RP63G. No clear relationship was found between soil erosion vulnerability and those locations which had high proportional gully expansion (Table 20). However, gullies located on soils attributed with lower soil erosion vulnerability rankings (<4) also had lower than average proportional growth. There were also no relationships apparent between original gully size, actual gully growth, yearly growth rates and Erosion Vulnerability rankings. However, these results may be due to the small sample size.

Table 20 The soil erosion characteristics and ranking of the gullies (based on products developed by RWQ Science Project RP63G), sorted by the proportional growth of gullies.

Gully	Gully growth			Soil erosion characteristics				Erosion Vulnerability Ranking			
	Total enc. m2	m ² /year	Prop. growth (%)	Erosion Vulnerability - Surface Soil	Erosion Vulnerability - Subsoil Dispersibility	Erosion Vulnerability - Combined	A	B	C	D	Total ranking
2	6,300	94	54	40% Non-dispersive surface soils, 60% Dispersive surface soils	100% Non-dispersive subsoils	40% Non-cohesive surface soils over non-dispersive subsoils, 60% Weakly dispersive clayey soils	4	11			8.2
8	3,600	62	50	60% Dispersive surface soils, 40% Non-cohesive surface soils	100% Non-dispersive subsoils	60% Weakly dispersive clayey soils, 40% Non-cohesive surface soils over non-dispersive subsoils	11	4			8.2
4	1,020	15	38	85% Non-cohesive surface soils, 5% Moderately stable surface soils, 10%	100% Non-dispersive subsoils	85 % Non-cohesive surface soils over non-dispersive subsoils, 5% Moderately stable surface soils over non-	4	2	11		4.6

RP66G Synthesis Report: Gully mapping and drivers in the grazing lands

9	3,600	75	33	Dispersive surface soils	100% Non-cohesive surface soils	100% Non-dispersive subsols	100% Non-cohesive surface soils over non-dispersive subsols	dispersive subsols, 10 % Weakly dispersive clayey soils	4									4
3	10,3500	94	31	85% Non-cohesive surface soils, 15% Dispersive surface soils	65% Non-dispersive subsols, 45% Highly dispersive subsols	50% Non-cohesive surface soils over non-dispersive subsols, 10% Weakly dispersive clayey soils, 20% Non-cohesive surface soils over highly dispersive subsols, 20% Dispersive clayey surface soils over highly dispersive subsols			4	11	12	17						9.2
1	54,000	1,059	30	80% Non-cohesive surface soils, 20% Dispersive surface soils	80 % Non-dispersive subsols, 20% Weakly dispersive subsols	80% Non-cohesive surface soils over non-dispersive subsols, 20% Weakly dispersive clayey soils			4	11								5.4
7	8,100	135	23	90% Non-cohesive surface soils, 10 % Moderately stable surface soils	100% Non-dispersive subsols	90% Non-cohesive surface soils over non-dispersive subsols, 10% Moderately stable surface soils over non-dispersive subsols			4	2								3.8
5	5,400	106	14	100% Dispersive surface soils	90% Non-dispersive subsols, 10% Moderately	90% Weakly dispersive clayey soils, 10% Dispersive clayey soils			11	13								11.2

Department of Science, Information Technology, Innovation and the Arts

6	900	17	4	40% Dispersive surface soils 30% Non-cohesive surface soils, 30% Moderately stable surface soils	100% Non-dispersive subsoils	40% Water Supply Division , 30% Non-cohesive surface soils over non-dispersive subsoils, 30 % Moderately stable surface soils over non-dispersive subsoils	4	2			3
10	0	0	0	75% Moderately stable surface soils, 25% Non-cohesive surface soils	100% Moderately stable surface soils	75% Moderately stable surface soils over non-dispersive subsoils, 25% Non-cohesive surface soils over non-dispersive subsoils	2	4			2.5

4 Discussion

This project aims to use three main lines of evidence to provide information about the location, extent and dynamics of gullies in the Burdekin catchment. These are:

- I. multi-scale mapping of gully locations and prediction of gully presence
- II. multi-temporal, very high-resolution mapping of changes to the extent and volume of gullies using airborne LiDAR technology
- III. historical 'chronosequence' mapping of gully evolution.

The use of multiple remote sensing technologies provides a comprehensive account of current knowledge and delivers new spatial products for extension, modelling and improved land management investment activities in the Burdekin catchment. This is discussed further below.

4.1 Mapping of gully locations

A range of products have been developed for the Burdekin. These provide regional-scale mapping or prediction of gully locations and presence or absence. These products are based on a range of information sources including satellite imagery, aerial photography, spatial layers of biophysical information, expert knowledge and visual interpretation.

4.1.1 Broad-scale (5km resolution) mapping

The 'No-Gully' Map is a regional-scale spatial description of areas of the Burdekin that are less likely to feature gullies or be at risk of gully formation in the future. The map is a simple, pragmatic attempt to use basic information combined with expert knowledge to enable more targeted mapping of gullies. Over 47 per cent of the Burdekin has been identified as having few or no gullies, which is a significant area. This information alone may inform Reef-related activities as knowing where gullies are unlikely to occur is just as important as knowing where they do occur in terms of targeting effort for gully management. For example, this map may:

- assist P2R modellers to better account for gully density in particular areas
- assist to indicate landscapes that are more stable and possibly more resilient to erosion
- provide key information to manage areas more susceptible to erosion.

The gully mapping was constrained to the location of 'gully-sensitive' areas in the 'No-Gully' Map. Assuming 'no-gully' areas are reasonably accurate, the mapping increased the area of the Burdekin catchment where gullies are mapped to about 5% (2.7% of the total area of the Burdekin catchment), a vast improvement on the 0.88% previously reported by Kuhnert et al. (2010). This mapping may be used to identify areas where gullies are prevalent and the approximate extent of individual gullies in those areas. However, it should not be considered representative of all gullied areas in the Burdekin. This is because mapping was targeted to areas with imagery of sufficient resolution to aid interpretation; and within those areas, gullies were not mapped systematically or comprehensively due to time and resource constraints. In addition, detecting gullies from imagery is reliant on a gully definition that can be

applied consistently for mapping purposes. This requires compilation of a set of readily identifiable characteristics which can be used to identify gullies in a consistent manner. This is not a straightforward task, especially when multiple image sources are used and land cover characteristics associated with gullied areas vary significantly in space and time. A gully mapping guideline has been developed as part of this project, in collaboration with DNRM, in an attempt to develop a more consistent approach state-wide to catchment scale gully mapping. This is also being supported by an increase in the capture of aerial orthophotography, which has sufficient resolution to accurately determine gully presence or absence.

The predictive gully model was also constrained to 'gully-sensitive' areas. This model used a simple set of rules and was based on the strong statistical relationship found between mapped gullies and elevation above drainage line. Further testing of this relationship is required as it is yet unknown if there is a stochastic element which leads to the initiation or presence of a gully or if we are lacking explanatory variables at the appropriate resolution. It is most likely a combination of both. The relationship with elevation above drainage line may also be somewhat biased by the fact that many gullies are mapped as drainage lines in the topographic data used in this project. Potential explanatory variables that may help improve future predictions include soil attribute data and information about grazing pressure and land management history.

Overlaying the predictive model against the gully mapping highlighted one of the key issues in locating or predicting gully presence. Results suggest that where the model predicts low probability of gully presence, there were indeed fewer gullies. However, where the model predicts high probability of gully presence, the probability of a gully being present is still only around 5 per cent. It is interesting to note that the mean area of gullies in the LiDAR transects was 6%, which suggests that gullies are not prevalent features in the landscape and supports the relatively low probability of gully presence in the predictive model. Further work would be required to refine gully predictions at the higher end of the probability scale to enable its separation into an improved actual gully or non-gully prediction. However, as has been reported by previous authors (e.g. Kuhnert et al., 2010), it is recommended that any future efforts focus on manual mapping of gullies, at least until explanatory variables are available at sufficient resolution to describe landscape processes which lead to gully formation.

The 5km Gully Presence Map integrated observations of gully prevalence with information derived from the 'No-Gully' Map and predictive model. This map also incorporated a further broad relationship between observed data and IBRA sub-bioregions (Interim Biogeographic Regionalisation for Australia). This relationship assumes that sub-bioregions are representative of a unique combination of soil/geology, landform, climate and vegetation. Levels of confidence were assigned to areas of the 5km Gully Presence Map based on the information source used to derive mapping at that location.

The approach taken to compile the map involved a simple, repeatable and relatively expedient method for identifying areas where gullies are most prevalent in a catchment. The approach is somewhat subjective. However, unlike previous gully maps in the Burdekin, it is based on extensive observations of actual gully presence, rather than complex models trained on limited localised information and a set of explanatory variables that are either models themselves, or of very low resolution.

There remain areas in the map where our confidence is low, and these may be improved by future mapping efforts.

Provided the limitations of the predictive model and gully presence map are understood and appropriately communicated, these products can inform Reef-related activities by highlighting areas in the Burdekin that are more likely to have gullies or be at risk of gully formation. This may be used with other information, such as ground cover and soil data and higher resolution gully mapping, to target extension efforts to areas which may be vulnerable to gully initiation or expansion.

4.1.2 Medium scale (1km resolution) mapping

The 1km Gully Presence Map is a medium-resolution visual observation of gully presence. Mapping of priority areas was informed by grid cells classified as 'High' and 'Very High' in the 5km Gully Presence Map. By applying a more objective count value rather than a subjective scale value (i.e. High, Medium, Low), the end user can determine how best to rank the data in accordance to their individual requirements.

As with the 5km Gully Presence Map, the 1km Gully Presence Map has relied heavily on Google Earth imagery. Whilst Google Earth provides high quality imagery, images are not always captured during the dry winter/spring seasons optimal for viewing gullies. Some cells were counted from 'wet season' imagery, when vegetation can hide gully presence. Improved satellite and airborne imagery is becoming more readily available in Queensland and this will provide opportunities for future mapping efforts. For example, the Spatial Imagery Subscription Plan (SISP) which is administered by DNRM, undertakes systematic image capture of large areas of the state, usually with very high resolution aerial photography. Repeat captures are on 1-5 year time scales, suitable for monitoring gully change. These image data sets are greatly improving the ability to apply the methods described in the mapping guidelines and is reducing the reliance on freely available Google Earth imagery which can be of varying quality and consistency.

To minimise differences between mapping operators, a grid based approach was applied to the manual editing components of this project. This approach has reduced the need for mapping operators to identify gully edges in imagery that is not suitable for such mapping. Instead, an operator simply makes a decision about the presence of a gully in a grid cell, reducing subjectivity and applying a consistent mapping approach in terms of scale and outputs. As previously mentioned, this approach has now been developed into a Catchment-scale Gully Mapping Guideline for Queensland which provides clear and repeatable instructions for operators to produce consistent mapping outputs for priority areas in Queensland.

Together, these developments have significantly improved consistency in gully mapping amongst multiple operators, especially with regard to the 1km Gully Presence Map. They have also simplified the task of mapping gullies and allowed officers who are unfamiliar with GIS packages to contribute to the project with minimal training and direction. Currently, regional DNRM officers in Toowoomba, Rockhampton and Bundaberg continue to work on the 1km Gully Presence Mapping in the Burdekin, Fitzroy and Burnett-Mary catchments.

4.2 Mapping gully extent, volume and change using airborne LiDAR

Airborne LiDAR is widely used for providing detailed and accurate measurements of the land surface topography. In the present study, airborne LiDAR was used to map the 3-dimensional morphology of gully systems and quantify changes through time at a number of locations in the Burdekin and Fitzroy. This involved capturing LiDAR on two (or more) separate dates with near-identical sensor configurations in an attempt to minimise any false gully change due to sensor effects. The sites in the Burdekin capture areas where Reef Rescue funding has been allocated by the NQDT regional group for gully management and two long-term gully and hillslope erosion monitoring sites which have been extensively studied by CSIRO. Automated methods for processing LiDAR data have been developed as part of this work to accurately map and quantify gully extent and volume. These methods can be applied to multi-temporal LiDAR data to quantify rates of gully volumetric change. The results showed significant potential to characterise gullies and gully change over time, but the work also presented many challenges.

The difference in DEM values over time showed numerous examples of gully head expansion, demonstrating LiDAR's ability to map fine scale gully change. Converting estimates of change into meaningful volumetric values produced unrealistic results (i.e. gully volume decreased rather than increased). This was attributed to 'noise' in the LiDAR data (i.e. erroneous data points resulting from capture and processing issues). Setting a minimum detectable change threshold provided results closer to expectations. Brasington et al. (2003) and Croke et al (2013) suggested that the minimum detectable change is around 40-45cm to account for signal to noise ratios in the data and survey control. Our results show that a threshold of 40cm accounts for more than half of the detected volumetric change. This is considerable and highlights the importance of optimising this parameter for assessing gully change / deriving sediment budgets.

Applying a noise threshold of 40cm, all sites showed at least some change in gully volume between 2010 and 2013. Some of these showed significant changes, including Marshes Creek, Parrot Creek, Starbright and Turrawulla. Absolute differences are difficult to calculate due to issues with the LiDAR data between dates and the difficulty in accurately mapping different gully morphologies using automated approaches. However, relative differences are still apparent and these data could be used to highlight those areas which have undergone more significant change in recent years. Results from the Fitzroy LiDAR captures and the chronosequence mapping suggest that gully change is largely event driven and any one location could change rapidly where erosion factors combine under favourable conditions such as low cover and high intensity localised rainfall. At least three dates of data are available for the Fitzroy sites. The two change periods measured in the Fitzroy LiDAR data were 2007-10 and 2010-13. The latter period was much wetter overall yet the earlier period showed greater change. It is hypothesised that this greater change was driven by a single intense rainfall event in the Fitzroy, at the end of a drought when ground cover was low. This provides some evidence that a whole-of-catchment approach is still required for gully prevention and management as any part of a catchment can be impacted by localised rainfall events, even during drier periods.

A major issue in mapping gully change using LiDAR relates to the classification of ground returns; a task undertaken by the data providers. To our knowledge no algorithm has been developed for ground returns in complex gully environments and as a consequence, there are likely to be errors in defining the ground surface. This will result in over/under mapping of change over time. Comparing the minimum height of returns with the DEM found that returns frequently occurred below the ground surface which should in fact be classified as ground returns (*i.e.* returns cannot occur below the ground surface). It is not possible, however, to quantify the magnitude of these errors without accurate field survey data, collected using appropriate surveying methods. The level of processing by the provider can have a significant impact on the accuracy of the ground return data. It is important that standards be followed by LiDAR data providers to ensure consistency and accuracy in data, especially data which is to be used for change detection. The 2013-14 capture was provided to DSITIA as Level 2 classification data, when capture specifications required Level 3. This means less rigorous filtering has been applied to the data to classify the ground returns and this may explain some of the issues identified, particularly less than the 40cm threshold applied. As a result, reprocessing has been requested (as Level 3 processing was specified in the contract with the provider), but results presented here are based on Level 2 classification. The methods will be reapplied once the Level 3 data is resupplied.

The automated method used to classify gully extents for individual dates was not robust enough to reliably compare and map change in gully extents between dates and over time. This is due in part to the issues discussed above, but also due to the limitations of applying a standard window size for deriving the difference from mean elevation in complex and variable environments, characterised by a range of different gully morphologies. Although the accuracy of the method is likely to be high (~90% of the same area was mapped as gullies in both dates), the proportion of total gully area that changed between 2010 and 2013 is small. We found a window of 5m was optimal, however, this meant wider gully heads were sometimes under-mapped. Further research is required to evaluate different algorithms to extract gully features from LiDAR data, although it is expected that there will be issues with whatever approach is taken. Any evaluation should focus on the required outcomes, and the balance of omission and commission error and what this may mean for change estimates.

At the landscape scale, LiDAR data provides a highly detailed and accurate measure of the land surface. Gullies are complex structures at micro and macro scales. Capturing a 3-dimensional profile of a gully system and changes to these structures through time from airborne LiDAR presents many challenges. Appropriate scanning specifications, in particular scan density and scan angle, are critical for observing and measuring subtle variations in gully structure. These factors are influenced by sensor type, flying height, vegetation and debris, and post-processing by the LiDAR provider. Further research is required to account for these factors and quantify minimum detectable changes to improve uncertainty in gully change data and derived sediment budget. Airborne LiDAR does provide detailed maps of gully extent and quantitative estimates of gully change over time. This information can be used by geomorphologists and modellers to improve gully process understanding and model parameterisation. Whilst it is known that a minimum detectable change threshold is required, there is a need to quantify the uncertainty in a more systematic and quantitative way to establish a point of reference, based on field data. These field

data have not been systematically collected for past acquisitions limiting our ability to validate the accuracy of previous LiDAR captures and any derived volume and change estimates. This could be improved through field based techniques, including Terrestrial Laser Scanning (TLS). TLS LiDAR data has been captured as part of this project but more research needs to be undertaken to determine how best to merge the two datasets to determine a point of reference. TLS also offers the potential for a more systematic and geographically-comprehensive sampling regime to be developed. Airborne LiDAR provides information at scales not previously possible, however it is limited in geographic coverage by cost and processing capacity. TLS is relatively inexpensive and systems are in place for the storage and processing of the data captured. An opportunity exists to develop and extend our knowledge of gully change using TLS, provided the time and resources required for development are available.

4.3 Gully chronosequence mapping

The chronosequence mapping component of this project has provided us with insight regarding current levels of activity, and varying rates of gully expansion, as well as the proportional growth of gullies on different soil types. It is best, however, to look at the results on a case by case basis due to the small sample size.

Whilst the method employed is robust and reasonably objective, it has posed some challenges associated with locating and mapping gullies in different image sources, potentially influencing the integrity of the results. In this study, most of these issues were addressed. The requirement to locate gullies in historical aerial photography limited the range of locations available for inclusion. Historical high resolution (large scale) aerial photography (from the 1940s and 1950s) is typically available around townships and near infrastructure projects. Despite this, we have found study sites within each of the main Burdekin sub-catchments, representative of the dominant land types. In locating these sites, we have investigated at least 40 other sites, which were excluded due to poor quality historical imagery, inappropriate scale and/or lack of repeated capture over the required dates. This has led to the small, but relatively well-distributed study sample.

As previously mentioned, results from this small sample and from the LiDAR change data suggest that most gullies are active and that larger, detectable changes to the gullies are possibly sporadic and (rainfall) event driven. It is difficult to assess this hypothesis without ongoing monitoring and more accurate information about where, when and how much rainfall was received at particular locations and points in time.

Ordering, checking, and ortho-rectifying historical imagery is resource and time intensive. All aerial photography is managed by DNRM through SmartMap. Whilst imagery is generally available for immediate download, much historical imagery requires ordering, which can take up to a week. Only once the image is received, only then can we verify its quality and determine if the gully in question can be located and mapped. Hence, whilst gullies of varying sizes have been studied, all gullies needed to be large enough to be recognised in the historical imagery before they could be included. Smaller gullies are therefore unlikely to be well represented in this study.

Ortho-rectifying historical imagery is difficult in rural settings due to a lack of optimal control points. Some image warping may have occurred whilst rectifying imagery

leading to misregistration between image dates. The impact of this warping on the accuracy of the results is in part offset by the use of a grid for counting gully sizes. However, the larger the surface area or edge of a gully, especially with dendritic gullies, small misregistration in imagery could have cumulative impacts on overall grid counts. Whilst using a grid approach reduces the impact of user-subjectivity and some of the ambiguities associated with identifying the edges of gullies, this method can lead to an overestimation in gully sizes. A simple rule was established to reduce this influence - at least 50 per cent of a cell had to be gullied before it could be included in the count. However, considering that each cell represents 900m² some overestimation is still expected. This rule can also lead to underestimation of gully expansion. In the case where a gully is active and expansion has not encompassed 50 per cent of the adjacent grid cell in subsequent image dates, the expansion will not be counted. This can lead to an underestimation of up to 450m², or up to half of a grid cell. This is particularly problematic with widening linear gullies.

Selection of suitable locations for application of this approach may have been biased by available imagery. However, where gully expansion has been mapped in this study, it is generally considered that the differences in imagery types used for mapping over time has not greatly influenced the results. That is, we have not simply measured improvements in photographic technology. It is important to note that the mapping of gully expansion, however, can be influenced by vegetation and other objects that may obstruct the view of a gully on aerial photography or satellite imagery. Figure 36 shows the limitations of aerial photography when compared with a DEM derived from LiDAR data. The three-dimensional representation provides a more accurate and clear representation of gully extent. The chronosequence mapping may be improved by using stereoscopic methods to better represent the elevation differences, particularly where vegetation obstructs the view of the ground surface. Future opportunities also exist to monitor gullies using 3-D surfaces derived from stereo-pairs of satellite imagery. RSC is working with space agencies in China to investigate this further.

A preliminary attempt was made to integrate the chronosequence mapping with land types and Erosion Vulnerability ranking scores (as developed under RWQ Science Project RP63G). It was difficult to establish any reliable conclusions about the relationships between these landscape variables and gully expansion rates due to the small number of samples obtained by the chronosequence mapping. It would be beneficial to integrate these datasets with the 1km Gully Presence Map to improve understanding of the relationships between land types, Erosion Vulnerability ranking scores and gully prevalence. However, developing and undertaking an appropriate methodology for this work is would require some time and resources which were beyond the scope of this project.

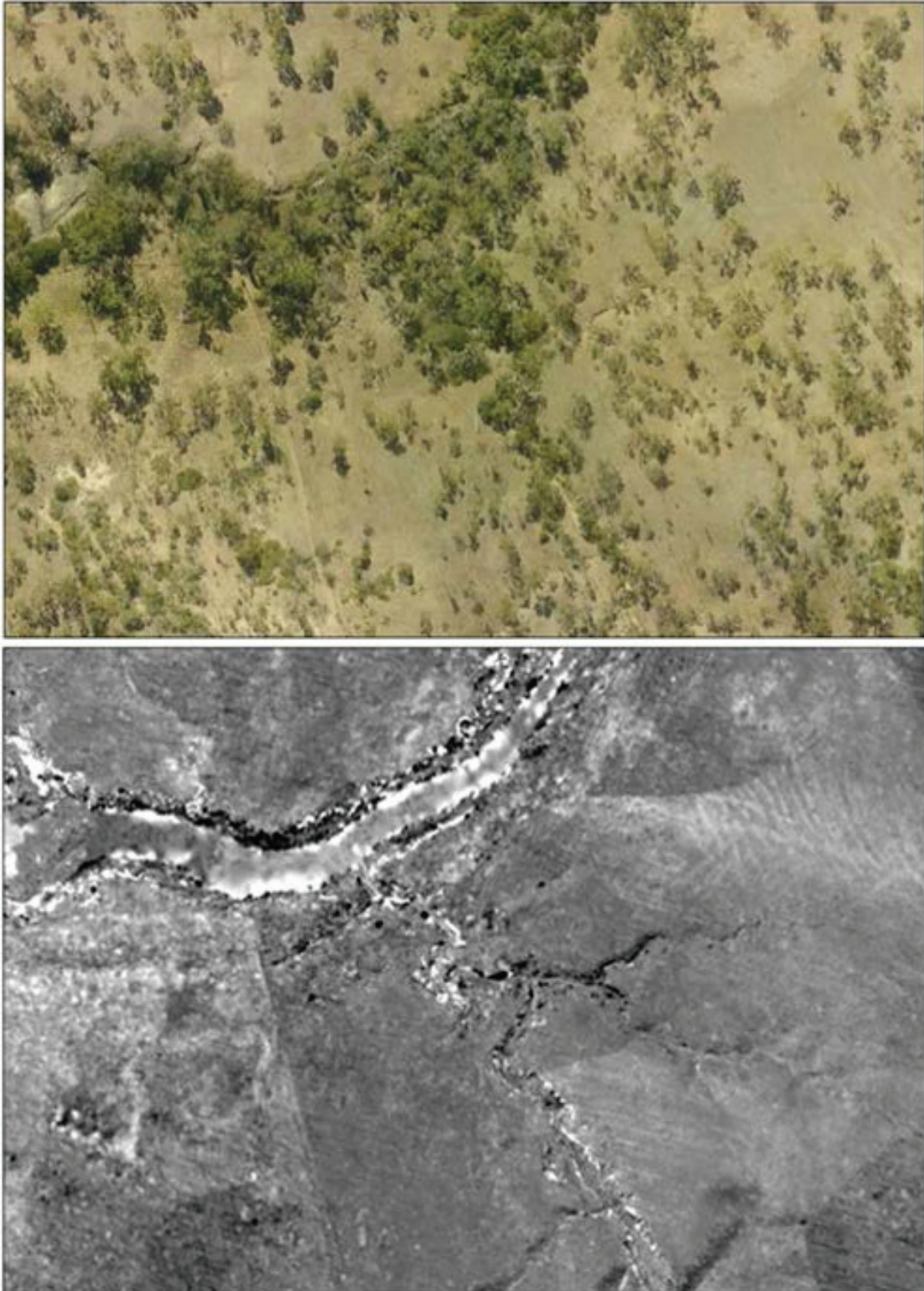


Figure 36 Top: high resolution aerial photography, Bottom: DEM derived from LiDAR data of the same area.

5 Conclusions

This project builds on previous work that provided consistent and reliable spatial data on the distribution of gullies in the Burdekin catchment. In undertaking this project, current knowledge of gully distribution and activity has been improved and multi-scale mapping products based on a range of methods and technologies have been derived. Key outputs and findings from the project are summarised below. A number of recommendations are also suggested based on knowledge gained through this project and emerging technologies.

Gullies are a significant contributor of sediment in Reef catchments. Outputs from this project, along with other projects funded by Reef Water Quality Science Program, Reef Plan and Reef Rescue will help to build understanding about the role of gullies in the sediment budget delivered to the GBR and identify areas vulnerable to future gully erosion. This information will be critical to inform future catchment-scale water quality modelling, policy development, extension and land management investment activities across grazing lands of the GBR catchments.

5.1 Key outputs

A number of key outputs have been produced from this project. These include:

- i. A **5km resolution gully presence map** compiled from high resolution mapping and broad scale visual observations and predictive modelling of gully presence. This map can be used to highlight areas in the Burdekin catchment which have higher prevalence of gully erosion or areas that may be at risk of future gully erosion, especially when assessed with soil erosion vulnerability mapping. The map also provides a foundation for extrapolating information derived from higher resolution mapping such as the 1km resolution gully presence map and the LiDAR data.
- ii. A **5km resolution gully density map** derived from the 5km resolution gully presence map and higher resolution mapping of gully networks. This map has been produced specifically to address the needs of the catchment water quality models, which require gully density grids as inputs.
- iii. **1km resolution gully presence mapping** for selected areas of the Burdekin. The mapping, which is based on the methods and guidelines developed for this project, provide medium-resolution information to augment the broad-scale mapping and help with more specific targeting of particular locations for gully prevention and management. The mapping also provides an intermediate level of information to enable scaling of gully volume change information derived from LiDAR and field data, to sub-catchment and catchment scale to support water quality models and whole-of-catchment management strategies. This mapping continues to be extended across the Burdekin, Fitzroy and Burnett-Mary regions through efforts of DNRM regional staff, an in-kind contribution.

- iv. **A method and accompanying guidelines for catchment-scale gully mapping.** This method and guidelines have been developed to facilitate consistent mapping of gully presence at 1km (or higher) resolution. This work has been collaboration with DNRM.
- v. **LiDAR data and derived change data** for 15 locations in the Burdekin and two dates (2010 and 2013/14), and 4 locations in the Fitzroy for three dates (2007, 2010 and 2013/14). These data provide very high resolution information about gully location, presence and volume, as well as volumetric change. The change estimates can be used to inform water quality models, providing improved gully erosion parameters for different locations and soil types. These data, and methods developed to analyse them, also establishes an accurate and objective foundation for ongoing monitoring, especially as many of the sites chosen coincide with, or are near, on-ground investment areas aimed at improving land condition.
- vi. **Historical gully change data** for 10 sample sites in the Burdekin, on dominant land types. These data are based on mapping and analysis of historical imagery and provide limited, but useful, information about rates of gully expansion over longer timeframes, in some cases over 50 years. These data can help indicate when different locations or regions experienced greater rates of change, and provide a mechanism for further investigation. The long-term rates of change can provide information to water quality models which are based on a longer initialisation period, more in line with climate records.

5.2 Key findings

The multiple scales of information, data and methods developed by this project have led to a number of key findings. Some of these relate to methodological issues and some relate to the location and dynamics of gullies, particularly in the Burdekin. These key findings are summarised as follows:

- i. Gully mapping across large areas using remotely sensed imagery is challenging. It relies on having a consistent, repeatable and mappable definition of gullies which can be applied at multiple scales and across multiple image capture platforms. Simple, pragmatic and efficient methods are required to ensure consistency in the application of any mapping approach. Outputs must balance available resources for mapping against end-user requirements. A key outcome of this project has been the development of a guideline for catchment-scale gully mapping in Queensland. The guideline provides clear definition, guiding principles and efficient methods for manual and semi-automated mapping of gullies.
- ii. Approximately 60% of the Burdekin catchment has low to very low presence and prevalence of gullies. This means there are very few or no gullies present in those areas. A large proportion of this area is in the Cape-Campaspe and Belyando sub-catchments and the southern half of the Suttor sub-catchment.
- iii. Approximately 3% of the Burdekin catchment has high to very high presence and prevalence of gullies. This means that there is severe or highly prevalent gullying in these areas. Gullies can be either linear or extensive systems. The majority of these are in the Upper Burdekin and Bowen-Broken-Bogie

catchments. A further 19% of the Burdekin catchment has medium or medium-high gullying present - gullies are frequent but are more likely to be relatively small and linear.

- iv. Based on a predictive model of gully presence, there is a strong relationship between elevation above drainage lines and gully presence. Ninety-six per cent of gullies occur within 1m of elevation above a drainage line. However, the probability of finding a gully in these areas is only about 4-5%. This suggests that although the model is useful for identify areas where gully probability is higher, the absolute prevalence of gullies in the landscape is still low.
- v. Mapping and monitoring gullies with LiDAR data requires accurate and consistent capture specifications, data processing and quality checking by LiDAR data providers. Thresholds are required when comparing differences in digital elevation models between multiple dates to account for noise and misclassification in the data. Based on the literature and testing as part of this project, these thresholds are nominally around 40-45cm, although this may vary depending on the quality of the data and the complexity of the terrain and land cover in the area of interest.
- vi. Automated mapping of gullies from LiDAR imagery requires an algorithm which is capable of detecting elevation differences over varying ranges. This is due to the differences in the morphology of individual gullies and gully systems. Any approach must balance errors of omission and commission.
- vii. Very high resolution mapping and change analysis of gullies using LiDAR data showed that of the 16 sites in the Burdekin and Fitzroy that were able to be analysed, all had at least some change in gully extent and volume between the two capture dates (2010 and 2013-14). The largest changes mapped were in excess of 10,000m³ at Marshes Creek, Parrot Creek, Starbright and Turrawulla sites. The exact timing and the fate of the sediment from these changes is unknown.
- viii. Very high resolution mapping and change analysis of gullies using LiDAR data also showed that there is a strong correlation between gully volume and gully area. This relationship could be used to extrapolate gully volume for areas where only gully area mapping was available. Further analysis should focus on relationships with soil erosion vulnerability to best approximate expected gully volume for different soil structural characteristics. Assumptions would need to be made about management history but this could improve gully volume estimates for water quality model parameterisation and regional prioritisation.
- ix. Mapping changes in gully extents using historical imagery is challenging and resource intensive, particularly for large areas. Locating historical imagery for a particular location requires extensive investigation of air photo archives to find suitable imagery that can be geo-located accurately to be able to reliably compare change over time. Identifying gullies in older imagery, and also in some new imagery, can be extremely difficult, resulting in a large degree of subjectivity in mapping outputs. It is suggested that gully chronosequence

mapping should only be undertaken where the study area is restricted to a local site and where reliable imagery is available.

- x. Ten gully sites were mapped over a 40-60 year period for some of the dominant land types of the Burdekin, using historical and recent aerial photography and satellite imagery. All but one of the sites demonstrated active gullying. Extension of gullies appeared to occur at different rates through time. From this limited sample, few relationships could be established between active gullying and soil erosion vulnerability or land type. A greater sample would be required to test these relationships.
- xi. Results of multi-temporal monitoring of gullies using LiDAR data and historical imagery suggest that significant gully change is largely event driven. Any one location could change rapidly where erosion causing factors combine under favourable conditions such as low cover and high intensity localised rainfall.

5.3 Recommendations for future work

This project has developed and tested a number of approaches for mapping and monitoring gullies. Based on experiences in this project, including resourcing levels and issues with third party data acquisition, the following six recommendations are made for future work. These are listed in a general order of priority however prioritisation of these future projects would be dependent on end user requirements and investment strategies.

- i. Continue development of the Catchment-scale Gully Mapping Guidelines and provide support for ongoing efforts by DNRM and DSITIA to continue mapping gully presence at 1km resolution (or higher) in the Burdekin, Fitzroy and Burnett-Mary catchments.
- ii. Provide support for the establishment of a yearly gully monitoring program based mainly around field-based terrestrial laser scanning, with the possibility for periodic (~5 year) acquisitions of airborne LiDAR for established sites, subject to available resources. This program would require approximately 6-12 months of development to design a sampling program and establish appropriate survey and processing specifications for the use of terrestrial laser scanning for monitoring gully changes. This program has the potential to include stream banks. The program should also include gully (and stream bank) prevention/remediation sites in order to help monitor and evaluate the cost-benefit of any intervention strategies.
- iii. Investigate and develop an appropriate mechanism to integrate key landscape indicators of land condition. This includes gully mapping, soil erosion vulnerability, ground cover and management practice data. The catchment-scale water quality modelling may be the most appropriate mechanism for this work. With respect to the multiple scales of gully mapping produced by this project, some methods based on machine learning approaches have been suggested by Griffith University. These approaches integrate data at multiple scales to predict gully presence and volume change. These approaches may warrant a small-scale, sub-catchment study to test the model outputs.
- iv. New technologies are emerging such as Unmanned Aerial Vehicles (UAVs) and space-borne stereo imagery. DAFF has previously demonstrated the application of UAVs for capturing imagery and generating digital surface models over a gully remediation trial on Spyglass Research Station in the Burdekin. Outputs still require testing and validation but the results did show some promise. It is suggested that further investigation of UAV technology for mapping and monitoring gullied areas be considered. With regards to space-borne stereo imagery, RSC has an agreement with the Chinese Satellite Applications Centre for Surveying and Mapping (SASMAC) who operate the ZY-3 satellite. This satellite has high resolution stereo-imagery capable of producing 4m digital surface models. Although this is still relatively coarse resolution for monitoring specific gullies, it is recommended that an assessment of these data be undertaken to determine the applicability of the imagery for catchment-scale mapping in three dimensions. Trial imagery will be provided free-of-charge as part of the collaboration with SASMAC.

- v. Mapping and monitoring of gullies can only provide part of the story when it comes to understanding gully contributions to sediment loads and impacts on the GBR. Improved understanding of transport pathways, residence times, and dominant processes is still required. It is recommended that future geomorphological studies be focussed on these key issues.
- vi. There is very limited information about the cost-benefit of gully prevention and remediation approaches. The gully mapping provides improved targeting of management, but, without adequate understanding of cost-benefit of different management approaches, this targeting may be misguided. It is recommended that, where possible, science and monitoring efforts be combined with on-ground efforts and economic modelling to improve knowledge of where and when to expend resources for gully management.

6 Data publication

A number of products and data have been developed as part of this project. These will be made available through Open Data portals in late 2014 or early 2015. Further releases of data and mapping will be undertaken as mapping is progressed by DNRM and LiDAR data is resupplied from the LiDAR data provider.

Table 21 lists those data sets to be released under Creative Commons (BY attribution) licencing in the near future. The data will be made available through approved Open Data portals, including, where possible, the Queensland Globe. These data will be of use to government agencies, regional NRM groups, academic researchers and Paddock to Reef modelling staff.

Table 21 List of data sources to be released as Open Data from this project

Data set name	Resolution	Format	Delivery mechanism
Burdekin catchment 5km gully presence map	5km grid	TIFF	SIR, QGIS
Burdekin catchment 1km gully presence mapping	1km grid	TIFF	SIR
2010 LiDAR data and derived DEMs	As per LiDAR specifications	LAS, TIFF	TERN Auscover
2013/14 LiDAR data and derived DEMs	As per LiDAR specifications	LAS, TIFF	TERN Auscover

7 References

- Armston, J.D., Denham, R.J., Danaher, T.J., Scarth, P.F., Moffiet, T.N., 2009. Prediction and validation of foliage projective cover from Landsat-5 TM and Landsat-7 ETM+ Imagery. *Journal of Applied Remote Sensing*. 3:033540.
- Bainbridge, Z., Lewis, S., Davis, A., Brodie, J., 2008. Event-based community water quality monitoring in the Burdekin Dry Tropics NRM Region: 2007/08 wet season update. ACTFR Report No. 08/19 for the North Queensland Dry Tropics. ACTFR, James Cook University, Townsville, Australia.
- Bartley, R., 2011. Sediment sources and grazing land management impacts in the Burdekin catchment: a review of existing research and projection of future research needs. Report to Queensland Department of Environment and Resource Management (Reef Protection Unit).
- Bartley, R., Hawdon, A., Post, D.A., Roth, C.H., 2007. A sediment budget for a grazed semi-arid catchment in the Burdekin basin, Australia. *Geomorphology*. 87(4), 302-321.
- Baruch, A., Filin, S., 2011. Detection of gullies in roughly textured terrain using airborne laser scanning data. *ISPRS Journal of Photogrammetry and Remote Sensing*. 66(5), 564-578.
- Bou Kheir, R., Wilson, J., Deng, Y., 2007. Use of terrain variables for mapping gully erosion susceptibility in Lebanon. *Earth Surface Processes and Landforms*. 32(12), 1770-1782.
- Brasington, J., Langham, J., and Rumsby, B., 2003. Methodological sensitivity of morphological estimates of coarse fluvial sediment transport. *Geomorphology*. 53, 299-316.
- Brodie, J., Waterhouse, J., Schaffelke, B., Kroon, F., Thorburn, P., Rolfe, J., Johnson, J., Fabricius, K., Lewis, S., Devlin, M., Warne, M., McKenzie, L. 2013. 2013 Scientific Consensus Statement. Land Use impacts on Great Barrier Reef water quality and ecosystem condition. The State of Queensland, Brisbane.
- Croke, J., Todd, P., Thompson, C., Watson, F., Denham, R., Khanal, G., 2013. The use of multi temporal LiDAR to assess basin-scale erosion and deposition following the catastrophic January 2011 Lockyer flood, SE Queensland, Australia. *Geomorphology*. 184, 111-126.
- Eustace, A.H., Pringle, M.J., Denham, R.J., 2011. A risk map for gully locations in central Queensland, Australia. *European Journal of Soil Science*. 62(3), 431-441.
- Evans, M., and Lindsay, J. 2010. High resolution quantification of gully erosion in upland peatlands at the landscape scale. *Earth Surface Processes and Landforms*, Vol. 35, 876-886.
- Gómez Gutiérrez, Á., Schnabel, S., Felicísimo, Á.M., 2009. Modelling the occurrence of gullies in rangelands of southwest Spain. *Earth Surface Processes and Landforms*. 34(14), 1894-1902.

Hughes, A.O., Prosser, I.P., Stevenson, J., Scott, A., Lu, H., Gallant, J., 2001. Gully Erosion Mapping for the National Land and Water Resources Audit. Technical Report 26/01. CSIRO, Land and Water, Canberra, Australia.

James, L.A., Watson, D.G., and Hansen, W.F. 2007. Using LiDAR to map gullies and headwater streams under forest canopy: South Carolina, USA. *Catena*, Vol., 132-144.

Johansen, K., Watson, F., Eustace, A., Tindall, D. and Phinn, S., 2011. Object-based mapping of gullies from SPOT-5 imagery and ancillary data in the Burdekin catchment, Queensland, Australia. Joint Remote Sensing Research Program. Unpublished report.

Kinsey-Henderson, A.E., Post, D.A. and Prosser, I.P., 2005. Modelling sources of sediment at sub-catchment scale: an example from the Burdekin Catchment, North Queensland, Australia. *Mathematics and Computers in Simulation*, 69(1-2), 90-102.

Knight, J., Spencer, J., Brooks, A. and Phinn, S., 2007. Large-area high-resolution remote sensing based mapping of alluvial gully erosion in Australia's tropical rivers. In, *Proceedings of the 5th Australian Stream Management Conference*. Australian rivers: making a difference. Charles Sturt University, Thurgoona, New South Wales.

Kuhnert, P., Kinsey-Henderson, A., Bartley, R. and Herr, A., 2010. Incorporating uncertainty in gully erosion calculations using the random forests modelling approach. *Environmetrics*, 21(5): 493-509, DOI: 10.1002/env.999.

Lewis, S., Brodie, J., Ledee, E., Alewijnse, M., 2006. The Spatial Extent of Delivery of Terrestrial Materials from the Burdekin Region in the Great Barrier Reef Lagoon. ACTFR report number 06/02, Townsville, Australia.

Martínez-Casasnovas, J.A., Ramos, M.C., Poesen, J., 2004. Assessment of sidewall erosion in large gullies using multi-temporal DEMs and logistic regression analysis. *Geomorphology*. 58(1-4), 305-321.

McKergow, L.A., Prosser, I.P., Hughes, A.O., Brodie, J., 2005. Sources of sediment to the Great Barrier Reef World Heritage Area. *Marine Pollution Bulletin*. 51(1-4), 200-211.

Meyer, A., Martínez-Casasnovas, J.A., 1999. Prediction of existing gully erosion in vineyard parcels of the NE Spain: a logistic modelling approach. *Soil & Tillage Research*. 50(3-4), 319-331.

Perroy, R.L., Bookhagen, B., Asner, G.P., Chadwick, O.A., 2010. Comparison of gully erosion estimates using airborne and ground-based LiDAR on Santa Cruz Island, California. *Geomorphology*. 118(3-4), 288-300.

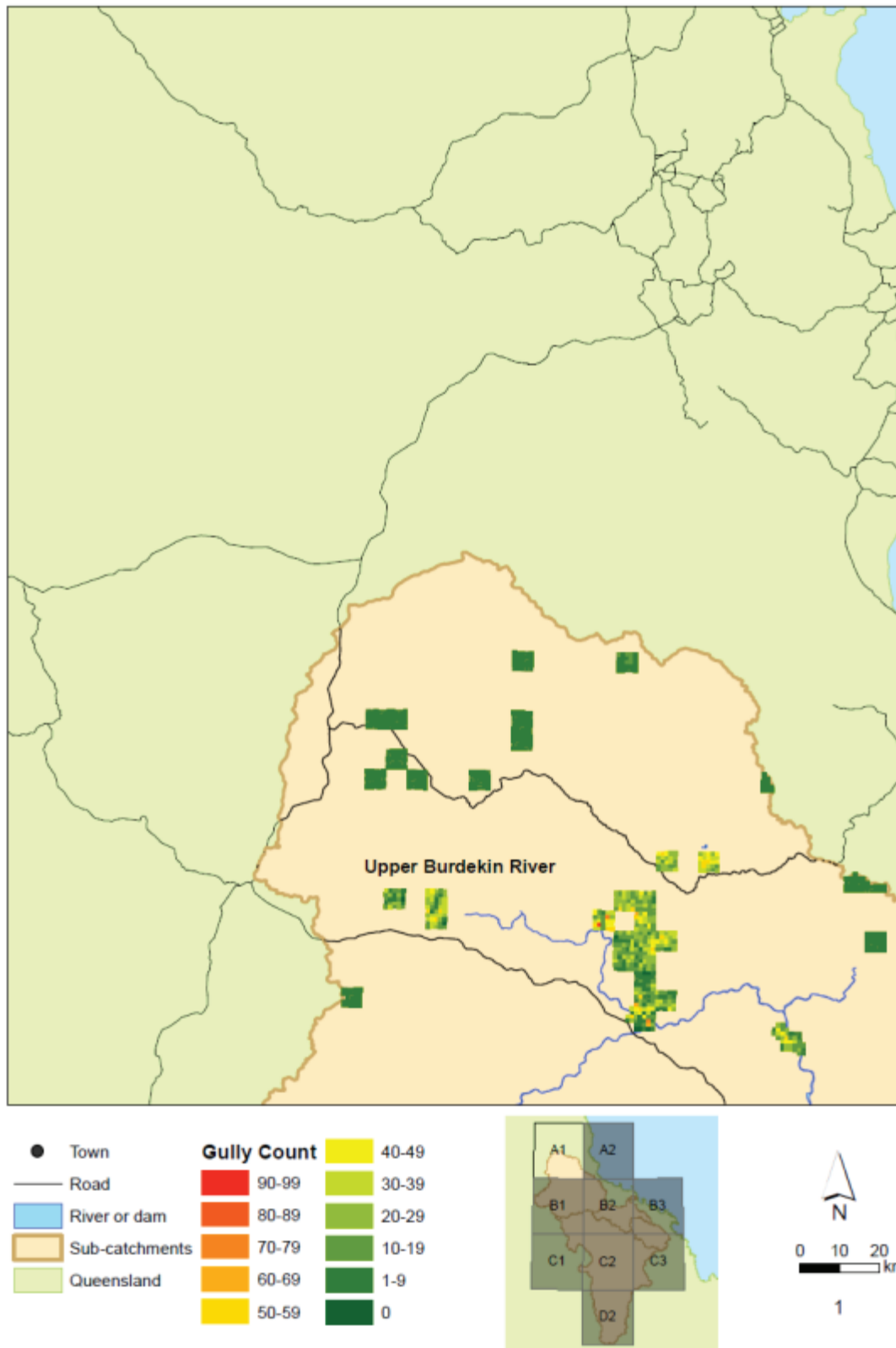
Prosser, I., Moran, C., Lu, H., Scott, A., Rustomji, P., Stevenson, J., Priestly, G., Roth, C.H., Post, D., 2002. Regional Patterns of Erosion and Sediment Transport in the Burdekin River Catchment. Technical report 5/02. CSIRO Land and Water, Brisbane, Australia.

Sibson, R., 1981. A Brief Description of Natural Neighbor Interpolation. Chapter 2 in *Interpolating multivariate data*, John Wiley & Sons, New York, 1981, 21-36.

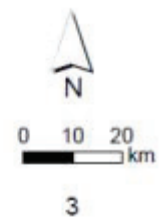
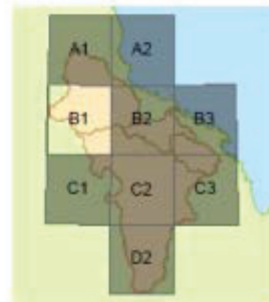
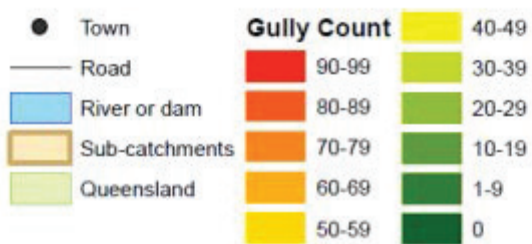
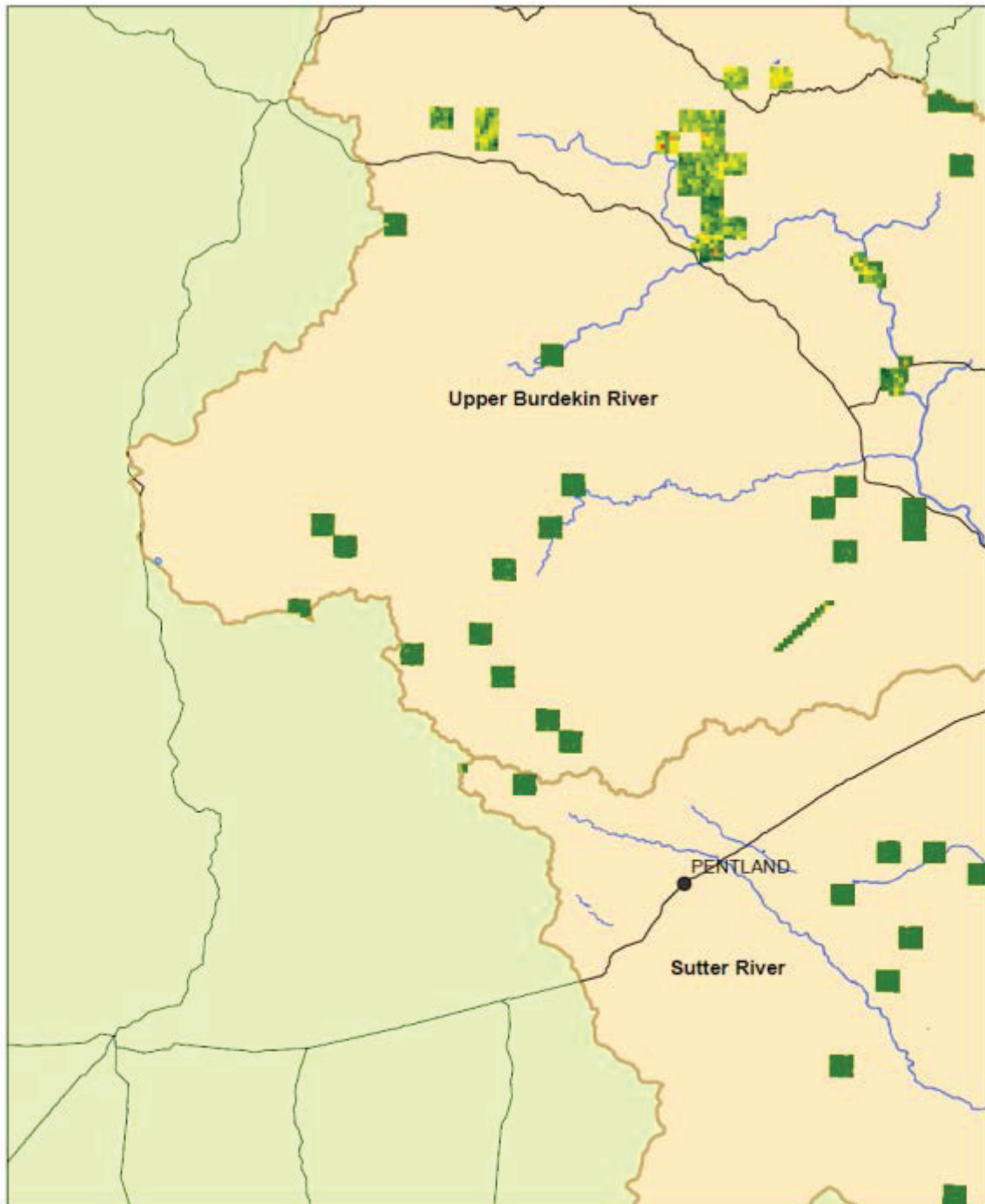
- Shruthi, R.B.V., Kerle, N., Jetten, V., 2011. Object-based gully feature extraction using high spatial resolution imagery. *Geomorphology*. 134(3-4), 260-268.
- Vanwallegem, T., Van Den Eeckhaut, M., Poesen, J., Govers, G., Deckers, J., 2008. Spatial analysis of factors controlling the presence of closed depressions and gullies under forest: Application of rare event logistic regression. *Geomorphology*. 95(3-4), 504-517.
- Vrieling, A., Rodrigues, S.C., Bartholomeus, H., Sterk, G., 2007. Automatic identification of erosion gullies with ASTER imagery in the Brazilian Cerrados. *Int.J.Remote Sens.* 28(12), 2723-2738.
- Zinck, J.A., López, J., Metternicht, G.I., Shrestha, D.P., Vázquez-Selem, L., 2001. Mapping and modelling mass movements and gullies in mountainous areas using remote sensing and GIS techniques. *International Journal of Applied Earth Observation and Geoinformation*. 3(1), 43-53.

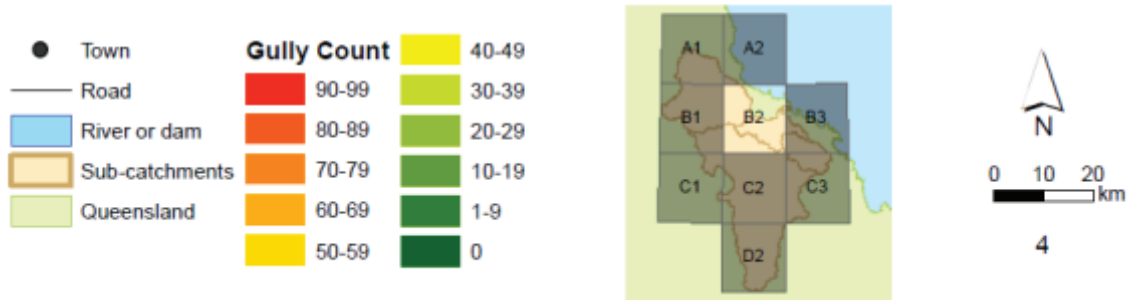
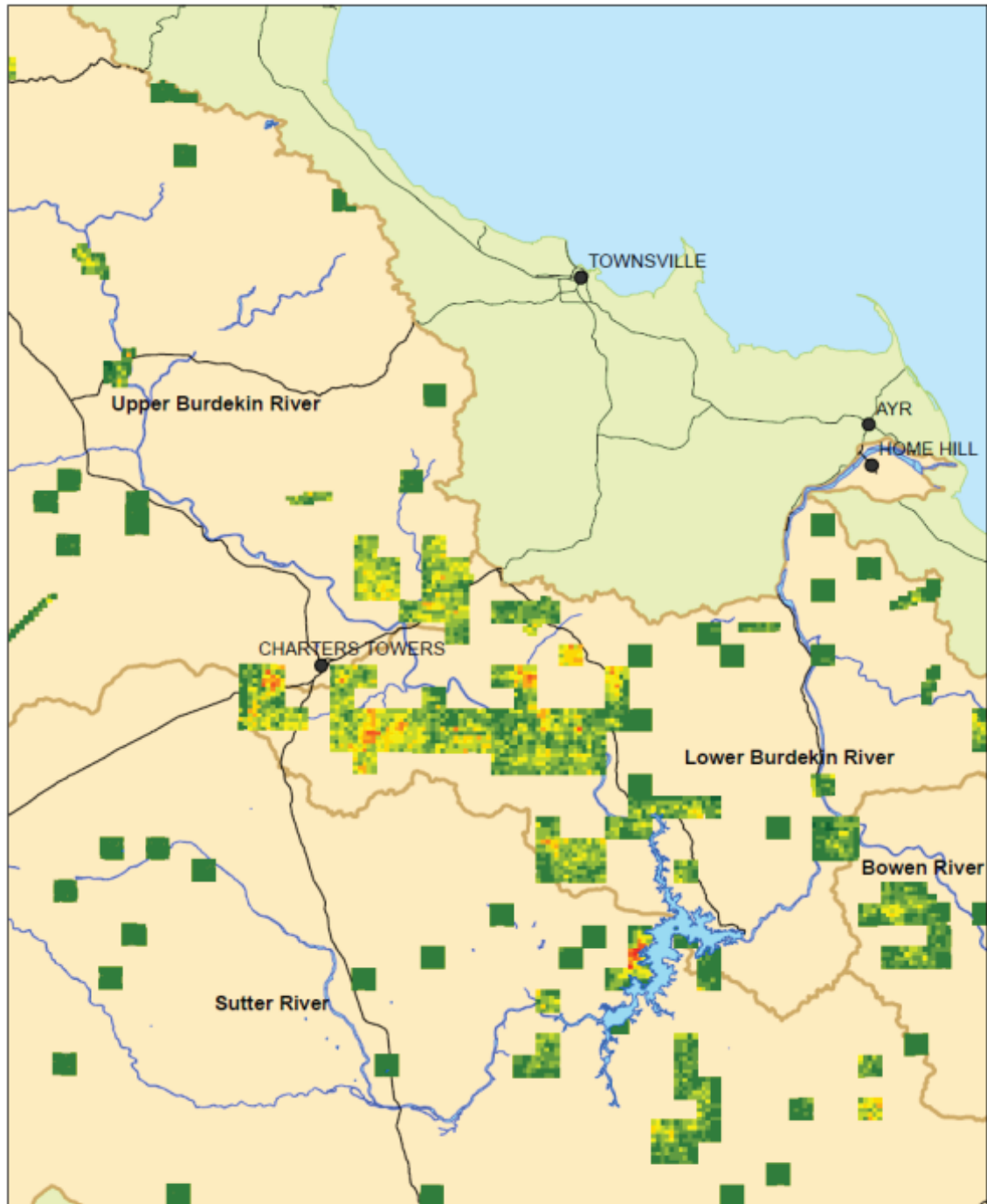
1. Appendices

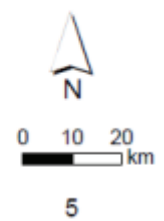
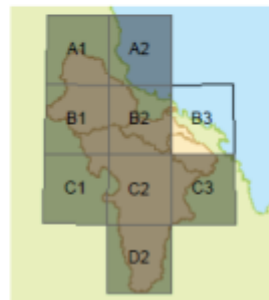
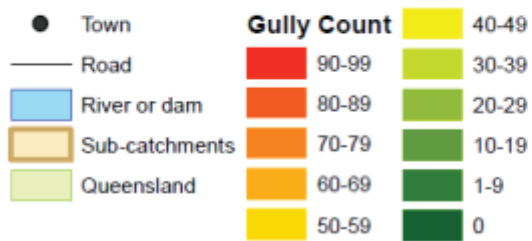
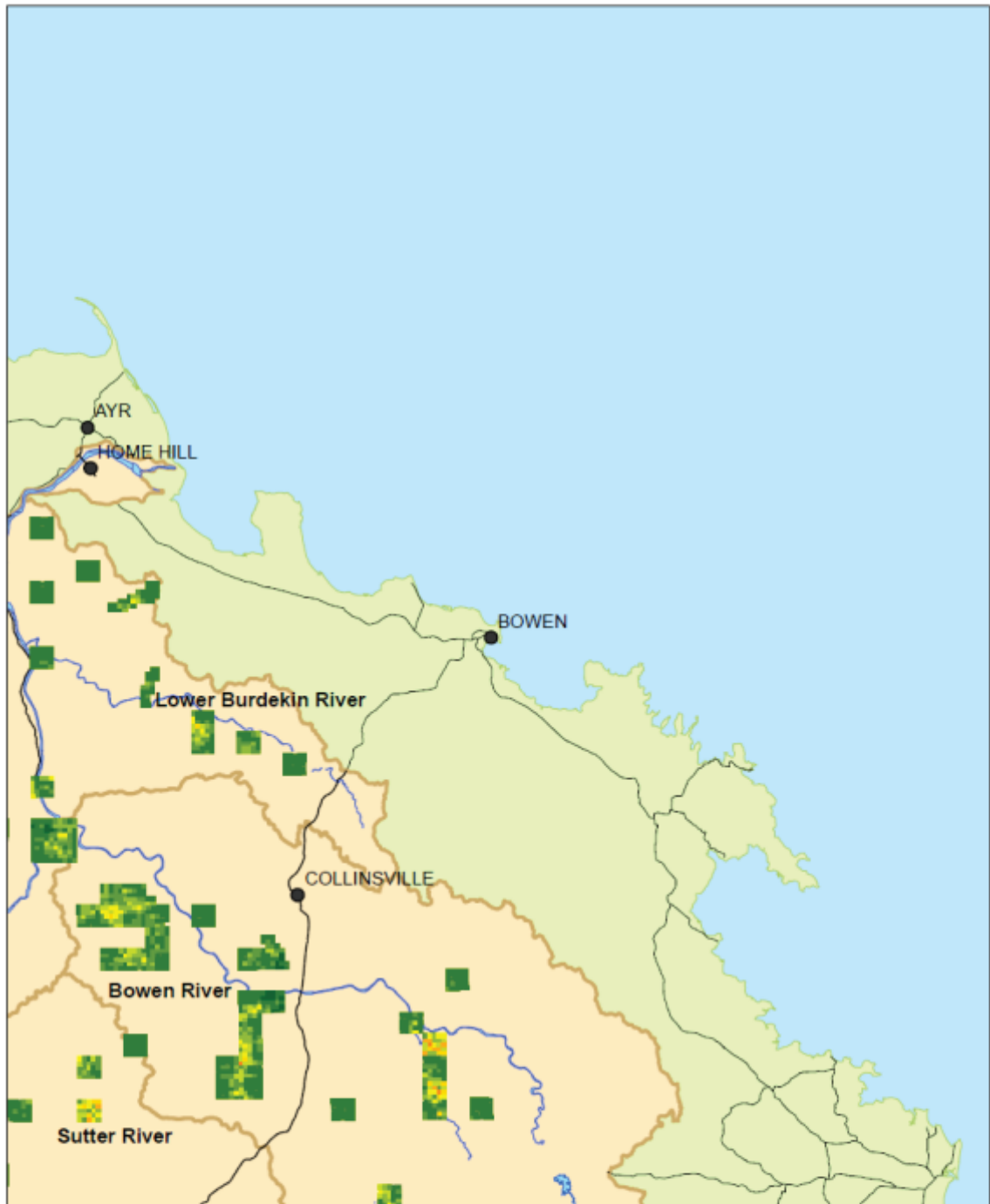
Appendix A Mapbook showing 1km resolution gully presence mapping.

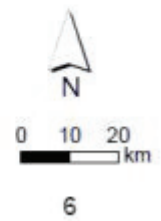
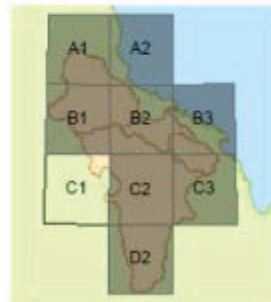
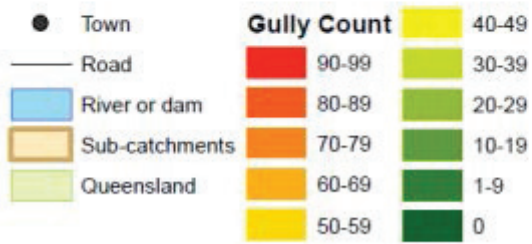
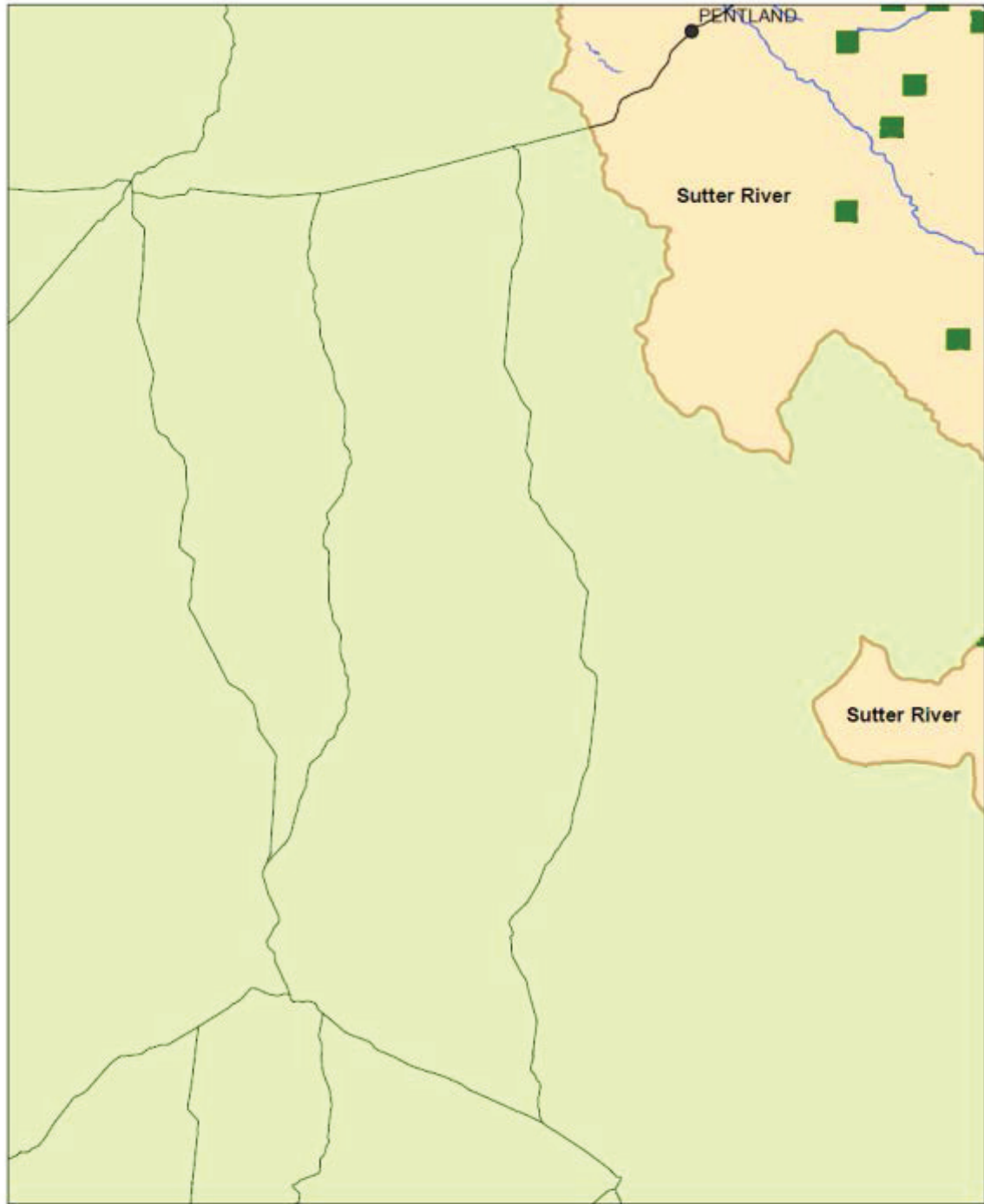


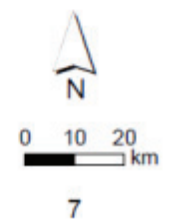
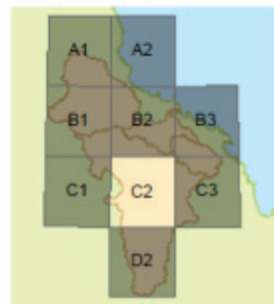
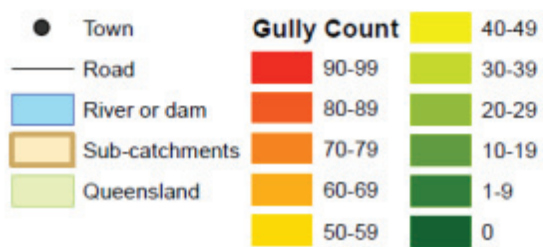
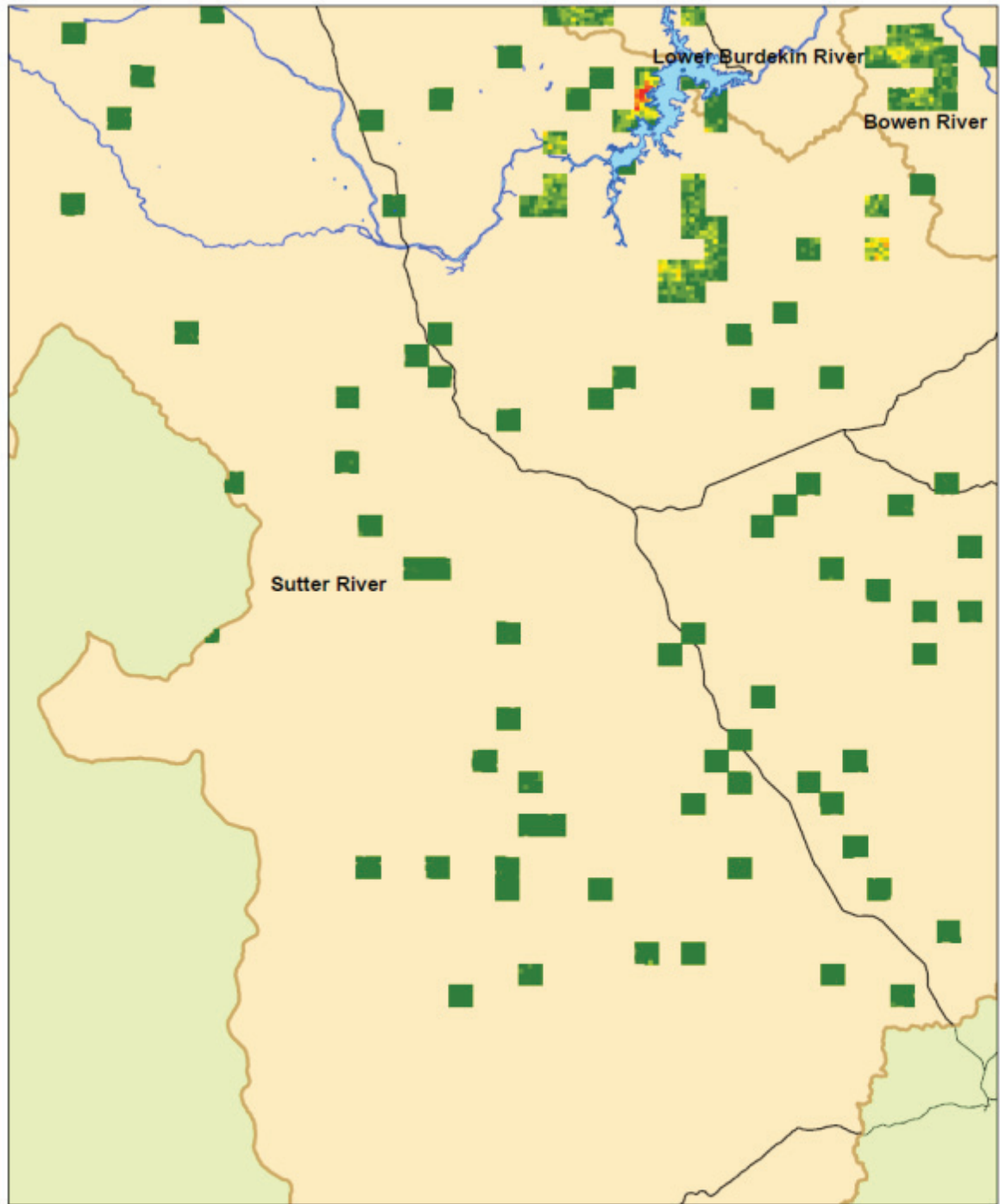


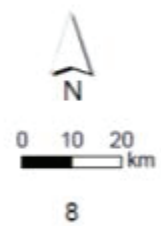
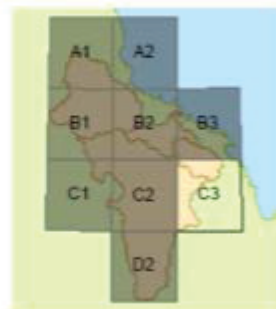
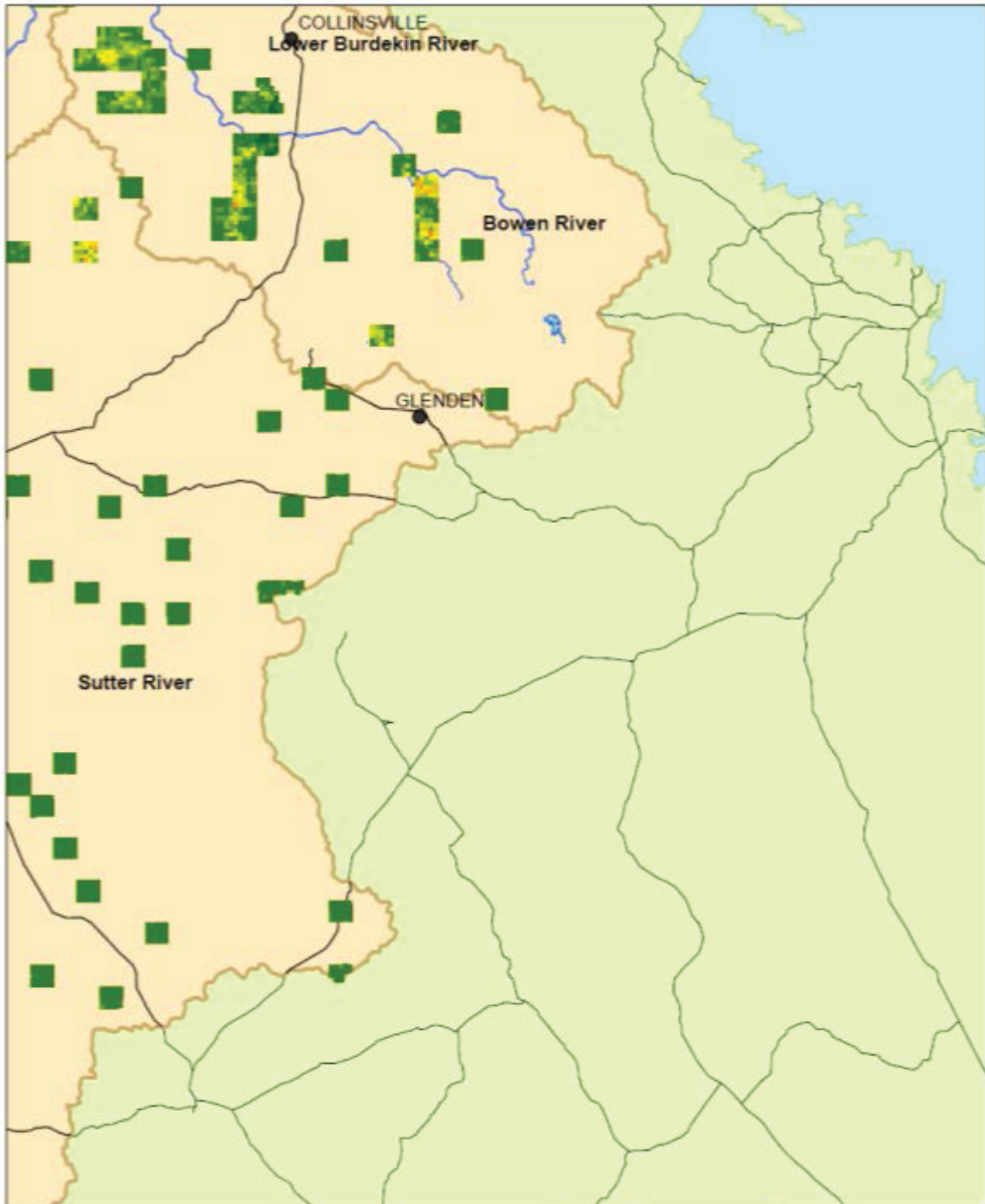


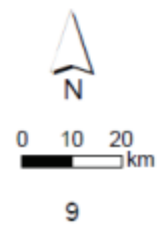
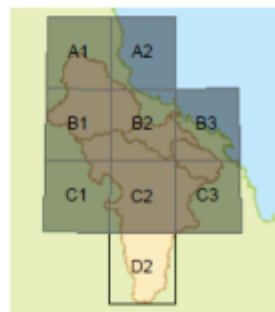
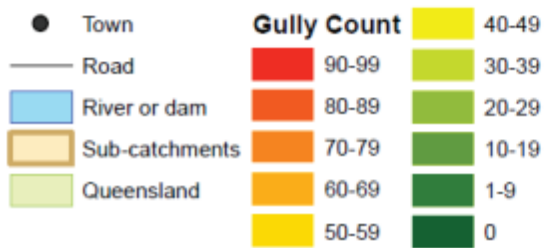
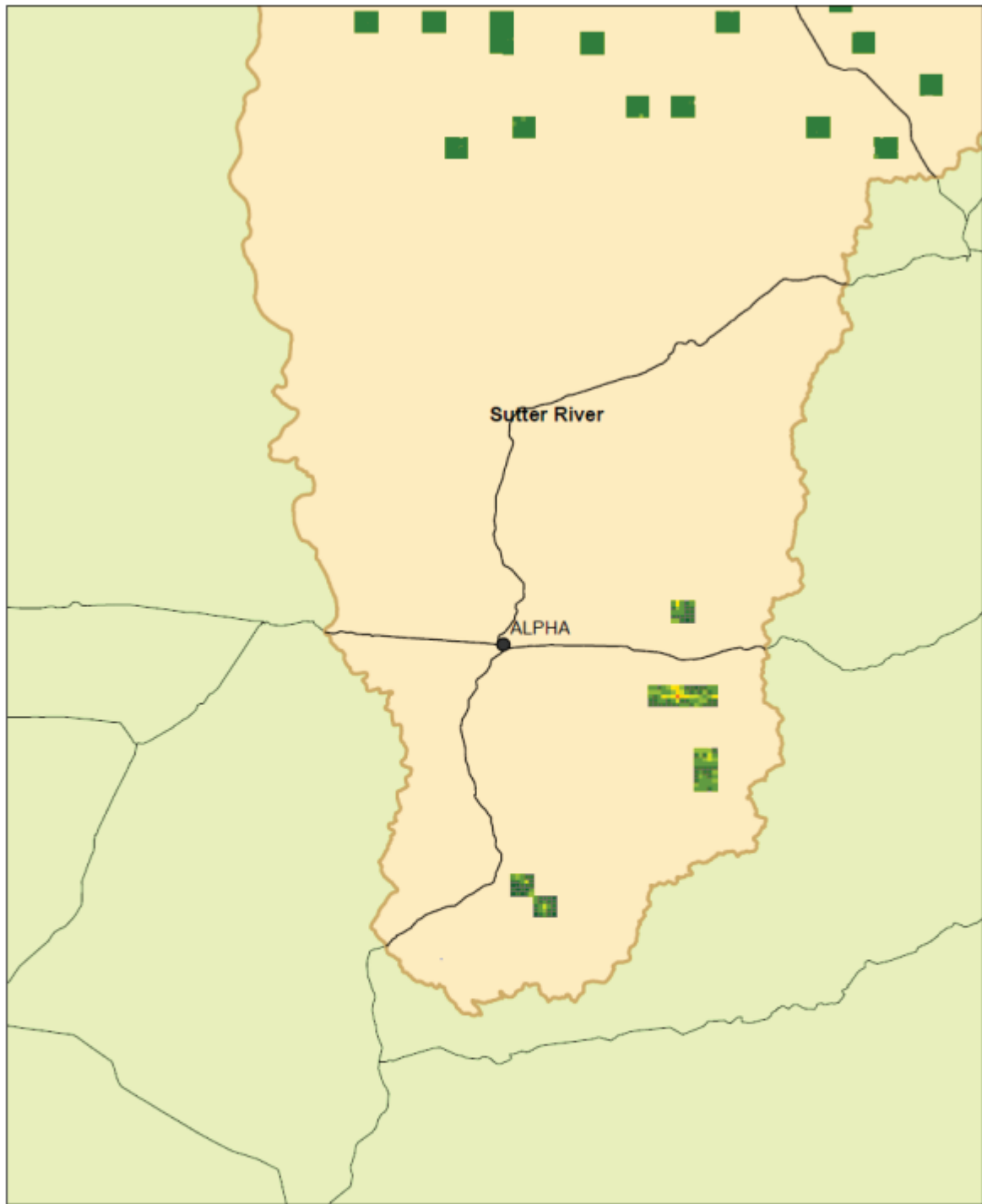




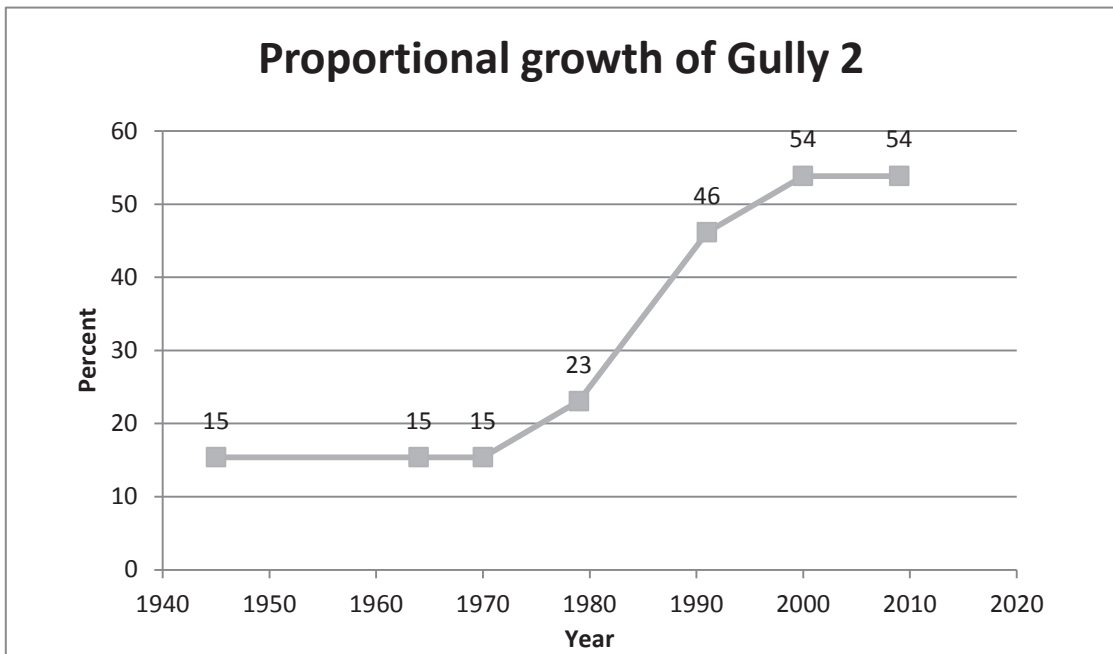
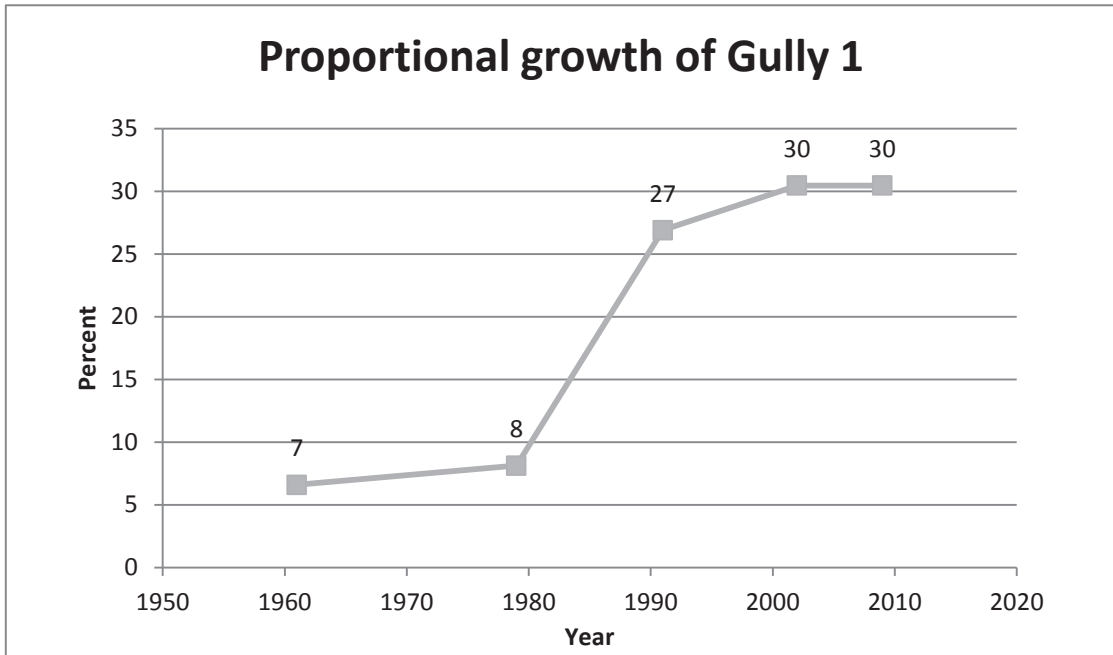




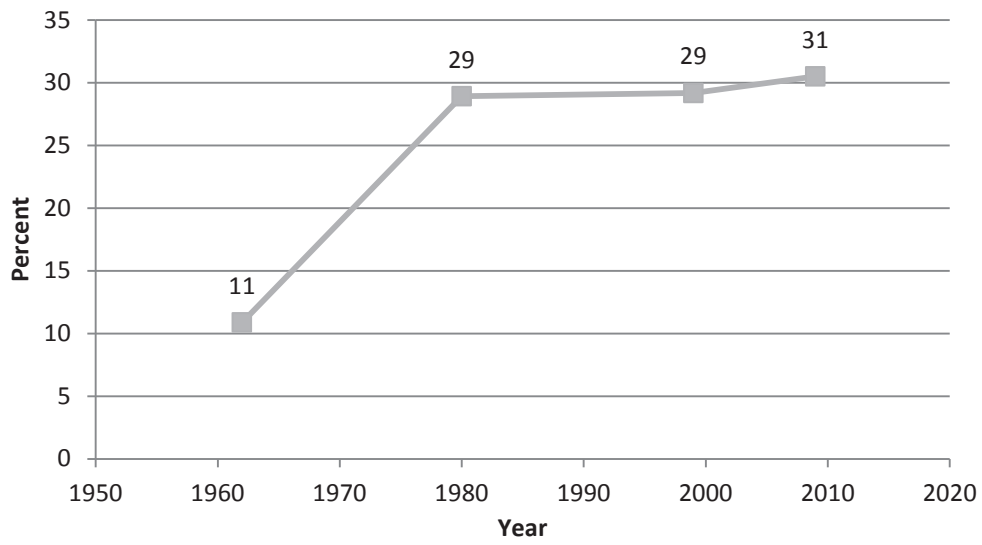




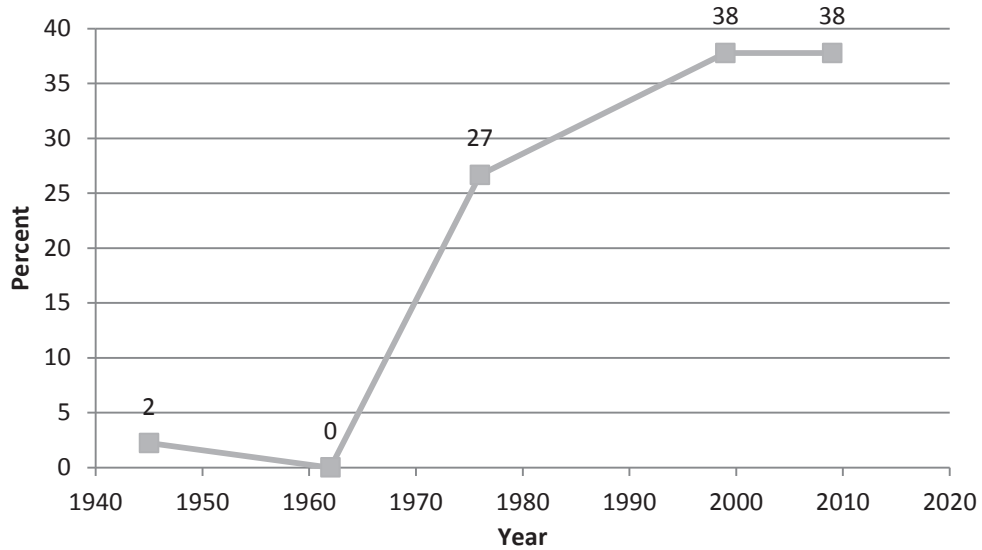
Appendix B – Proportional growth of the 10 gullies studied through gully chronosequence mapping.



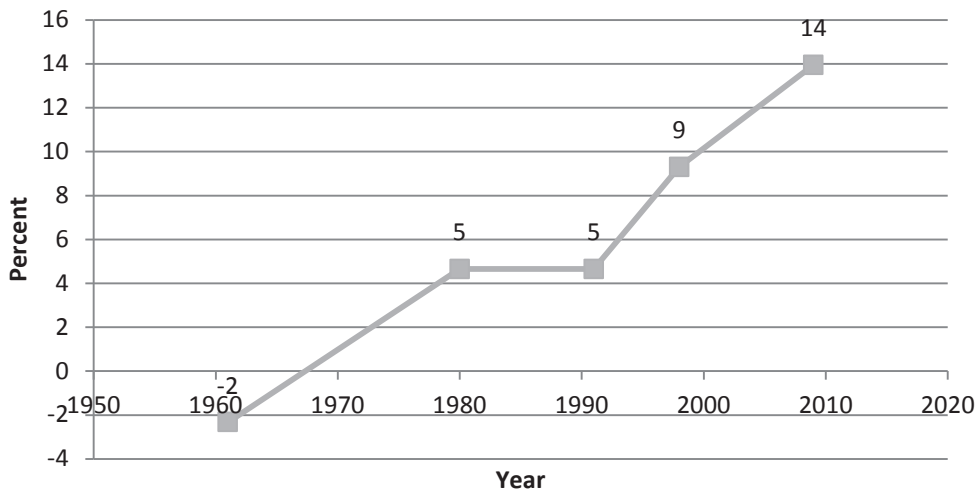
Proportional growth of Gully 3



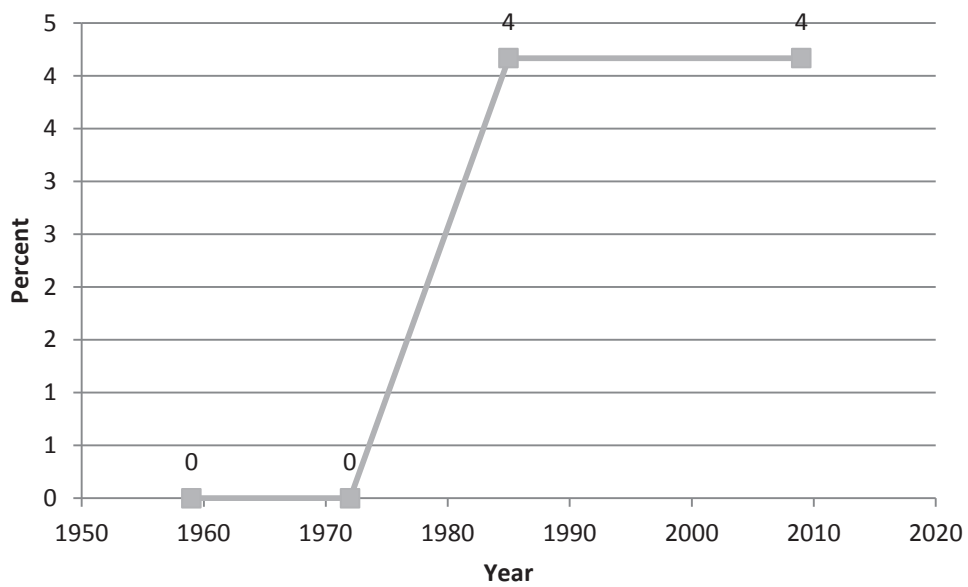
Proportional growth of Gully 4



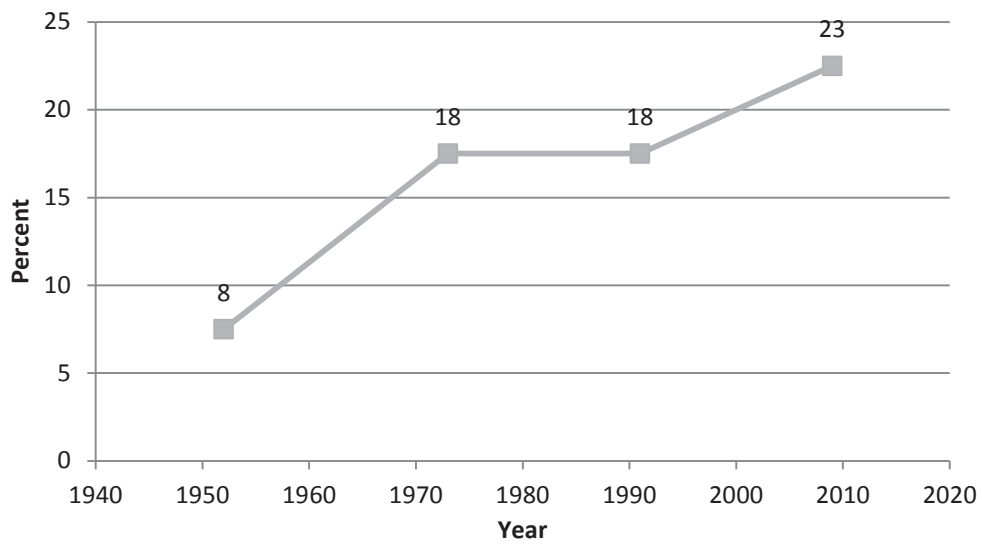
Proportional growth of Gully 5



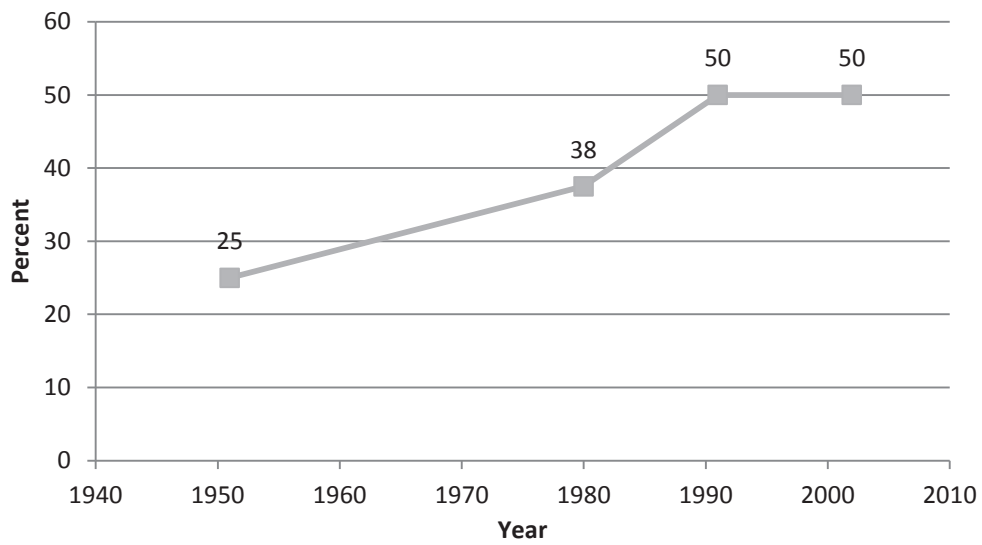
Proportional growth of Gully 6



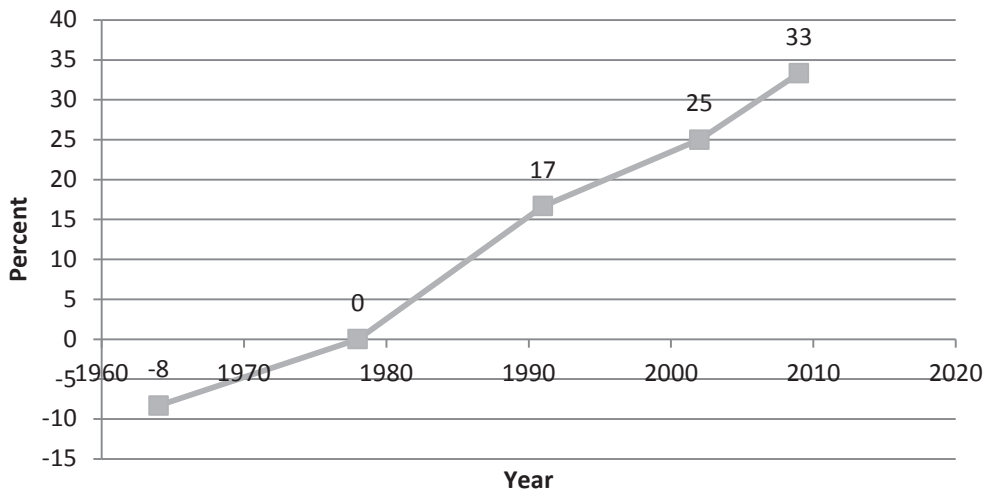
Proportional growth of Gully 7



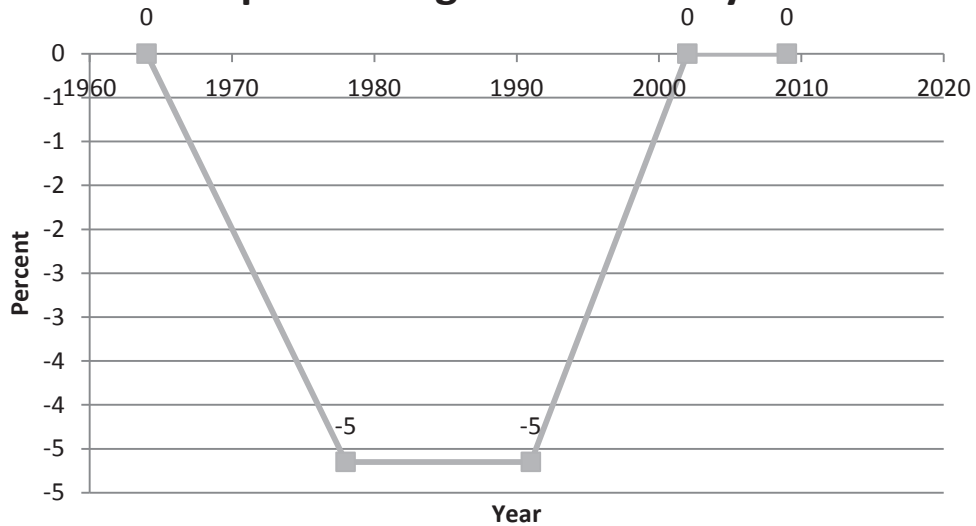
Proportional growth of Gully 8



Proportional growth of Gully 9



Proportional growth of Gully 10



Appendix C – Table of results of the Gully Chronosequence Mapping

Gully	Shape	Image Year	Count	Gully size m ²	Intervening years	Change during intervening years (m ²)	Yearly rate of change during intervening years (m ²)	Proportional change from first image date (%)	Change between 1 st and last year (m ²)	Rate of change between 1 st and last year (m ² /year)	Greatest change period
1	L	1961 BW	197	177300	NA	NA	NA	NA	NA	NA	
1	L	1979 BW	210	189000	18	11700	650	7	NA	NA	NA
1	L	1991 BW	213	191700	12	2700	225	8	NA	NA	NA
1	L	2002 C	250	225000	11	33300	3027	27	NA	NA	NA
1	L	2009 S	257	231300	7	6300	900	30	NA	NA	NA
1	L	2012 S	257	231300	3	0	0	30	54,000	1059	1991-2002
2	B	1945 BW	13	11700	NA	NA	NA	NA	NA	NA	NA
2	B	1964 BW	15	13500	19	1800	95	15	NA	NA	NA
2	B	1970 BW	15	13500	6	0	0	15	NA	NA	NA
2	B	1979 BW	15	13500	9	0	0	15	NA	NA	NA

2	B	1991 BW	16	14400	12	900	75	23	NA	NA	NA	NA
2	B	2000 C	19	17100	9	2700	300	46	NA	NA	NA	NA
2	B	2009 S	20	18000	7	900	129	54	NA	NA	NA	NA
2	B	2012 S	20	18000	3	0	0	54	6300	94	1991-2000	NA
3	B	1962 BW	377	339300	NA	NA	NA	NA	NA	NA	NA	NA
3	B	1980 BW	418	376200	18	36900	2050	11	NA	NA	NA	NA
3	B	1999 C	486	437400	19	61200	3221	29	NA	NA	NA	NA
3	B	2009 S	487	438300	10	900	90	29	NA	NA	NA	NA
3	B	2012 S	492	442800	3	4500	1500	31	103500	2070	1980-1999	NA
4	L	1945 BW	90	2700	NA	NA	NA	NA	NA	NA	NA	NA
4	L	1962 BW	92	2760	17	60	4	2	NA	NA	NA	NA

4	L	1976 BW	90	2700	14	-60	-4	0	NA	NA	NA	NA	NA
4	L	1999 C	114	3420	23	720	31	27	NA	NA	NA	NA	NA
4	L	2009 S	124	3720	10	300	30	38	NA	NA	NA	NA	NA
4	L	2012 S	124	3720	3	0	0	38	1020	15	1999-2009		
5	L	1961 BW	43	38700	NA	NA	NA	NA	NA	NA	NA	NA	NA
5	L	1980 BW	42	37800	19	-900	-47.3684	-2	NA	NA	NA	NA	NA
5	L	1991 BW	45	40500	11	2700	245.4545	5	NA	NA	NA	NA	NA
5	L	1998 C	45	40500	7	0	0	5	NA	NA	NA	NA	NA
5	L	2009 S	47	42300	11	1800	163.6364	9	NA	NA	NA	NA	NA
5	L	2012 S	49	44100	3	1800	600	14	5400	106	1998-2009		

6	L	1959 BW	24	21600	NA	NA	NA	NA	NA	NA	NA	NA	NA	NA	NA	NA	NA
6	L	1972 BW	24	21600	26	0	0	0	NA	0	NA	NA	NA	NA	NA	NA	NA
6	L	1985 BW	24	21600	13	0	0	0	NA	0	NA	NA	NA	NA	NA	NA	NA
6	L	2009 S	25	22500	24	900	38	4	NA	4	NA	NA	NA	NA	NA	NA	NA
6	L	2012 S	25	22500	3	0	0	4	NA	4	900	17	1985-2009				
7	B	1952 BW	40	36000	NA	NA	NA	NA	NA	NA	NA	NA	NA	NA	NA	NA	NA
7	B	1973 BW	43	38700	21	2700	129	8	NA	8	NA	NA	NA	NA	NA	NA	NA
7	B	1991 BW	47	42300	18	3600	200	18	NA	18	NA	NA	NA	NA	NA	NA	NA
7	B	2009 S	47	42300	18	0	0	18	NA	18	NA	NA	NA	NA	NA	NA	NA

7	B	2012 S	49	44100	3	1800	600	23	8100	135	2009-2012 (historically 1973-1991)
8	L	1951 BW	8	7200	NA	NA	NA	NA	NA	NA	NA
8	L	1980 BW	10	9000	29	1800	62	25	NA	NA	NA
8	L	1991 BW	11	9900	11	900	82	38	NA	NA	NA
8	L	2002 C	12	10800	11	900	82	50	NA	NA	NA
8	L	2009 S	12	10800	7	0	0	50	3600	62	Similar between 1980-1991 & 1991-2002
9	L	1964 BW	12	10800	NA	NA	NA	NA	NA	NA	NA
9	L	1978 BW	11	9900	14	-900	-64	-8	NA	NA	NA
9	L	1991	12	10800	13	900	69	0	NA	NA	NA

